Nataša Hulak

TESIS DOCTORAL

2014

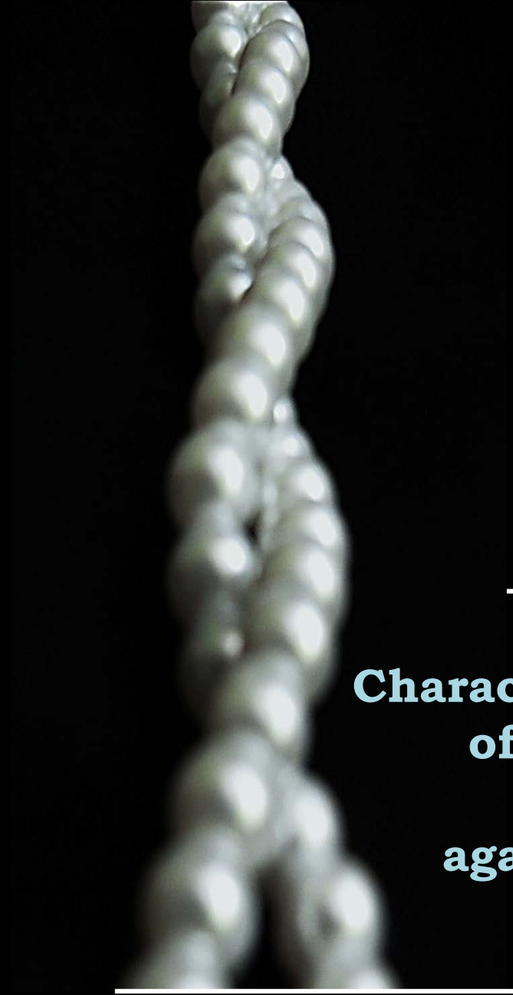

Nataša Hulak

Characterization of the expression of transcriptionally silent loci during the plant response against *Pseudomonas syringae*

TESIS DOCTORAL
2014

Universidad de Málaga-CSIC
Departamento de Biología Celular, Genética y Fisiología
Instituto de Hortofruticultura Subtropical y Mediterránea
(IHSM)

FEDER
Fondo Europeo de Desarrollo Regional
JUNTA DE ANDALUCIA
IHSM La Mayora
Instituto de Hortofruticultura Subtropical y Mediterránea
CSIC
Consejo Superior de Investigaciones Científicas
ma
UNIVERSIDAD DE MÁLAGA

Publicaciones y
Divulgación Científica

AUTOR: Nataša Hulak

EDITA: Publicaciones y Divulgación Científica. Universidad de Málaga

Nataša Hulak

Characterization of the expression of transcriptionally silent loci during the plant response against *Pseudomonas syringae*

TESIS DOCTORAL

Málaga, 2014

Memoria presentada por

Nataša Hulak

para optar al grado de Doctora por la Universidad de Málaga

Characterization of the expression of transcriptionally silent loci during the plant response against *Pseudomonas syringae*

Directores:

Dra. Carmen R. Beuzón López

Dra. Araceli Castillo Garriga

Área de Genética

Departamento de Biología Celular, Genética y Fisiología.

Instituto de Hortofruticultura Subtropical y Mediterránea "La Mayora" (IHSM)

Universidad de Málaga

IHSM-UMA-CSIC

Málaga, 2014

Este trabajo ha sido financiado por el proyecto P07-CVI-2605 de "Junta de Andalucía" (co-financiado por FEDER) y por la Beca para la Formación de Personal Investigador, JAE-Pre-111 (2009-2013), concedida por Consejo Superior de Investigaciones Científicas, CSIC.

Área de Genética.
Departamento de Biología Celular, Genética y Fisiología.
Instituto de Hortofruticultura Subtropical y Mediterrénea (IHSM).
Universidad de Málaga-Consejo Superior de Investigaciones Científicas.

La Dra. Araceli Castillo Garriga, Profesor Contratado Doctor, y la Dra. Carmen R. Beuzón López, Profesor Titular, del Área de Genética del Departamento de Biología Celular, Genética y Fisiología

INFORMAN:

Que la tesis doctoral titulada "Characterization of the expression of transcriptionally silent loci during the plant response against *Pseudomonas syringae*.", presentada por Natasa Hulak en esta memoria para optar al título de Doctor por la Universidad de Málaga, ha sido realizada bajo su dirección y supervisión en el Área de Genética, y de que reúne los requisitos exigidos para su defensa pública.

Y para que así conste y tenga los efectos que correspondan en cumplimiento de la legislación vigente, extienden el presente informe.

En Málaga a 7 de noviembre de 2014

Araceli Castillo Garriga

Carmen R. Beuzón López

COMITÉ EVALUADOR

Presidente

Dr. Miguel Á. Botella Mesa

Departamento de Biología Molecular y Bioquímica,

Universidad de Málaga

Secretario

Dr. David Posé Padilla

Departamento de Biología Molecular y Bioquímica,

Universidad de Málaga

Vocal #1

Dr. Alberto P. Macho Escribano

The Sainsbury Laboratory, Reino Unido

Vocal #2

Dr. Rosa Lozano Durán

The Sainsbury Laboratory, Reino Unido

Vocal #3

Dr. Juan Antonio Díaz Pendón

Departamento de Interacción Planta-Patógeno,

IHSM-CSIC-UMA "La Mayora", Algarrobo Costa, Málaga

Suplente #1

Dr. Cayo J. Ramos Rodríguez

Departamento de Biología Celular, Genética y Fisiología

Universidad de Málaga

Suplente #2

Dr. M. Clara Pliego Prieto

IFAPA, Centro de Churriana, Málaga

For those I love

For Thiago

"*The only real mistake is the one from which we learn nothing.*"

— Henry Ford

Acknowledgments•Agradecimientos•Zahvalnica

It is very hard to go way back and think on the beginnings and not get sad because in a way it is a reminder that I also have to say goodbye and farewell. I will start from somewhat chronological way in which I met people from the department; hopefully I won't forget anyone like that. I would like to say that the unconditional help and kindness that I received from **Javi** and **Eduardo** regarding Spanish bureaucracy made me see how everything is possible. **Eduardo**, thank you for the opportunity to work in your group and in the department of genetics. My genuine thanks to my supervisors, **Carmen** and **Araceli** for guiding me in these 4 years and for taking the time to teach me, direct my thesis and help me not only professionally but personally as well. I have gained a new perception of life and work throughout our journey in the last 5 years together. Thank you for never giving up on me. Thank you **Edgar**, I appreciate a lot all the scientific and wisdom-solving-all-situation conversations that we shared. Thank you for all the needed motivation, help and support. I would like to thank all the professors from the department especially Ana Grande (for great dialysis advices and tricks, for all the kind words); Enrique (for his kindness); Cayo (for the most entertaining classes and stories during lunch); Miguel Angel and Victoriano (for all the advices and comments regarding my work on our seminars). I would like to express my gratitude to Antonio Heredia for all the scientific and cultural debates and concerts and José Campos for useful advices regarding qPCRs. Finally to all of my colleagues and by now dear friends that I have met and shared these last 6 years with. Tabata (*Morena mia*) thank you for being you, for giving me those hugs and kisses and contagious laughs, even when I did not deserve them, for the optimistic yet down-to-earth dreams and conversations. One big hug (*the ones you like*) for Ana (Chiqui) that went far but is still here close. I miss our conversations about everything by sipping vanilla tea. I owe so much to Migue, thank you for having the patience and the will to teach me in the lab. Manolo, for teaching me how to "defend" my Spanish (*for guiris*), thank you for the best transcendent conversations and all shared chapters of first and second season of "*Game of Thrones*" during lunch. Alberto, thank you for showing me how to work with *Arabidopsis,* I appreciate a lot your good will to help always, as well as, your unconditional guidance in my beginnings. Rosa, thank you for the advices, optimism and friendship; Adela, for being a good friend and a great "*boss*", for having the patience and for making me laugh; Jose, for being a loyal, good friend. For, being there when I needed you. Zaira (and family), thank you for the advices, help, conversations and for being my "*older sister figure*" in Spain.

Apreciare a Ana Luna por los "*cafelitos*" y las charlas; a Ainhoa por su eternamente optimistica manera de ver el mundo; a Clara por ser una calida amiga; Willie, Eli, Carlos, Nono, Spy, Inma Ortiz, Isa X, Isa A. (por transmitirme alegría), Pi (que me enseño como combinar colores), Eloy (*mi arma*), Isa P (por hacer todos los viajes que quiero hacer yo algún día), Candelas (y nuestros tríceps intrépidos y feroces), y a todos los nuevos becarios y alumnos internos; Pepe, Alvaro, Miguelito, Sito (AKA "*achichincles*"), Tamara, Carlos, Inma, Begoña, Blanca. Los "Bioquímicos"; Abel, Jessy, Eli, Delphine, Vitor, Sonia, José (el "*Chileno*"), Vero e Ian (Mòran taing mo cariad), David, Paqui y Alicia os doy las gracias por compartir conmigo el laboratorio y por ser parte de mis últimos 3 años en la Torre, por compartir sonrisas, seminarios y charlas. Lucia (la "*apaña*"), Mayte, Silvia, Ana G. y Pablo por ayudarme siempre sin vuestras consejos y recetas una andaría perdida. Por las conversaciones y consejos, os doy las gracias.

A mis "*Mamis Canguros*" por apoyarme siempre y ayudarme en las etapas mas emocionantes de mi vida. A Christian por machacarme por mí bien. A mi família política por ser mi família Española, por tratarme como una más os agradezco muchisimo por darme vuestro apoyo y ánimos y por todas las noches de "*mesa camilla-Divinity–ensalada Manhattan*".

Željela bih se zahvaliti svim dragim prijateljima koji su mi pružili ruku kada mi je to zbilja bilo najpotrebnije, možda su to za vas bili nebitni trenutci u vremenu, ali meni su to bili djelići života koji su vas smjestili na sam vrh moje "piramide". Nikola, hvala ti sto si mi bio prijatelj, prijateljica i laboratorijski partner. Sve te vježbe iz organske kemije koje smo prošli (i ništa nismo zapalili), sve te ispite koje smo zajedno položili, počevši od onog prvog iz biolgije stanica...zbilja čuvam u najljepšem sjećanju. Mislim da sam ti to već davno rekla, ali hvala ti što si uvijek bio tu, nadam se da sam ti barem djelićem uzvratila svu toplinu i prijateljstvo i stiskave zagrljaje koje si mi pružio. Hvala ti što si me nasmijavao i kada sam plakala.

Marina, ako netko želi imati veliku dozu dobrote, iskrenosti, dragosti, uzora za slijediti, ponekad jedinog glasa razuma, ljubavi i odanog prijatelja na kojeg uvijek može računati, onda treba imati tebe u životu. Hvala ti što si dio mog'! Zbilja sam ponosa što imam tako dobru prijateljicu još od srednje škole. Želim ti reći hvala za sve tvoje poruke optimizma koje čuvam i redovito "otpakiram" svako malo kada mi je potrebno "staviti" osmijeh na lice.

Nado, puno puta se vratim kući da "napunim baterije" i obožavam naše rituale čavrljanja tipa *"što se dogodilo u posljednjih godinu dana..."*. Osoba si koja me poznaje i koja je sa mnom prošla kroz sve "tinejdžerske egzibicije", koja me nasmije

do suza onako iskreno dok ne zaboli trbuh. Hvala ti što me nisi nikada zaboravila i još uvijek me smatraš prijeteljicom i u meni "vratiš" ono iskreno, autentično i dobro.

Mojoj Obitelji, volim vas sve! Uvijek me začudi koliko me život "nosi" daleko a ja se uvijek želim vratiti. Vi ste moja svjetlost, vrijednost i tolerancija. Predanost koju imam je ona koju ste mi vi usadili. Hvala vam što ste ponosni na mene i kada ja to nisam, hvala vam za vašu bezuvjetnu ljubav koja daje krila za savladati i one najveće prepreke na putu. Znajte da vas uvijek sve nosim sa sobom gdje god bila i kuda god otišla. Uvijek smo skupa i kada smo daleko! Nema niti jedne isplakane suze bez vaše podrške i snage da krenem dalje s još više entuzijazma kada pakleknem i kada mi je teško.

Thiago, moja ljubav, moja sreća, moje sunce, zvijezde i mjesec, moje sve. Hvala ti za toliko puno stvari koje si mi unio u život, što si mi pokazao koliko je sve ostalo nebitno. Kada se ti smiješ, kada mi ti kažeš da me voliš vrijeme stane i sve ponovno ima smisao i sve kockice se poslože na svoje mjesto. Ušao si u moj život, uzdrmao ga i promijenio na najbolji mogući način. Znaj da svi moji uspjesi idu uvijek za tebe, jer si ti ono što mi daje snagu i što me tjera dalje, više i bolje. Volim te, imaj to uvijek na umu jer ljubav je ono bitno i ono što vrijedi. Jako sam ponosna na tebe, osjećam se povlaštenom što te imam i što si onaj najbolji dio mene.

Juanjo, teško je pronaći prave riječi kojima bih mogla reći koliko sam ti ustvari zahvlana. Samo ti i ja znamo kroz sve što smo morali proći da stignemo do kraja i početka. Hvala ti što mi pomažeš u svemu i što dijeliš svaki komadić svog dana u mom društvu. Hvala ti na ljubavi, strpljenju, upornosti i odanosti. I hvala ti za još mnoštvo stvari i za tu našu "magiju" koja nas veže. ***You've been one of the best people I shared my life with.***

Index

Introduction

1. Pseudomonas syringae

Pseudomonas syringae is a rod shaped, Gram-negative, hemibiotrophic bacterium with polar flagella, which elicits a wide variety of symptoms in plants, including blights, leaf spots and galls (**Figure 1**).

The species is divided into pathogenic variants (pathovars) which vary in host range (Peñaloza-Vazquez et al., 2000). There are more than 50 different pathovars described, some of which are further divided into races based on host range among cultivars of the host species (González et al., 2000; Hirano and Upper, 2000). *Pseudomonas syringae* survives on the leaf surfaces of plants as an epiphyte before it enters into the intercellular space, through natural openings such as stomata or wounds, to initiate the infection process (Hirano and Upper, 2000). *P. syringae* pv. *tomato* (hereafter *Pto*) DC3000, the main model strain for studying *P. syringae* interaction with the host, is the causing agent of bacterial speck in tomato, and is also capable of causing disease in the model plant *Arabidopsis thaliana.*

Figure 1. Symptoms exhibited by *Arabidopsis* leaves infected with *Pseudomonas syringae* pv. *tomato* strain DC3000. Water-soaked areas of collapsed tissue are surrounded by chlorotic tissue 48 hours after initial infection.

The *Pto* DC3000 genome (6.5 megabases) contains a circular chromosome and two plasmids, which collectively encode 5,763 ORFs (Collmer et al., 2002). The genetic basis of pathogenicity and virulence in *P. syringae* is complex and includes global regulators (Hrabak and Willis, 1992; Kitten et al., 1998; Rich et al., 1994), the *hrp* cluster, which encodes a type III secretion system (T3SS), as well as virulence factors such as phytotoxins (*e.g.* coronatine) and exopolysaccharides (Bender et al., 1999; Yu et al., 1999). Once inside its host, *P. syringae* survives and proliferates within the intercellular spaces between plant cells, the apoplast, where through the action of the *Hrp* T3SS translocates a set of highly specialized proteins, called effectors, across the host cell wall into the neighbouring plant cells. Once

inside the host cytosol, the effector proteins work to suppress the plant immune system, allowing bacterial growth within the apoplast (Göhre and Robatzek, 2008). Mutant derivatives unable to translocate effectors, *i.e.* T3SS mutants, are severely restricted for growth within the host by the plant immune system and do not cause disease (Mohr et al., 2008).

1.1. The type III secretion system

The T3SS is a complex secretion apparatus composed of approximately 30 different proteins. This sophisticated apparatus couples secretion across the bacterial inner and outer membranes with translocation across eukaryotic cytoplasmic membranes, as well as across the cell wall in the case of T3SS from plant pathogenic bacteria (Nguyen et al., 2000). T3SS are essential for pathogenicity (Cunnac et al., 2009). The genes encoding type III secretion systems—especially those genes which encode the secretion apparatus—are clustered. In some organisms, these gene clusters are located on plasmids which are unique to the pathogen and are not found in non-pathogenic relatives (*Yersinia* spp., *Shigella flexneri*, and *Ralstonia solanacearum*) (Galán and Collmer, 1999). In other pathogens (*Salmonella typhimurium*, Enteropathogenic *E. coli* (EPEC), *Pseudomonas aeruginosa*, *P. syringae*, *Erwinia amylovora*, and *Xanthomonas campestris*) (Orth et al., 2000), the T3SS gene clusters are located on the chromosome and often appear to have been acquired by horizontal transfer, since related non-pathogenic bacteria lack these pathogenicity islands but share the corresponding adjacent sequences.

The function of the T3SS apparatus involves three different protein classes; (i) Structural proteins: build the base, the inner rod and the needle, (ii) Effector proteins: get secreted into the host cell and promote infection through suppressing host cell defences, (iii) Chaperones: bind effectors in the bacterial cytoplasm, protect them from aggregation and degradation and direct them towards the needle complex (Anderson et al., 2010). *P. syringae* strains also encode some helper proteins, type III-secreted proteins which assist effectors to translocate across the plant cell membrane, but do not enter themselves into the cytoplasm of the host cell, and harpins, proteins

secreted in a type III–dependent manner that remain outside the host cell where they can elicit host responses (Choi et al., 2013). Functional analysis of the *Pto* DC3000 genome showed several clusters of genes jointly encoding type III effectors (T3Es), 31 confirmed, and 19 predicted (Collmer et al., 2002). The *Pto* DC3000 T3Es, known as Hop (HR and pathogenicity outer protein) or Avr (avirulence) proteins based on the phenotype by which they were discovered (Collmer et al., 2002), have been comprehensively analyzed and 28 of them have been shown to be well-expressed and deployed during infection (Lindeberg et al., 2006). T3Es are collectively essential for pathogenicity, but individually dispensable for the bacteria to defeat defences, grow, and produce symptoms in plants. Eighteen of the *Pto* DC3000 effector genes are clustered in six genomic islands/islets (Collmer et al., 2009). Members of effector gene paralogous families are scattered around the genome and have an unusually low G+C content, indicating that such families may have been acquired by sequential horizontal acquisitions (Collmer et al., 2002).

2. The plant response against P. syringae

Plants react to pathogen attack using layered defence responses which mostly differ in the type of molecules from the pathogen that each one detects, and the speed and intensity of the resulting responses. The first layer of defence is activated upon pathogen detection through the action of pattern recognition receptors.

2.1. Pattern recognition receptors and pathogen-associated molecular patterns

Plants are capable of restricting colonization and growth of a very large number of microbial pathogens. This successful outcome is mostly due to the activation of receptors located on the plant cell surface called Pattern Recognition Receptors (PRRs). These receptors are proteins that recognize well-conserved microbe-specific molecules known as pathogen-associated molecular patterns (PAMPs, or microbe-associated molecular pattern or MAMPs, depending on the authors). *Arabidopsis* encodes numerous PRRs (47 identified to date). One of the best characterized PRR is FLS2, which perceives flagellin, the main component of the bacterial flagella (Boller and Felix, 2009). FLS2 is highly conserved among plants species (Zipfel et al., 2004) and is capable of alerting the plant of an incoming intruder, even before the bacteria penetrate into the leaf (Melotto et al., 2006). Many pathogen bacteria possess flagella, which is mostly formed by a polymer of flagellin. Even though the entire flagellin is considered to acts as a PAMP, only a conserved 22 amino acid segment from the N-terminus is required for recognition (Felix et al., 1999). This 22 amino acid peptide is commercially available and is known as flg22. Most mutations that allows flagellin to avoid recognition by FLS2 render non-motile bacteria (Naito et al., 2008).

Upon recognition of these conserved microbial features or PAMPs, the plant triggers an immune response, which involves activation of MAPK (mitogen-activated protein kinase) signalling and downstream signalling cascades that lead to the induction of defence genes (pathogen-response genes), production of reactive oxygen species in an oxidative burst, and callose deposition at the sites of infection to reinforce the cell walls, all of which contribute to restrict bacterial growth (Schwessinger and Zipfel, 2008). This process is known as PAMP-triggered immunity or PTI (**Figure 2**). PTI activation is a slow process and the intensity of the response builds up with time. This slow activation is befitting of an immune response that does not discriminate between pathogenic and non-pathogenic microorganisms and allows the plant to prevent colonization by most microbes. However, the slow initial kinetics of its activation can be exploited by adapted pathogens, which have evolved to

acquire additional functions that specifically target and suppress PTI, preventing the response from reaching enough intensity to effectively protect the plant.

2.2. Effector-mediated suppression of PAMP-triggered immunity

Effectors have evolved to contribute to the virulence capacity of the pathogen and to overcome the host. A mayor function of the T3SS in plant pathogenic bacteria is to suppress PTI in the host (**Figure 2**). PTI suppressing activity has been demonstrated for many T3 secreted effectors (T3Es), although the molecular mechanisms involved are their suppression is still to be determined for most of them.

In recent years, many reports have shown different ways in which pathogens are able to overcome the host basal defences. There are three main strategies by which pathogens overcome PTI: (a) suppressing the PTI activation through the action of effectors, (b) circumnavigating PTI activities through the production of toxin type effectors or (c) degrading bioactive products of PTI through sophisticated detoxification mechanisms (Anderson and Singh, 2011). There are several examples of pathogen effectors capable of suppressing specific aspects of the plant's defence. One of these examples in *Arabidopsis*, is the suppression of the activation of PTI following perception of flg22 by T3Es AvrPto, AvrPtoB and HopAI1. These *Pto* effectors have been shown to suppress PTI by blocking MAPK activation (De Torres et al., 2006; He et al., 2006; Zhang et al., 2007). In addition to suppression of host defences, some effectors may also assist the pathogen in evading detection by PRRs by suppressing signalling directly downstream of PRR (Boller and He, 2009).

Thus, adapted pathogens use effectors to effectively overcome the PTI and as a result the pathogen can proliferate and the plant undergoes a process known as effector-triggered susceptibility or ETS (**Figure 2**). ETS leads to the development of disease as an outcome from the pathogen interaction with the host. This is also known as a compatible interaction. However, during plant-pathogen co-evolution, plants have evolved resistance (R) genes that allows them to detect pathogen effectors (or the effect of the effectors on a plant

target) and activate stronger and faster defence responses. This recognition leads to the establishment of resistance against the pathogen and is known as effector-triggered immunity or ETI (Jones and Dangl, 2006).

2.3. Effector-triggered immunity and suppression of effector-triggered immunity

Invading microorganisms can also be detected through effector recognition. The effectors specifically recognized by 'matching' resistance proteins (R proteins) are termed avirulence *(*Avr*)* proteins. This type of recognition is often indirect, through the detection of the modifications generated through the activity of the effector on a host target. The model by which this indirect detection occurs is known as the *guard hypothesis* (Van Der Biezen and Jones, 1998). This hypothesis states that *R* proteins interact or *guard* a protein known as the *guardee* which is the target of an Avr protein. When it detects interference with the *guardee* protein, the R protein activates a strong resistance response against the pathogen known as ETI. R proteins are intracellular receptors of the NB-LRR (Nucleotide-Binding, Leucine-Rich Repeat-containing proteins) type.

During the activation of ETI, the host cells neighbouring the pathogen undergo a process of programme cell death known as the hypersensitive response or HR, resulting in senescence of the infected area and restricting growth and spread of the pathogen (Jones and Dangl, 2006). The HR is characterized by localized tissue necrosis and the production of phenolics and antimicrobial agents at the site of contact with the pathogen. This interaction is also known as an incompatible interaction, the pathogen is then considered to be avirulent, and the host resistant.

In contrast to PAMPs, effectors are pathogen-specific molecules and their recognition leads to a faster and more intense defence response, more efficient against adapted pathogens and presumable more difficult to suppress (Katagiri and Tsuda, 2010). ETI usually prevents further spread of the invading bacteria to more distant parts of the plant and is associated to the activation of systemic immunity known as systemic acquired resistance or SAR (Cameron et al., 1994). Thus, SAR protects distant parts of the plant

from further attack. However, some pathogens have also gained, through evolution, the ability to prevent activation of ETI, presumably suppressing ETI before is triggered, or targeting downstream signalling components to avoid gene expression and ETI derived activities. This step leads to proliferation of the pathogen and the development of disease and is also known as ETS (effector-triggered susceptibility) (**Figure 2**). Less is known about the mechanisms through which T3Es suppress ETI, some of which appear to be highly specific while others do so in a more general manner (Macho and Beuzón, 2010; Macho et al., 2010).

Yet, plants can also detect ETI-suppressing effectors through additional R proteins thus triggering ETI. Thus, an evolutionary arms race is establish with the plant-pathogen interaction going from ETS (pathogen success and defense development) to ETI (host-plant success and establishment of resistence) according to the suit of effectors and R-proteins available at each side of the interaction.

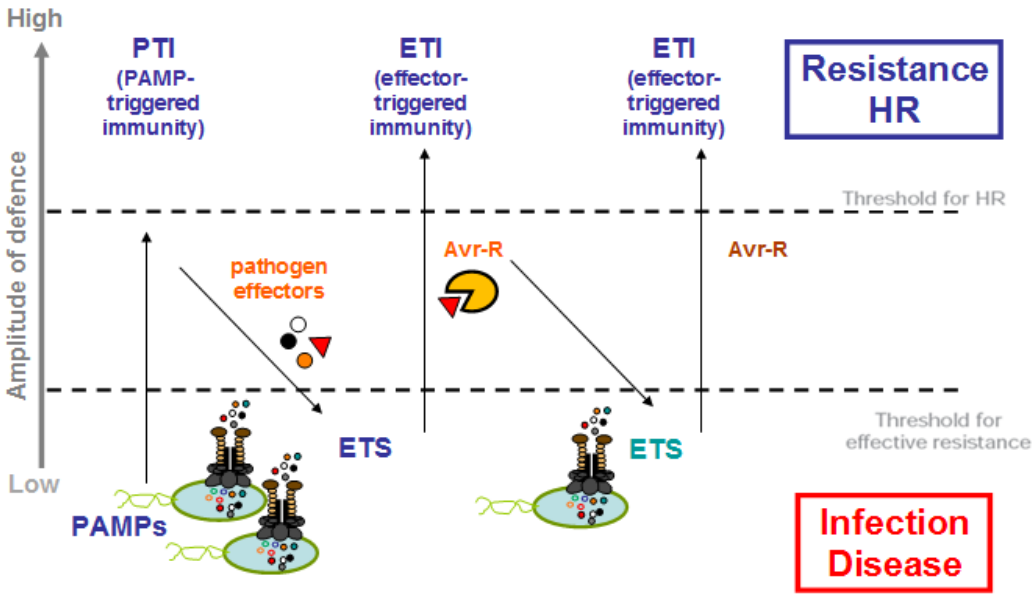

Figure 2. Modified version of zig-zag model proposed by Jones and Dangl (Jones and Dangl, 2006), which illustrates the outputs of the plants immune system.

2.4. The role of salicylic acid and coronatine during plant interaction with *Pto*

Plant defence against pathogens is influenced by systemic endogenous signalling mediated by plant hormones (Hayat et al., 2007). *Arabidopsis* has two main hormone-mediated responses involved in induced defence signalling pathways: the responses mediated by salicylic acid (SA), and those mediated by mehyl jasmonic acid (MeJA). These pathways suppress the growth of a wide range of microbial pathogens, including many different types of bacterial pathogens (Bostock, 2005; Glazebrook, 2005; Kunkel and Brooks, 2002).

Normally, SA signalling mediates resistance against biotrophic and hemibiotrophic pathogens such as *P. syringae*, whereas MeJA is commonly triggered in response to insect chewing, wounding, and necrotrophic pathogens (Ryan and Pearce, 1998). Accumulation of SA is triggered when plant receptors perceive PAMPs (Tsuda et al., 2008) and leads to activation of basal defence gene expression (Asai et al., 2002). Remarkably, *Pto* produces a phytotoxin called coronatine (COR) that functionally and structurally mimics MeJA and has the same effects as MeJA activating the MeJA response (Brooks et al., 2005). MeJA and SA signalling can be antagonistic (Kunkel and Brooks, 2002), thus activation of MeJA-induced signalling can, as a consequence, suppress the SA signalling pathway, necessary for effective basal defence against *P. syringae* (Delaney et al., 1995; Nawrath et al., 2002; Wildermuth et al., 2001). COR production is controlled by HrpL, which also regulates expression of the T3SS, and is implicated in suppressing closure of stomata associated to PTI (Melotto et al., 2008), and required to overcome SA-dependent defences (Brooks et al., 2005). Evidence of this is the resistant phenotype of the coronatine insensitive *Arabidopsis* mutant *coi1* (plants exhibit constitutive expression of SA-dependent defences) (Feys et al., 1994), which provides genetic evidence that the MeJA signalling pathway negatively regulates the expression of SA-dependent defences. Thus, *P. syringae* may utilize coronatine to activate the MeJA signalling pathway, thereby interfering with the induction of SA dependent signalling (Kloek et al., 2001). This could

inhibit or delay defences, thus giving the pathogen an opportunity to colonize host tissue (Reymond and Farmer, 1998).

3. Epigenetic mechanisms: DNA methylation in plants

Epigenetics in its classic definition, describes mitotically heritable modifications of DNA or chromatin that do not alter the primary nucleotide sequence (Bird, 2002; Jaenisch and Bird, 2003). Epigenetic modifications of DNA and histones, the core components of chromatin, consist of chemical additions to DNA and histones that are associated with changes in gene expression and are heritable, but do not alter the primary DNA sequence. The epigenetic modifications of chromatin constitute what is defined as "the epigenome" and represent an additional layer of information that influences the expression of the underlying genes (Law and Jacobsen, 2010). Epigenetic modifications of DNA and histones are crucial for development and differentiation of different cell types. In plants, DNA methylation is implicated in maintenance of chromatin structure and epigenetic states (Martienssen and Richards, 1995), control of plant development by enabling a single cell to grow into multiple organs or perform multiple functions (Finnegan et al., 1996; Kakutani et al., 1996; Ronemus et al., 1996), genomic imprinting, prevention of homologous recombination (Bender, 2004), transition into reproductive phase (Soppe et al., 2000) and silencing of foreign genes that have been incorporated into the host genome (Matzke et al., 2000).

In plants, DNA methylation commonly occurs at cytosine bases in all sequence contexts: the symmetric CG and CHG contexts (in which H = A, T or C) and the asymmetric CHH context. In *Arabidopsis*, genome-wide DNA methylation levels of approximately 24%, 6.7% and 1.7% are observed for CG, CHG and CHH contexts, respectively, and DNA methylation predominantly occurs on transposons and other repetitive DNA elements (Law and Jacobsen, 2010). DNA methyltransferases have been well characterized in *Arabidopsis*. *De novo* methylation is catalysed by DOMAINS REARRANGED METHYLTRANSFERASE 1 and 2 (DRM1 and DRM2) and maintained by three different pathways: CG methylation is maintained by DNA METHYLTRANSFERASE 1 (MET1); CHG methylation is maintained by

CHROMOMETHYLASE 3 (CMT3), a plant-specific DNA methyltransferase; and asymmetric CHH methylation is maintained through persistent *de novo* methylation by DRM1/DRM2 (Law and Jacobsen, 2010).

The establishment of DNA methylation in plants is controlled by a mechanism known as RNA-directed DNA methylation (RdDM) (Henderson and Jacobsen, 2007; Matzke et al., 2009). Throughout plant development, small RNAs target homologous genomic DNA sequences for cytosine methylation in all sequence contexts. In addition to the canonical RNA interference (RNAi) machinery (members of the Dicer and Argonaute families) and DRM2, RdDM requires two plant-specific RNA polymerases, Pol IV and Pol V, two putative chromatin-remodelling factors and several other recently identified proteins (Matzke and Mosher, 2014). In brief, the canonical view of RdDM involves the following steps (**Figure 3**). Transcripts from Pol IV are copied into long dsRNAs, processed by DICER-LIKE 3 (DCL3) into siRNAs (small interfering RNAs) and exported to the cytoplasm. Following loading of one strand of these siRNAs onto AGO4, they are re-imported to the nucleus, where the siRNA guides the targeting of nascent scaffold transcripts from Pol V by sequence complementarity. Ultimately, this targeting recruits DNA methyltransferase activity to mediate *de novo* methylation of cytosines in all classes of sequence contexts. Once established, global DNA methylation patterns must be stably maintained (genome will become hemimethylated after each cell division) to ensure that transposons remain in a silenced state and to preserve cell type identity.

RdDM seems to act preferentially at transposons located in euchromatic regions, like the retroelement *AtSN1* that is an endogenous model target of RdDM and is transcriptionally gene-silenced (TGS) (Haag et al., 2009; Wierzbicki et al., 2009). However, RdDM seems to be excluded to some extent from pericentromeric heterochromatin, which is enriched in larger transposons. Instead, the modifications at pericentromeric heterochromatin (mainly DNA methylation and methylation of histone H3 at K9, H3K9me) mostly occur in an siRNA-independent manner and rely on MET1, CMT3 and the chromatin remodeller DECREASED DNA METHYLATION 1 (DDM1) (Stroud et al., 2014; Zemach et al., 2013).

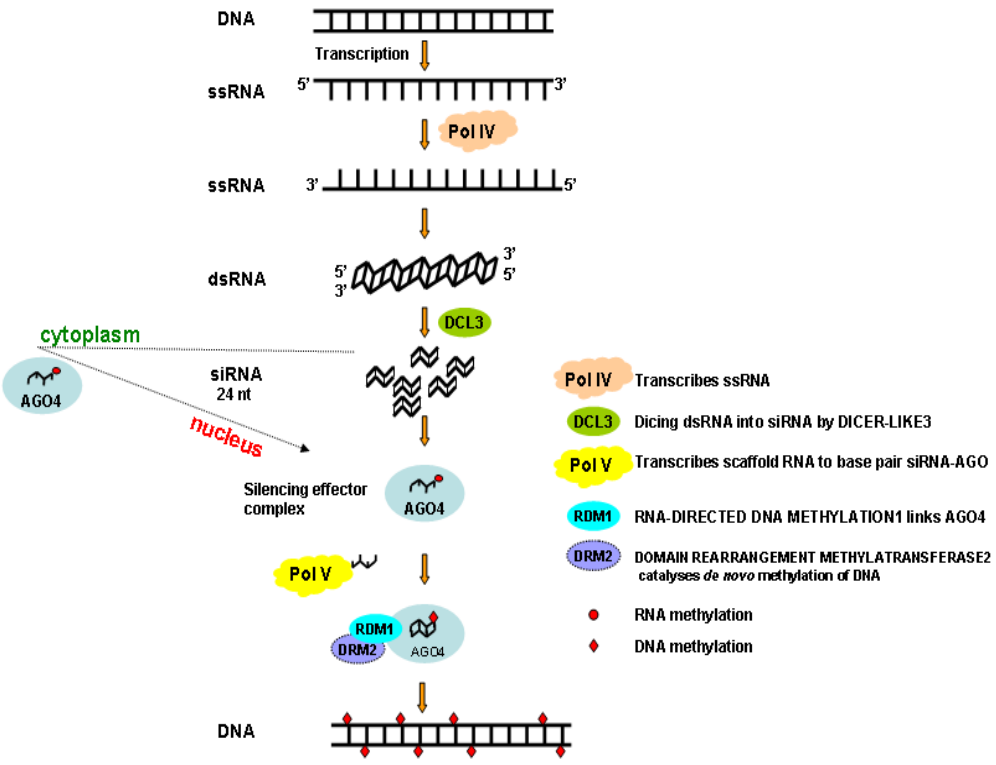

Figure 3. Simplified schematic representation of the *Arabidopsis* RdDM pathway in plant defence (Adapted from the Matzke and Mosher, Nature Reviews, 2014)(Matzke and Mosher, 2014).

Plants accomplish DNA demethylation by passive and active mechanisms. Passive demethylation is achieved by inhibition of maintenance activity for DNA methylation throughout replication (Law and Jacobsen, 2010) while active demethylation mechanisms are those that actively remove methyl groups from DNA. In plants, genetic and biochemical studies have revealed that the *Arabidopsis* DNA glycosylase domain-containing proteins ROS1 (REPRESSOR OF SILENCING 1), DME (DEMETER) and DEMETER-like proteins (DML2 and DML3) function as DNA demethylases, being ROS1 the best characterized (Furner and Matzke, 2011). ROS1 is involved in active demethylation through a base excision repair pathway and preferentially counteracts RdDM-induced methylation (Zhang and Zhu, 2012).

4. Role of DNA methylation and demethylation in response to pathogen attack

In the last few years works with mammalian pathogens have demonstrated that histone modifications and chromatin remodelling regulate gene expression and are thus key targets for mammalian pathogen manipulation during infection (Hamon and Cossart, 2008). One such obvious target is the host's immune system. In recent years, the epigenetic modulation of the host's transcriptional program linked to host defence genes has emerged as a relatively common event of pathogenic viral and bacterial infections (Gómez-Díaz et al., 2012; Paschos and Allday, 2010).

In plants, less is known about how pathogens alter the host epigenome and its consequences. It has been proposed that cytosine methylation is one of the major host defence mechanisms against plant DNA viruses, such as geminiviruses, and therefore these viruses have evolved different suppressor proteins to interfere with repressive methylation and transcriptional silencing of viral DNA (Raja et al., 2010). By interfering with the proper functioning of the plant methylation machinery, geminiviral proteins implicated in suppression of cytosine methylation can reverse transcriptional gene silencing (TGS) at transgenic and endogenous loci repressed by cytosine methylation (Raja et al., 2010; Rodríguez-Negrete et al., 2013; Zhang et al., 2011) confirming that plant pathogens modify the plant epigenome during infection.

Studies using phytopatogenic bacteria have brought increasing evidence that bacterial plant pathogens alter the host epigenome during their interaction with the plant and that plants have evolved specific defences against the TGS suppression orchestrated by pathogens.

Pavet and collaborators were the first to report that infection with *Pto* DC3000 induces rapid DNA hypomethylation at pericentromeric repeats, including repeats such as the 180-bp unit and *Athila* retrotransposon, and decondensation of chromocentres on *Arabidopsis* (Pavet et al., 2006). The authors showed that these responses occur 24 hours after the inoculation and that the DNA hypomethylation induced by *Pto* was not associated to DNA

replication, suggesting that it involves an active demethylation process (Pavet et al., 2006).

A second study that profiled the entire *Arabidopsis* DNA methylation status, revealed that many genomic regions enriched in transposon sequences become differentially methylated on infection by virulent and avirulent *Pto*, or following treatment with exogenous SA. Moreover, many of these changes in methylation affect expression of neighbouring protein-coding genes, including defence-related genes (Dowen et al., 2012). In addition, they demonstrated that bacterial growth of avirulent or non pathogenic *P. syringae* strains was restricted in mutants presenting genome-wide changes in DNA methylation, such as *met1-3* (null allele of the CG maintenance DNA methyltransferase, MET1) or *ddc* (triple mutant *drm1-2 drm2-2 cmt3-11*, affected on DRM1, DRM2 and CMT3 DNA methyltransferases) mutants, indicating that loss of DNA methylation enhances resistance to bacteria in an unspecific manner.

A third study revealed that treatment of *Arabidopsis* plants with the flagellin peptide flg22, causes a rapid and transient downregulation of key RdDM pathway components, including AGO4 and the RNA polymerase IV (Pol IV) subunit NUCLEAR RNA POLYMERASE D 1A (Yu et al., 2013). This downregulation occurred as early as 3 hours post-treatment and was sufficient to reactivate several well-characterized endogenous RdDM target loci such as the transposons *Onsen*, *EVADE* and *AtSN1,* as well as a transposon-based reporter transgene undergoing TGS. This effect was reversible, as DNA methylation and TGS were already restored to previous levels, 9 hours after flg22 treatment. This response induced by flg22 was facilitated by the DNA glycosylase ROS1, which is the main *de novo* demethylase in vegetative tissues. A mild enhanced bacterial growth was observed in *ros1*-infected plants, but not in the *DEMETER-like 2* (*dml2*) and *dml3*-infected loss-of-function mutants, supporting a role for *ROS1*-dependent DNA demethylation in antibacterial resistance (Yu et al., 2013).

Spontaneous HR and increased SA-mediated signalling observed in RdDM mutants are all indicative of the constitutive activation of R genes, suggesting that RdDM might negatively regulate the expression of at least some R genes. Yu and collaborators demonstrated that at least two R genes, *RESISTANCE*

METHYLATED GENE 1 (*RMG1*) in wild-type plants and *WRKY22* in flg22-treated plants, are subjected to extensive RdDM and were overexpressed in RdDM mutants (Yu et al., 2013).

These recent studies with phytopatogenic bacteria suggest that RNA-directed DNA methylation (RdDM) and transcriptional gene silencing (TGS) have an important role in plant disease (Pumplin and Voinnet, 2013). Dampening defence gene expression through RdDM could provide an effective mode of regulation since RdDM can be rapidly reversed by biotic and abiotic stresses. The rapid activation of plant defences would require the presence of RdDM-prone genomic segments (transposons and repeats) in the vicinity of defence-related genes and the involvement of active demethylation pathways to ensure optimal and rapid defence gene induction upon pathogen attack. In addition, the dampening of RdDM and the resulting defence gene activation occurs only transiently, to prevent the prolonged induction of these stress-responsive plant genes. This feature is foreseeably advantageous in the case of defence-related genes whose continuous expression reduces plant fitness.

Objectives

- To analyse changes in *Arabidopsis thaliana* DNA methylation levels during its interaction with *Pseudomonas syringae* and their implication on the activation of transcriptionally silenced loci (TGS loci).

- To determine the role of *P. syringae* virulence determinants in the activation of TGS loci in *Arabidopsis*.

- To analyse the transcriptional state of *Pto* DC3000-activated TGS loci in *Arabidopsis* during different defence responses.

- To investigate the role of genes involved in establishing and maintaining plant DNA methylation in the defence responses of *Arabidopsis* against *P. syringae*.

Material and methods

1. Bacterial strains and growth conditions

Bacterial strains used in this work are listed in **Table M1**. Bacteria were grown at 37ºC (*Escherichia coli*) or 28ºC (*Pto* DC3000 and its derivative strains) in Lennox Broth (LB), a modification of Luria-Bertani broth with the NaCl concentration halved (tryptone 20 g/L, yeast extract 10 g/L, NaCl 10 g/L, bacteriological agar 16 g/L) (Lennox, 1955) or SOB liquid medium (tryptone 20 g/L, yeast extract 5 g/L, NaCl 0.5 g/L, 10 ml/L of 250 mM of KCl, pH adjusted to 7.0 using 5 M NaOH) (Hanahan, 1983). King's B (KB) medium (King et al., 1954) (29 g/L of bactoproteose peptone, 1.5 g/L of K_2HPO_4, 8 ml/L of glycerol, pH adjusted to 5.7 with KOH) was used for motility assays. When needed, media were supplemented with antibiotics at the concentrations detailed in **Table M2**.

2. Motility test (swimming)

Strains were grown at 21ºC for 72 hours on LB plates. Bacterial lawns were re-suspended in 10 mM $MgCl_2$ to reach an OD_{600} of 2. Two µL of bacterial suspension were deposited at the centre of a soft agar plate containing KB medium supplemented with 2.5 g/L of agar. Five ml/L of sterile 1 M $MgSO_4$ was additionally added after autoclaving, to avoid the medium from becoming cloudy. The diameter of the bacterial growth halo was assessed after 2-3 days of incubation in darkness at 25ºC.

3. Plasmids and cloning procedures

Vectors used in this project were pGEM-T Vector System (Promega; Madison, WI, USA), pKD4 (Datsenko and Wanner, 2000) and pBluescript SK(+) ($pBSSK^+$) (Agilent Technologies, Inc. 2010).

To generate pGEMT -CMP (*CMP*, repetitive centromeric sequences, 180-bp repeats) and pGEMT -Athila, a PCR was performed using genomic DNA from *Arabidopsis* as a template, and the corresponding primers listed in **Table M3**. PCR for pGEMT -CMP was performed as follows: 94ºC for 3 min, followed by 30 cycles at 94ºC for 20 s, 60ºC for 30 s, and 72ºC for 30 s, and followed by 7 min at 72ºC. PCR for pGEMT -Athila was performed as follows: 94ºC for 3 min, followed by 33 cycles at 94ºC for 30 s, 58ºC for 50 s, and 72ºC for 1

min, and followed by 5 min at 72ºC. The PCR products were A/T cloned into pGEM-T, confirmed by restriction analysis, and sequenced using commercially available primers SP6 and T7 (**Table M3**). Gel and PCR purification was performed using FavorPrep™ GEL/PCR Purification Mini Kit (Favorgene Bioteck Corp., Taiwan). Routine analysis of transformant clones obtained was carried out using the DNA extraction method described by Holmes and Quigley (Holmes and Quigley, 1981), with certain modifications. Three mL of bacterial cultures grown at 37ºC in LB overnight were collected by centrifugation. The pellets were resuspended in 112 µL of STETL (sacarose 8 % (p/v), Triton X-100 0.5 % (p/v), Tris- HCl 50 mM, Lysozime 0.5 mg/ml), and incubated for 30 s in boiling water, followed by centrifugation at 5,000 *g* for 15 min. The resulting pellets were removed from the sample using a sterile toothpick, previously dipped into a RNAse solution (10 mg/ml). The remaining supernatants were mixed with 112 µL of isopropanol and gently mixed prior to centrifugation at 5,000 *g* for 15 min. The supernatants were then discarded and the pellets air dried and resuspended in 30 µL of sterile miliQ water. Restriction analysis were carried out using the appropriate restriction enzymes (Takara Bio Company, Madison, USA). DNA electrophoresis was carried out using the appropriate concentration of agarose (Gellyphor, Euroclone, Italy) supplemented with ethidium bromide (EtBr) (5 µg/ml) in TBE 1x (Tris-boric acid 45 mM, EDTA 1 mM, pH 8). Loading buffer used was prepared to a concentration 5x (0.125% bromophenol, 12.5% Ficoll 400). Markers used to determine the molecular weight were either bacteriophage lambda DNA digested with *Hin*dIII (New England Bio Labs), or 1Kb Plus Ladder (Invitrogen, USA).

To construct the vectors necessary for generating knockout mutants in *Pto* DC3000 we used a protocol previously described in the laboratory (Zumaquero et al., 2010). First, two regions of approximately 500 bp, unless otherwise indicated, flanking the ORF of the gene to be deleted, were amplified using PCR. A genomic DNA extraction of *Pto* DC3000 was used as template, and primers specially designed to include an *Eco*RI or *Bam*HI site fused to the T7 primer sequence, in such a manner as to provide homology and a cloning site between both flanking fragments (**Table M3**). Expand High

Fidelity polymerase (Roche, Germany) was used for each reaction containing 0.64 mM dNTPs, 1x Buffer 2, 5% DMSO, 0.4 µM of each of the corresponding primers (**Table M3**), 10 ng genomic DNA, and $_{dd}H_2O$ (Nalgene; Rochester, NY, USA). The first PCRs were carried out as follows: 94ºC for 3 min, followed by 20 cycles at 94ºC for 20 s, 55ºC for 30 s, and 72ºC for 50 s, and followed by 7 min at 72ºC. Five µl of each gel-purified PCR product was used for the second PCR consisting on 8 cycles of polymerization at 94ºC for 30 min, 52ºC for 1 min, and 72ºC for 1 min, finishing with 7 min at 72ºC, without primers or template. The product from this step was used as template in a reaction mix (5 µL per reaction) that also contained 0.64 mM dNTP mix, 1x Buffer 2, 5% DMSO, 0.4 µM of each of the forward primer for the 5' flanking region and the reverse primer for the 3' flanking region to amplify the entire fragment (**Table M3**), and commercial water (Nalgene). The mix was incubated at 94ºC for 3 min, followed by 20 cycles at 94ºC for 20 s, 53ºC for 30 s, and 72ºC for 1 min, finishing with 7 min at 72ºC. The resulting products, the deletion alleles, were A/T cloned into pGEM-T Vector System, and fully sequenced to discard mutations on flanking sequences. DNA plasmid extractions for sequencing were carried out using the Miniprep kit from Macherery-Nagel (Düren, Germany). Sequencing results were later analyzed using programs Chromas 1.45 and Seqman (DNA Star). After confirmation of the deletion alleles, the knockout vectors, carrying the *nptII* gene cloned into the deletion alleles were generated as follows. As appropriate, *Eco*RI, or *Ba*mHI fragments containing the *nptII* gene were obtained from pGEMT-*nptII*-*Eco*RI, or pGEMT-*nptII*-*Bam*HI (Zumaquero *et al.*, 2010), respectively, and ligated into the *Eco*RI, or *Ba*mHI, fragments of the corresponding pGEM-T derivatives carrying the deletion alleles. Ligation was performed using the Takara enzyme T4 DNA ligase (Takara Bio Company, Madison, USA). DH5α transformants were selected directly on LB plates supplemented with kanamycin, and confirmed by restriction analysis, rendering a collection of allelic exchange knockout vectors for *Pto* DC3000.

4. Generation of knockout mutants in Pseudomonas syringae pv. tomato

Allelic exchange knockout vectors were transformed by electroporation into *Pto* DC3000. We used a modified electroporation protocol, previously described for *P. aeruginosa* (Choi et al., 2005), and adapted to *P. syringae* by our laboratory (Zumaquero et al., 2010). Transformants were plated onto LB plates supplemented with kanamycin. Since pGEMT cannot replicate in *P. syringae* strains, kanamycin resistant clones must be originated through recombination between the plasmid and the bacterial chromosome. Single recombination events between the plasmid and the chromosome would result in plasmid integration and produce clones resistant to both kanamycin and ampicillin, whereas double recombination events will lead to allelic exchange and to clones resistant to kanamycin only. Thus, replica plates of the resulting colonies were carried out in LB plates supplemented with ampicillin (300 µg/ml). Since ampicillin selection is typically a problem in *P. syringae,* potential clones were further tested for growth in liquid LB medium with 100 µg/ml of ampicillin and 50 µg/ml of nitrofurantoin. Since *Pseudomonas* species are naturally resistant to nitrofurantoin (Gilardi, 1972), and this antibiotic has been shown to be effective against *E. coli* (Sandegren et al., 2008), we routinely use nitrofurantoin to eliminate any possible contamination from unwanted bacteria. Southern blot analysis, using *nptII*-FRT as a probe (a 1,495 bp fragment amplified with primers P1 and P2 from pKD4), was used to confirm that allelic exchange occurred at a single and correct position within the genome (see section 8 of Material and Methods).

5. Plant material, growth, and treatment conditions

Unless otherwise stated, wild-type *Arabidopsis thaliana* used in this thesis corresponds to the Columbia ecotype (Col-0). Mutants were obtained from the European Arabidopsis Stock Centre (NASC) or kindly provided by different groups (see below). The following seed stocks were used: *rpm1-1* ((Grant et al., 1995)/AT3G07040), *rps2* (SALK_087581/AT4G26090, AT4G26095), *rps4* (SAIL_519-B09/AT5G45250), *zar1-1* (SALK_013297/AT3G50950), *ago4-2* (Dr. Pablo Vera, (Agorio and Vera, 2007); AT2G27040), *met1-3* (Dr. César

Llave, AT5G49160), *ros1-4* (Dr. Teresa Roldan Arjona; AT2G36490), *ddc* (*drm1-2 drm2-2 cmt3-11*) (CS16384/AT5G15380 AT5G14620 AT1G69770), *AtGP1 LTR:GUS* (Dr. Lionel Navarro, (Yu et al., 2013)), *ddm1* (Dr. Oliver Voinnet/AT5G66750).

Seeds were surface-sterilized by vortexing for 10 min in a 30% household bleach solution with 0.05% Tween 20 detergent, and rinse 5-7 times with distilled sterile water. Seeds were sown on MS plates (4.33 g/L Murashige and Skoog basal medium (Sigma M5519), 20 g/L sucrose; pH was adjusted to 5.7 with 2N KOH), sealed with Micropore paper tape (to prevent desiccation while allowing slight aeration), and placed for stratification at 4°C for 3 days in darkness. Then, plates were placed into growth chambers at 21°C under 8 hours of light followed by 16 hours of darkness. Plants were transferred to soil after 2 weeks, covered with plastic foil for 1.5 week and watered with distilled water enriched with Hakaphos (once per week). They were kept in growth chambers for 3-4 weeks (5-6 weeks since germination) before performing infection experiments (section 6).

For SA treatment (Dowen et al., 2012) 4 week old plants grown in short-day conditions were sprayed with 1mM SA (Fisher Scientific, UK), containing 0,01% Silwet L-77, every day for 5 consecutive days. Tissue was collected on day 6 (*i.e.* 5 days of exposure). Control plants were grown in the same conditions as treated ones. Mock plants were treated with Silwet L-77 and collected on the 6th day. Naïve plants were collected prior to any treatment. Leaves were collected and immediately macerated in liquid nitrogen. RNA was extracted and cDNA synthesis performed using SuperScript II Reverse Transcriptase Kit (Invitrogen, CA, USA) (see section 10 of Material and Methods).

6. Bacterial inoculation procedure in plants

When analyzing bacterial replication in the plant or performing a competitive index (CI), *P. syringae* strains (**Table M1**) were grown on LB plates supplemented with the appropriate antibiotic for 48 h at 28ºC. When infecting *Arabidopsis* to assess the effect of *Pto* on the plant epigenome or on the expression of silent loci, bacterial strains were grown on the appropriate

LB/antibiotic plates for 72 h at 21ºC. In any case, bacterial lawns were re-suspended in 30 mL of 10 mM $MgCl_2$, OD_{600} was adjusted to 0.1 (equivalent to $5x10^7$ colony-forming units (cfu/ml), and serial dilutions carried out when necessary, to reach a final inoculation dose of $5x10^4$ cfu/ml unless otherwise stated. Three fully-grown leaves from 5-6 weeks old *Arabidopsis* plants were inoculated using 1 mL needless syringes. Three rosette leaves were used per biological replicate and a minimum of three biological replicates were performed on each experiment. For Southern blot analysis and RT-*q*PCR assays, inoculated leaves were collected at 0 hours post-inoculation (hpi) and 24 hpi, macerated in liquid nitrogen and kept at -80ºC. They were later processed and used for either DNA or RNA extraction.

For bacterial replication and Competitive Index analysis (CI, section 7 of Material and Methods), 3 disc leaves of 10 mm-diameter were collected at 0 hpi and 96 hpi and macerated in 1 mL of 10 mM $MgCl_2$. To determine the amount of bacteria, serial dilutions were plated onto LB plates supplemented with the appropriate antibiotic. The number of bacteria was counted from the plated dilution that displayed from 50-500 bacterial colonies per plate.

For visualization of Pto-induced disease symptoms (protection assay) in *Arabidopsis,* 3-4 weeks old plants were sprayed with a bacterial suspension containing $5x10^7$ cfu/ml in 10 mM $MgCl_2$ and 0.02% Silwet-L77. Plants were then covered with plastic foil for 24 hours to keep the humidity level, and symptoms were documented at 3, 7, 9 and 14 days post inoculation (dpi).

7. Mixed infection assay (Competitive Index, CI)

Competitive index (CI) assays are a established method for determining the attenuation of bacterial growth (Macho and Beuzón, 2010; Macho et al., 2007). Briefly, 5-6 weeks old plants (*Arabidopsis* Col-0 or its derivatives) were inoculated using a blunt syringe, with $5x10^4$ cfu/ml of a mixed bacterial suspension containing equal cfu from wild type and mutant or gene-expressing strains. In this work, all strains analysed by CI against wild type bacteria were resistant to kanamycin. Serial dilutions of the inoculum were plated onto LB agar plates supplemented with cycloheximide or with cycloheximide and kanamycin to confirm the relative cfu proportion between

co-inoculated strains. Cycloheximide was used as fungicide when growing *P. syringae* isolated from plant tissues. Four days post-inoculation (dpi), three 10 mm-diameter leaf discs were homogenized by mechanical disruption into 1 mL of 10 mM $MgCl_2$. Bacterial enumeration was performed by serial dilutions and plating of the samples onto agar plates with cycloheximide and cycloheximide plus kanamycin, to differentiate between the strains used in the mixed infections. The CI is defined as the mutant-to-wild type ratio within the output sample divided by the mutant-to-wild type ratio within the input (*inoculum*) (Freter et al., 1981; Taylor et al., 1987). CI assays are presented as mean values of three independent experiments (three replicates per experiment). Error bars represent standard error. To determine statistically significant growth attenuation each CI was analyzed as established by Student T-test and the null hypothesis: mean index is not significantly different from 1.0 (P value <0.05). When CI values for different strains, or CI values for the same strain in different plant genotypes were compared, we used One Way ANOVA and Bonferroni test for multiple comparison, or One Way ANOVA on Ranks and Tukey test for multiple comparison when Equal Variance Test failed (P<0.05).

8. Southern blot

Two different Southern blot protocols were used depending on the labelling procedure used, chemiluminiscence using digoxigenin or radioactivity using α-^{32}P.The first one was used to confirm the correct disruption of the locus in the effector-knockout mutant strains generated by allelic exchange, and the second procedure was used to analyze the DNA methylation pattern of *Arabidopsis* Col-0 genome.

8.1. Chemiluminescence (Digoxigenin)

Genomic DNA extraction of *Pto* was carried out using Jet Flex Extraction Kit (Genomed; Löhne, Germany). Two µg of genomic DNA was digested. The reactions were left overnight at the corresponding temperature in a volume of 50 µL. The restriction enzymes were selected by detailed analysis of the DNA sequence flanking the deletion sites, using the DNAStar suite (DNASTAR Inc., USA) or an online tool for restriction analysis, such as WatCut (WatCut: An on-line tool for restriction analysis, silent mutation scanning and SNP-RFLP analysis, http://watcut.uwaterloo.ca/template.php). Samples were run in a 0.8% agarose gel at 60 V for 4-5 hours, and stained with EtBr for visualization. Gels were treated with HCl 0.25 M during 15 min, washed 3 times with distilled water, then treated for 30 minutes with denaturing buffer (1.5 M NaCl, 0.5 M NaOH), and neutralized (3 M NaCl, 0.5 Tris, pH 7) for 30 min. DNA transfer was done by setting 15-20 kitchen paper towels, 3 Whatman papers, previously sunken into SSC 20x buffer (3 M NaCl, 0.3 M $C_6H_5Na_3O_7$ (sodium citrate), the agarose gel, a Nylon membrane (Sigma, 0.45 µm pore size), and 3 Whatman papers, previously sunken in SSC 20x buffer and 15-20 kitchen paper towels under a weight, and let the transfer take place overnight. The membrane was cross-linked using UV light at 1,200 J/m^2. Prehybridization of the membrane was done for 2 hours at 65ºC with the corresponding prehybridization buffer (SSC 5x, 1% of blocking reagent, 0.1 % N-lauryl sarcosine (p/v), 0.1% NaCl (p/v), 0.02% SDS (p/v)). Hybridization with the probe (previously denatured and diluted into prehybridization buffer), was performed at 65ºC, overnight. A fragment containing the *nptII* kanamycin resistance gene was used as a probe and labelled by PCR using the chemiluminescent digoxigenin-dNTPs DIG Labelling Mix (Roche; Mannheim, Germany), plasmid pKD4 (GenBank AY048743) as a template and primers P1 and P2 (**Table M3**). After incubation with the probe, the membrane was rinsed with SSC1x (0.30 M $NaC_6H_5O_7$, 0.030 M NaCl buffer), and incubated twice for 5 min at room temperature with 0.1% SDS. The membrane was then incubated three times with SSC 0.5% and 0.1% SDS for 10 min at 65ºC, and finally washed with Washing buffer (70 mM maleic acid, 150 mM NaCl, pH 7.5 and 0.3% Tween 20) for 5

min. The membrane was then incubated for 30 min with Buffer 2 (70 mM maleic acid, 150 mM NaCl, pH 7.5, 1% blocking reagent (w/v)), previously warmed up to 60ºC . The membrane was then incubated for 1h and 30 min in a solution containing the anti-digoxigenin antibody (dilution of 1:10,000 of DIG DNA Labelling Mix, 10x., Roche Diagnostics GMBH, Germany, in Buffer 2), at room temperature. The membrane was washed twice for 15 min at room temperature with Washing buffer and for 5 min with 20 mL of Buffer 3 (0.1 M Tris, 10 mM NaCl, 50 mM $MgCl_2$, pH 9.5). Finally, the membrane was incubated at 37°C for 15 min in CSPD, a substrate that belongs to the group of the dioxetane phenyl phosphates that upon dephosphorylation by alkaline phosphatase, forms an intermediate that when decomposed results in light emission which can be recorded on X-ray film (Roche, Mannheim, Germany).

8.2. Radioactivity (*radioisotope alpha* phosphate ^{32}P)

Arabidopsis genomic DNA was extracted using Jet Flex Extraction Kit (Genomed; Löhne, Germany). Three to five micrograms were digested with *Sau*3AI. *Sau*3AI is a type II endonuclease that cleaves GATC sequences. Its activity is inhibited by cytosine C5-methylation. The reaction was performed in a final volume of 200 µL for 2 h 30 min at 37ºC. The DNA was precipitated (NaOAc 3 M, pH 5.2, 1 µL glycogen) with 2 volumes of ice-cold 100% ethanol, incubated at -20ºC for 20 min, and centrifuged for 20 min at 5,000 *g*. The pellet was washed with 500 µL of ice-cold 70% ethanol, centrifuged for 5 more min at 5,000 *g* and dried for 5 min at 65ºC. The pellet was resuspended in 50 µL of miliQ water and left at 4ºC overnight. Samples were run in 1.2% agarose gels at 80 V for 5 h. The gel was treated for 10 min with 0.25M HCl, rinse 3 times with $_dH_20$, then denatured for 30 minutes (1.5 M NaCl, 0.5 M NaOH), rinsed 3 times with miliQ water, and neutralized (3 M NaCl, 0.5 Tris, pH 7) for 30 minutes followed with 3 rinses in $_dH_20$. The DNA in the gel was transferred onto a nylon membrane overnight as described above for digoxigenin labelling. After transfer, the membrane (Sigma, 0.45 µm pore size) was treated in a UV cross-linker at 1,200 J/m^2 and left at 70°C for 3 hours.

Probes (*CMP* or *Athila)* were denatured by 5 min incubation at 100°C and kept on ice. Fifty ng of the probe were mixed with 50 µCi of α-^{32}P using Amersham Ready-To-Go DNA Labelling Beads (-dCTP) (GE Healthcare, UK). The mix was incubated at 1 h at 37°C. Removal of unincorporated nucleotides, prior to hybridization was done by using a ProbeQuant™ G-50 Micro Column, (GE Healthcare, UK) with a sephadex resin. The columns were prepared as recommended by the manufacturers. The sample was purified and 13.5 µL of 2M NaOH added to stop the enzymatic reaction. The labelled probe was added to Church buffer (NaH_2PO_4 0.25 M, pH 7.2, EDTA 1 mM, SDS 7%) previously incubated at 65°C with the membrane, and left overnight at 65°C. After hybridization, the membranes were washed sequentially in 2 x SSC and 2% SDS at 65°C for 3 min and in 0.1 x SSC and 0.1% SDS at 65°C for 10 min twice. Then the membrane was placed into plastic foil and exposed to a Fujifilm BAS-MS3543 Imaging Plate and BAS 4043 IP Cassette, the signal was detected after 4 hours using a FUJIFILM Fluorescent Image Analyzer FLA-3000. The cassette enclosing the membrane and exposed film were kept at -80°C and the film later developed by placing it into a developing solution (Kodak D76 or Ilford ID11) for 10 seconds in agitation, placing into a stop bath (tap water) for 5 seconds, and finally fixed by incubation into a fixative solution (Kodak Rapid Fixor) for 10 seconds in agitation followed by a rinse in distilled water.

9. Plant genome methylation status by Chop-PCR

Arabidopsis leaves were infected with *Pto* DC3000 as indicated above (section 5) and tissue was collected 0, 3, 9, and 24 hpi. Macerated frozen tissue was used to extract RNA and quantify the accumulation of *AtSN1* transcripts (section 10 of Material and Methods) or to extract DNA and perform a chop-PCR analysis. For the latter, genomic DNA was extracted using Jet Flex Extraction Kit (Genomed; Löhne, Germany) and 250 ng of genomic DNA were digested ('chopped') with *McrBC* restriction enzyme (a DNA methylation-dependent enzyme) in 20 µL of final volume of the reaction mix, at 37°C for 4 hours. After the restriction reaction, the samples were diluted 1:2, and 4 µL of the digested DNA was used as template for *q*PCR in a 20 µL reaction mix.

Primers used for Chop-PCR (**Table M3**) helped us to monitor the positions 84459 to 84304 of BAC clone T15B3-Accession AL163975 (http://www.arabidopsis.org/), that correspond to *AtSN1* site. Primers designed for locus *At3g18780* were used as the normalizing control (loci described to be non-methylated (Widman et al., 2009). Error bars represent standard error. Statistics was applied as established by One-way ANOVA (Bonferroni's pos-hoc test).

10. RNA extraction, qRT-PCR and semi-quantitative RT-PCRs

Leaves from 5-6 week old *Arabidopsis* plants, were infected with *Pto* DC3000 as indicated above (section 5). Tissue was collected, macerated in liquid nitrogen and kept at -80ºC. Three rosette leaves were used per biological replicate and a minimum of three biological replicates were performed on each experiment. Following the manufacturer's manual for extraction of RNA with TRIzol® (Invitrogen, Carlsbad, USA), 100 mg of tissue was used and homogenized into 1 mL of TRIzol, and centrifuged at 14,000 *g* for 10 min at 4ºC. Supernatant was then recovered and mixed with 200 µL of chloroform by vortexing. Samples were centrifuged at 14,000 *g* for 15 min at 4ºC and the upper soluble fraction was recovered. An extra 300 µL of chloroform was added to the fraction and the procedure repeated (an extra step to purify the sample from TRIzol). The 500 µL fraction recovered was added to 500 µL of 2-propanol and centrifuged at 14,000 *g* for 15 min at 4ºC. The pellet was washed with 1 mL of 75% ethanol, carefully dried and resuspended in 30 µL of RNAse-free commercial water (Qiagen, Hilden, Germany). Any DNA contaminants were eliminated after digestion with RNAse-free DNAse (Takara, Otsu, Japan). Two µg of total RNA were treated with the enzyme in a final volume of 20 µL. The reaction was incubated at 37ºC for 45 min and the enzyme inactivated by incubating at 80ºC for 15 min. A control PCR using Actin primers (**Table M3**) was carried out using the RNA extraction as a template to confirm the absence of DNA prior to cDNA synthesis. For the first-strand cDNA synthesis we used the instructions provided by the manufacturer for SuperScript II reverse transcriptase reagent (Invitrogen, Carlsbad, USA). The first mix contained (dNTPs, dT^{17}:Random primers in 1:1

amount) and 1 µg of RNA with miliQ water up to 17.5 µL. The reaction was placed in the thermocycler (65ºC-3 min, 4ºC-3 min) then the second mix was added (buffers DDT, ES and enzyme SSII and RRI (Takara, Otsu, Japan) and the synthesis continued (42ºC-90 min, 70ºC-15 min, 4ºC-stop).

For RT-*q*PCR, the reaction mixture consisted of cDNA first-strand template, primer mix, forward and reverse (10 µmol each) and SsoFast EvaGreen® Supermix, (BIO-RAD) in a total volume of 20 µL. The PCR conditions were as follows: 30 s at 95ºC, 35 cycles (for actin), 45 cycles (for *AtSN1*) of 10 s at 95ºC and 15 s at 60ºC. The reactions were performed using a MyiQ real time cycler (Bio-Rad, USA.). The data was analyzed using the BIO-RAD software. A relative quantification RT-*q*PCR method was used to compare gene expression *versus* control samples (using ΔΔCt). Actin signal was used to normalize samples. Each data point is a mean value from 2-3 independent experiments (3-6 biological replicate per experiment). Error bars represent standard error. Statistics was applied as established by One-way ANOVA, (Bonferroni's pos-hoc test) and/or Student's t-test.

All semi-quantitative RT-PCRs were performed by using *Taq* DNA Polymerase (Thermo Scientific, USA) with the appropriate primers (**Table M3**), and containing 0.64 mM, dNTP mix, 1x Buffer MIX with $MgCl_2$, 0.5 µM corresponding primers, 10 ng cDNA, and commercial water (Nalgene; Rochester, NY, USA) per reaction. The programme used was: 94ºC for 3 min, followed by 22- 24 cycles (Actin), 30- 33 cycles (*AtSN1*), 19- 20 cycles (PR1), 25- 28 cycles (*At1g13470*), 25-27 cycles (PHI-1), 33-35 cycles (Ulp-*like*) and 36-37 cycles (CACTA) at 94ºC for 30 s, 58ºC for 45 s, and 72ºC for 50 s, and followed by 5 min at 72ºC. PCR products were analyses by electrophoresis into a 1.5% agarose gel with EtBr.

Primers for RT-*q*PCR were designed using Primer 3 software (http://frodo.wi.mit.edu/primer3/); and can be found in **Table M3**. Designed primers generate an amplicon of 100-300 bp.

11. Histochemical staining of GUS activity

GUS staining was performed according to the protocol previously described by (Ranjan et al., 2012) with minor modifications. Plant tissues were

immersed in histochemical GUS staining buffer (100 mM $NaPO_4$ pH 7, 0.5 mM $K_3[Fe(CN)_6]$, 0.5 mM $K_4[Fe(CN)_6]$, 20% Methanol, 0.3% Triton X-100 and 0.1% mg mL 5-bromo-4-chloro-3-indolyl-b-D-glucuronide (X-gluc) (Duchefa Biochemie, Nederlands) on plates (Corning Synthemax-R surface multiwell plates, SIGMA-ALDRICH), vacuum-infiltrated (75 cm Hg) for 10 min three times, and then wrapped in aluminium foil and incubated at 37°C for 12 h. Samples were then washed several times with 95% ethanol until complete tissue clarification. Then stored in 50% glycerol and photographed.

Table M1. Bacterial strains used in this thesis[a].

Strain	***Description***	***Source of reference***	***Antibiotic resistance***
DH5α	F-*endA1 hsdR17 supE44 thi-1 recA1 gyrA96 relA1* Δ*lacU189 f80* Δ-*lacZDM15*	(Hanahan, 1983)	
DH5α	pGEMT-Athila, Amp^R	This work	Amp^R
DH5α	pGEMT-CMP (180 bp repeats)	This work	Amp^R
DH5α	pGEMT-KmFRT-*Eco*RI (pGEMT derivative containing Km resistance gene flanked by FRT and *Eco*RI sites	Dr. Zumaquero A and Dr. Beuzón C.R. unpublished results)	Amp^RKm^R
DH5α	pGEMT-KmFRT-*Bam*HI (pGEMT derivative containing Km resistance gene flanked by FRT and *Bam*HI sites	Dr. Zumaquero A and Dr. Beuzón C.R. unpublished results)	Amp^RKm^R
DH5α	pGEMT derivative containing the Δ*hopO1-2::*KmFRT knockout allele	This work	Amp^RKm^R
DH5α	pGEMT derivative containing the Δ*hopX1::*KmFRT knockout allele	This work	Amp^RKm^R
DH5α	pGEMT derivative containing the Δ*hopA1::*KmFRT knockout allele	This work	Amp^RKm^R
DH5α	pGEMT derivative containing the Δ*hopAA1-2::*KmFRT knockout allele	This work	Amp^RKm^R
DH5α	pGEMT derivative containing the Δ*hopD1::*KmFRT knockout allele	This work	Amp^RKm^R
DH5α	pGEMT derivative containing the Δ*hopV1::*KmFRT knockout allele	This work	Amp^RKm^R
DH5α	pGEMT derivative containing the Δ*hopR1::*KmFRT knockout allele	This work	Amp^RKm^R
DH5α	pGEMT derivative containing the Δ*avrPto1::*KmFRT knockout allele	This work	Amp^RKm^R
DH5α	pGEMT derivative containing the Δ*hopB1::*KmFRT knockout allele	This work	Amp^RKm^R
DH5α	pGEMT derivative containing the Δ*hopAM1-2::*KmFRT knockout allele	This work	Amp^RKm^R
DH5α	pGEMT derivative containing the Δ*hopT1-2::*KmFRT knockout allele	This work	Amp^RKm^R
DH5α	pGEMT derivative containing the Δ*hrpL::*KmFRT knockout allele	This work	Amp^RKm^R
1448a	*Pseudomonas syringae pv. phaseolicola* (*Pph*), wild type strain, Race6	(Taylor et al., 1996)	
DC3000	*P. syringae pv. Tomato (Pto),* wild type strain	(Cuppels, 1986)	Rif^R
DC3000 Δ*hrcV*	DC3000 derivative, Δ*hrcV* ::Tn*3*Gus7	(Ronald et al., 1992), (Mudgett and Staskawicz,	Km^R

Strain	*Description*	*Source of reference*	*Antibiotic resistance*
		1999)	
DC3000 Δ*hop01-2*	DC3000 derivative, Δ*hop01-2* (knockout mutant)	This work	Km^R
DC3000 Δ*hopX1*	DC3000 derivative, Δ*hopX1* (knockout mutant)	This work	Km^R
DC3000 Δ*hopA1*	DC3000 derivative, Δ*hopA1* (knockout mutant)	This work	Km^R
DC3000 Δ*hopAA1-2*	DC3000 derivative, Δ*hopAA1-2* (knockout mutant)	This work	Km^R
DC3000 Δ*hopD1*	DC3000 derivative, Δ*hopD1* (knockout mutant)	This work	Km^R
DC3000 Δ*hopV1*	DC3000 derivative, Δ*hopV1* (knockout mutant)	This work	Km^R
DC3000 Δ*hopR1*	DC3000 derivative, Δ*hopR1* (knockout mutant)	This work	Km^R
DC3000 Δ*avrPto1*	DC3000 derivative, Δ *avrPto1* (knockout mutant)	This work	Km^R
DC3000 Δ*hopB1*	DC3000 derivative, Δ*hopB1* (knockout mutant)	This work	Km^R
DC3000 Δ*hopAM1-2*	DC3000 derivative, Δ*hopAM1-2* (knockout mutant)	This work	Km^R
DC3000 Δ*hopT1-2*	DC3000 derivative, Δ*hopT1-2* (knockout mutant)	This work	Km^R
DC3000 Δ*hrpL*	DC3000 derivative, Δ*hrpL* (knockout mutant)	This work	Km^R
DC3000 COR⁻	DC3000-DB29 *cmaA*::Tn5 *uidA* Sm/Spr; *cfa6*::Tn5 *uidA* Km^r (CFA^- CMA^- COR^-)	(Brooks et al., 2004)	Km^R
DC3000 Δ *fliC*	DC3000 derivative, Δ*fliC*	(Kvitko et al., 2009)	
DC3000 Δ28E CUCPB5500	DC3000 derivative, Δ28E (Δcluster I,II,III,IV,V,VI,VII,VIII, IX,pDC3000A, pDC3000B)[b] *ΔhopU1-hopF2 ΔhopC1-hopH1*::FRT *ΔhopD1- hopR1*::FRT *ΔavrE-shcN ΔhopAA1-2-hopG1*::FRT $pDC3000A^-$ $pDC3000B^-$	(Kvitko et al., 2009)	

Strain	***Description***	***Source of reference***	***Antibiotic resistance***
DC3000 CUCPB5459	(Δcluster I,II,IV, IX,pDC3000A, pDC3000B)[b] Δ*hopU1-hopF2* Δ*hopC1-hopH1*::FRT Δ*hopD1-hopR1*::FRT Δ*hopAA1-2-hopG1*::FRT pDC3000A2B2	(Kvitko et al., 2009)	
DC3000 CUCPB5451	(Δcluster II,IV, IX)[b] Δ*hopC1-hopH1*::FRT Δ*hopD1-hopR1*::FRT Δ*hopAA1-2-hopG1*::FRT	(Wei et al., 2007)	
DC3000 *hopZ1a*	pAME30 pAMEx *nptII::hopZ1a*	(Macho et al., 2010)	Amp^R, Km^R
DC3000 *avrRpm1*	pAME31 pAMEX-*nptII::avrRpm1*	(Macho et al., 2010)	Amp^R, Km^R
DC3000 *avrRps4*	pAME32 pAMEX-*nptII::avrRps4*	(Macho et al., 2010)	Amp^R, Km^R
DC3000 avrRpt2	pAME8 pAME4-*nptII:: avrRpt2*	(Macho et al., 2010)	Amp^R, Km^R

[a] Rif^R, Spc^R, and Km^R indicate resistance to rifampicin, spectinomycin and kanamycin.

Table M2. Antibiotics used in this study.

Antibiotic	*E. coli*	*P. syringae*
Ampicillin	100 µg/ml	300 µg/ml
Kanamycin	50 µg/ml	15 µg/ml (liquid medium), 25 µg/ml (solid medium)
Rifampicin	n.a.	15 µg/ml
Nitrofurantoin	n.a.	30 µg/ml
Cycloheximide*	n.a.	2 µg/ml

*Cycloheximide was used as fungicide when growing *P. syringae* isolated from plant tissues. n. a. (not applicable).

Table M3. Oligonucleotides used in this thesis.

Name	*Sequence 5' - 3'*	*Observation*	*Restriction site*
PCR amplification, Southern blot probe		**Reference**	
180bp 1[a]	gatc**m**agtcatattcgactcc	This work	
180bp 2[b]	gatctcatgtgtatgattgag	This work	
180bp 3[a]	gattgatcaagtcatattcgactcc	This work, *nested PCR*	
180bp 4[b]	gacttgatctcatgtgtatgattgag	This work, *nested PCR*	
Athila[a]	ttcttctccaactccagg	(Pavet et al., 2006)	
Athila[b]	tacccttttgttggagccg	(Pavet et al., 2006)	
Allelic exchange		**Localization**	
hopO1-2-A	ccctatagtgagtcgaattcatgatcaaaacagtcagcg	chromosome	*EcoRI*
hopO1-2-B	gaattcgactcactatagggcagcgtctcttatagtcc	chromosome	*EcoRI*
hopO1-2-2	cttgccaatctgttcacg	chromosome	*EcoRI*
hopO1-2-3	gagtttcccttggtcacc	chromosome	*EcoRI*
hopX1-A	ccctatagtgagtcgaattccgttaagaataagcgccc	plasmid	*EcoRI*
hopX1-B	gaattcgactcactatagggcatgctagctatgtcgtc	plasmid	*EcoRI*
hopX1-2	tgatcctccacacacgtc	plasmid	*EcoRI*
hopX1-3	tattcccaaggtctgccg	plasmid	*EcoRI*
hopA1-A	ccctatagtgagtcgaattcatcgagagtcttaaggcg	chromosome	*EcoRI*
hopA1-B	gaattcgactcactatagggaagtgcagcgattctgag	chromosome	*EcoRI*
hopA1-2	acccgcaaatcaaaaccc	chromosome	*EcoRI*
hopA1-3	ctgtctcttctggtcagc	chromosome	*EcoRI*
hopAA1-2-A	ccctatagtgagtcgaattcattccctctcgttctacg	chromosome	*BamHI*
hopAA1-2-B	gaattcgactcactatagggaagtgcagcgattctgag	chromosome	*BamHI*
hopAA1-2-2	acccgcaaatcaaaaccc	chromosome	*BamHI*
hopAA1-2-3	ctgtctcttctggtcagc	chromosome	*BamHI*
hopD1-A	ccctatagtgagtcgaattctcccggatgaagtaatcg	chromosome	*EcoRI*
hopD1-B	gaattcgactcactataggggatctactggacttcacg	chromosome	*EcoRI*
hopD1-2	gcctttgtattctgtggc	chromosome	*EcoRI*
hopD1-3	atagtgacaaaggaggcg	chromosome	*EcoRI*
hopV1-A	ccctatagtgagtcggatccggtctgaagtaggcatcg	chromosome	*BamHI*

Name	***Sequence 5′ - 3′***	***Observation***	***Restriction site***
hopV1-B	ggatccgactcactatagggggcattatctacacgag	chromosome	*BamHI*
hopV1-2	ttccatcgctgcactacc	chromosome	*BamHI*
hopV1-3	tacgcatcgctatgaagc	chromosome	*BamHI*
hopR1-A	ccctatagtgagtcgaattctattacccacgaagcacc	chromosome	*EcoRI*
hopR1-B	gaattcgactcactatagggtattgcgcttctccctgg	chromosome	*EcoRI*
hopR1-2	taagttctgctgacacgg	chromosome	*EcoRI*
hopR1-3	tgacagcagccttgtcag	chromosome	*EcoRI*
avrPto1-A	ccctatagtgagtcgaattctgtggcgtcataatgtcg	chromosome	*EcoRI*
avrPto1-B	gaattcgactcactatagggcacttgagtggtcatagg	chromosome	*EcoRI*
avrPto1-2	ttgcccttatcgaaccac	chromosome	*EcoRI*
avrPto1-3	cgacgcaataaagcgcag	chromosome	*EcoRI*
hopB1-A	ccctatagtgagtcgaattcattgaatctccgcgtacg	chromosome	*EcoRI*
hopB1-B	gaattcgactcactataggggaggttaaggaaggtctg	chromosome	*EcoRI*
hopB1-2	ttgggtacgctgcaagac	chromosome	*EcoRI*
hopB1-3	gatcccgaaatgcatcag	chromosome	*EcoRI*
hopAM1-2-A	ccctatagtgagtcgaattcactcaaatcagagtgccc	plasmid	*EcoRI*
hopAM1-2-B	gaattcgactcactatagggcaacttagctcttcgtgg	plasmid	*EcoRI*
hopAM1-2-2	acgcgttatcgacgactc	plasmid	*EcoRI*
hopAM1-2-3	cagatatccatcagcagc	plasmid	*EcoRI*
hopT1-2-A	ccctatagtgagtcgaattcccctcttattatcagaggc	chromosome	*EcoRI*
hopT1-2-B	gaattcgactcactataggggatcatatgagtcactcg	chromosome	*EcoRI*
hopT1-2-2	atgggcgtatctgacagg	chromosome	*EcoRI*
hopT1-2-3	tcatctctatacgagctc	chromosome	*EcoRI*
hrpL-A	ccctatagtgagtcgaattctgtacaagccctatagcg	chromosome	*EcoRI*
hrpL-B	gaattcgactcactatagggcaacttgcaccttcaacc	chromosome	*EcoRI*
hrpL-2	tgcaacaccacatgagcc	chromosome	*EcoRI*
hrpL-3	tgcaatcgggcgattgag	chromosome	*EcoRI*
P1-*EcoRI*	tcagaattcgtgtaggctggagctgcttc	primer	*EcoRI*
P2-*EcoRI*	tcagaattccatatgaatatcctccttag	primer	*EcoRI*
P1-BamHI	tcaggatccgtgtaggctggagctgcttc	primer	*BamHI*
P2-BamHI	tcaggatcccatatgaatatcctccttag	primer	*BamHI*
SP6	gatttaggtgacactatag	Promega, USA, Cat.# Q5011	
T7	gtaatacgactcactatagg	Promega, USA, Cat.# Q5021	
Semi quantitative PCR		**Reference**	
Actin[a]	actaaaacgcaaaacgaaagcggtt	(Bertrand et al., 2003)	
Actin[b]	ctaagctctcaagatcaaaggctta	(Bertrand et al., 2003)	
Athila[a]	cggcgtcactacttcaccacctgt	(Pavet et al., 2006)	
Athila[b]	ccccttcttgaattacgctgtcct	(Pavet et al., 2006)	
AtSN1[a]	gaatatctggaagttcaggcccaaaggccttac	(Buchmann et al., 2009)	
AtSN1[b]	accaacgtgttgttggcccagtggtaaatctc	(Buchmann et al., 2009)	
PR1[a]	tcagtgagactcggatgtg	Dr. Alberto Macho	
PR1[b]	cctgcatatgatgctcctt	Dr. Alberto Macho	
At1g13470[a]	gcgaaagaggaagacagagtcc	(Dowen et al., 2012)	
At1g13470[b]	ccgttaggagcaacagaagtg	(Dowen et al., 2012)	

Name	***Sequence 5′ - 3′***	***Observation***
Ulp-like[a]	tggatgtctctccatttagca	(Zhang et al., 2006)
Ulp-like[b]	caaggtttgaatggctggta	(Zhang et al., 2006)
CACTA[a]	tcgcaggagtggaggagttcttgacat	(Rodríguez-Negrete et al., 2013)
CACTA[b]	taatctggcataaatccttgactaaaca	(Rodríguez-Negrete et al., 2013)
PH-1[a]	actagtggcaccaaacaacg	(Zhang et al., 2006)
PH-1[b]	actccagtacaagccgatcc	(Zhang et al., 2006)
***q*RT-PCR**		**Reference**
Actin[a]	actaaaacgcaaaacgaaagcggtt	(Bertrand et al., 2003)
Actin[b]	ctaagctctcaagatcaaaggctta	(Bertrand et al., 2003)
Athila[a]	tgcatacacggtcacaaggaaatc	This work
Athila[b]	gctggttgtggttgtgagggaagt	This work
AtSN1[a]	tggtggttgtacaagcctagttt	This work
AtSN1[b]	attcgagacacgttgggaag	This work
Chop-PCR		**Reference**
At3g18780[a]	gccatcccaagctgttctctc	(Widman et al., 2009)
At3g18780[b]	ccctcgtagattggcacagt	(Widman et al., 2009)
AtSN1[a]	caaaggccttacatctcccagagg	(Rodríguez-Negrete et al., 2013)
AtSN1[b]	gtgttgttggcccagtggtaaatct	(Rodríguez-Negrete et al., 2013)
Genotyping		**Reference**
fliC[a]	accttcctgccgcgcaaaga	(Kvitko et al., 2009)
fliC[b]	cgagttgatcttgtcgcgcact	(Kvitko et al., 2009)

[a] indicate forward.

[b] indicate reverse.

Chapter 1

Pseudomonas syringae pathovar *tomato* induces changes on *Arabidopsis* DNA methylation pattern and up-regulates transcriptionally silent loci

1.1. Arabidopsis thaliana infections with Pto DC3000

It has been previously described by Pavet and collaborators (2006), that *Arabidopsis* shows centromeric DNA hypomethylation and cytological alterations of heterochromatic regions upon attack by *Pto* DC3000. In this chapter, we will evaluate the reproducibility of the results published by Pavet and collaborators (2006) and determine if the DNA hypomethylation induced by *Pto* DC3000 at *Arabidopsis* transcriptionally silent loci (Athila, centromeric DNA etc.) also leads to their transcriptional activation

To perform *Arabidopsis* infections, Pavet *et al.* (2006) obtained the *Pto* DC3000 inoculum by growing the bacteria in liquid rich medium (King´s B). In our laboratory, *Pto* DC3000 cultures used for infections, are obtained from direct plate-grown harvested inoculum (LB) to avoid potential contaminations that can occur in liquid rich medium. In order to compare both inoculum-growing methods, we infected *Arabidopsis* plants with *Pto* DC3000 grown by either strategy and monitored bacterial replication. Three leaves from *Arabidopsis* Col-0 were infiltrated with a moderate titre ($5x10^4$ cfu/ml) of *Pto* DC3000 grown on rich media, either liquid or solid, and resuspended on 10 mM $MgCl_2$. Three disc leaves (one per leave) were collected and macerated at day 0 (just after the inoculation) and 4 days post-inoculation (dpi) and used to determine bacterial growth within the plant (**Figure 1.1**). The results suggest that the inoculum growing method prior to plant inoculation has no significant impact on bacterial replication within plant.

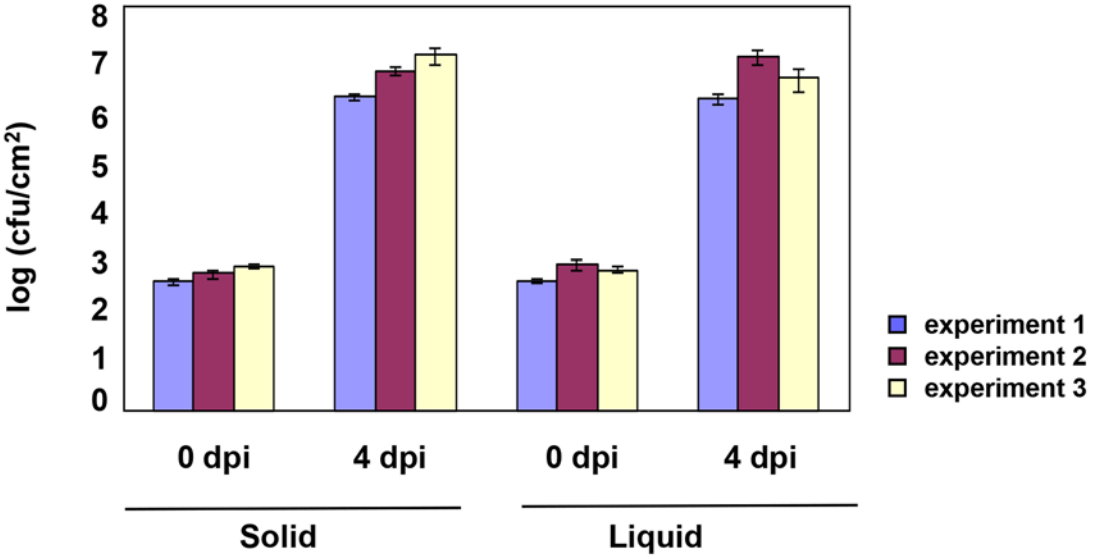

Figure 1.1. Bacterial (*Pto* DC3000) proliferation is not altered if the inoculum is harvested directly from the plate or liquid culture. *Arabidopsis* plants (Col-0) were grown in a short day conditions and infiltrated with an inoculation dose of $5x10^4$ cfu/ml. Three disc leaves per plant were collected and processed just after the inoculation (0 dpi), and 4 days after (4 dpi). Bacterial colonies were counted and represented in logarithmical scale. Each colour bar represents an independent experiment and for each experiment 4 plants were used. Error bars represent the standard error.

1.2. DNA hypomethylation upon Pto DC3000 infection

In order to corroborate if plant genome methylation levels are reduced during *Pto* DC3000 infection, we obtained Southern blot probes similar to the ones used by Pavet *et al.* (2006).

First, we amplified by Nested-PCR and the appropriate primers (**Table M3**), AL1a (GenBank X04322), a homologue to the centromeric 180-bp repeat (**Figure 1.2A**). The final PCR product was cloned into pGEM-T Vector. Transformants were analyzed by restriction (*Sac*I + *Apa*I) to confirm the fragment size (289 pb) (**Figure 1.2B**) and two of the recombinant clones were sequenced. Both clones showed homology to the centromeric 180-bp repeat but only one (clone 180.2) contained the complete sequence (**Figure 1.2C**). We used clone 180.2 (from now on would be referred to as CMP, *centromeric probe*) as a probe for Southern blot hybridization. Second, *Athila* probe was generated using the primers described in Pavet *et al.* (2006) (**Table M3**).

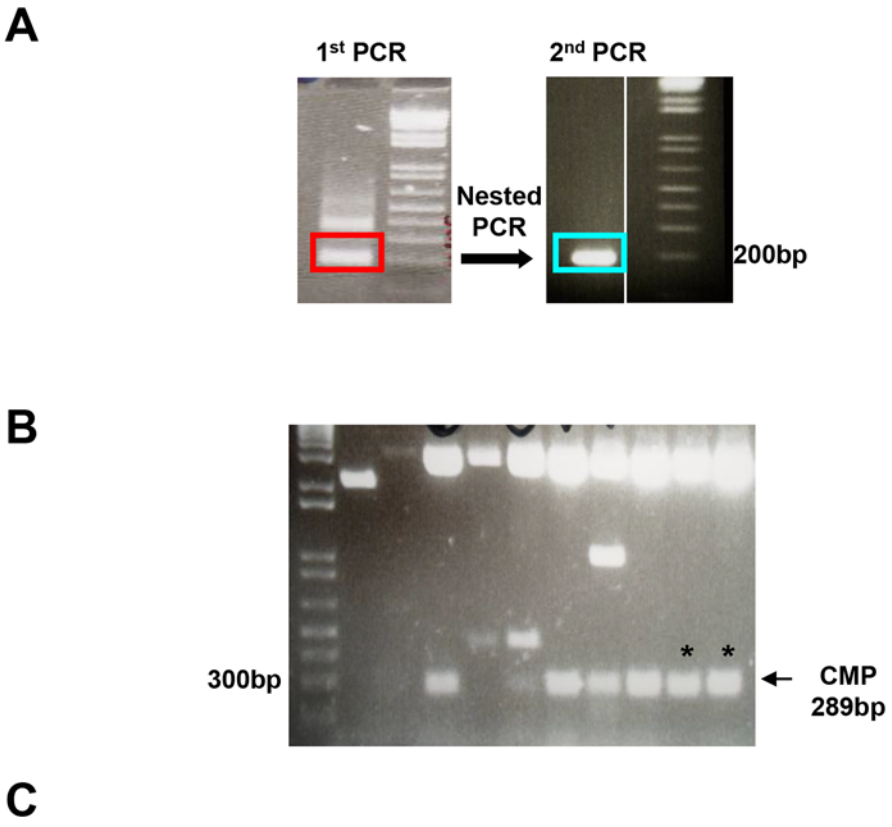

Figure 1.2. Generation of the centromeric repeat probe (CMP) for Southern blot analysis. (**A**) To generate the CMP probe a first PCR was carried out using primers 180bp1+180bp2 and *Arabidopsis* genomic DNA as template. The following *Nested PCR* was performed using primers 180bp3+180bp4 and the band obtained in the previous PCR as a template**.** The band of approximately 200 bp obtained in the first PCR was purified prior to its use as template. The fragment of 200 bp obtained from the second PCR was cloned into pGemT-Vector. (**B**) Restriction analysis (*Sac*I + *Apa*I) of transformants of the pGEM-T ligation to the 200 bp fragment. A fragment of 289 bp was generated in the correct recombinant clones. The clones marked with asterisks were confirmed by DNA sequencing. (**C**) Clone 180.2 contains identical nucleotide sequences (indicated with asterisk) of centromeric satellite repeat homologues up to 180bp repeats, called AL1 AL1a (X04322), and was therefore used as probe for Southern blot analysis.

The 509 bp PCR fragment obtained (**Figure 1.3A**) was also cloned into pGEM-T Vector, and the transformants analyzed as described for CMP (**Figure 1.3B**). The two clones contained a 509 pb *Athila* fragment (**Figure 1.3C**) and clone A1, was used as a probe for Southern blot hybridization.

In order to corroborate that *Arabidopsis* centromeric DNA is hypomethylated during infection with *Pto* DC3000 (Pavet et al., 2006), we performed a Southern blot using the CMP probe. *Arabidopsis* plants were infiltrated with *Pto* DC3000 grown in rich media, either liquid (King´s B) or solid (LB). Although we had previously described that the source of inoculum had no impact on the bacterial replication efficiency (**Figure 1.1**), we wanted to rule out any possible impact of the source of inoculum on *Pto* DC3000 effect on plant DNA methylation. We inoculated two sets of plants with different bacterial dilutions from the same inoculum: a first set inoculated with $5x10^4$ cfu/ml used to check bacterial replication, and a second inoculated with $5x10^6$ cfu/ml used for the Southern blot analysis. Growth 4 dpi confirmed bacteria were growing as expected displaying a 10^4-fold increase- regardless of the source of the inoculum (**Figure 1.4A**), a requirement for analysing the second set of plants and test their DNA methylation levels at 24 hpi. Genomic DNA was isolated from naïve, mock (infiltrated with $MgCl_2$) and infected leaves, digested with *Sau*3AI, a methylation-sensitive restriction enzyme which does not cut if DNA is methylated in GAT^{5m}C, and separated on an agarose gel. Genomic DNA from *ddm1* plants was used as a positive control as this mutant shows genome-wide hypomethylation (Vongs et al., 1993). DDM1 (DECREASED IN DNA METHYLATION 1) is a chromatin remodeler required for maintenance of DNA methylation as it facilitates access of DNA methyltransferases to heterochromatin (Law and Jacobsen, 2010). The blot was hybridized with the CMP probe and as shown on **Figure 1.4B**, we did not observed an increase on small size bands on *Pto*-infected plants (with either type of inoculum), and no differences were detected either between Pto-infected plants and mock or naïve plants, while a clear increase on the intensity of smaller bands, in keeping with reduce levels of DNA methylation, was clearly observed in the *ddm1* mutant.

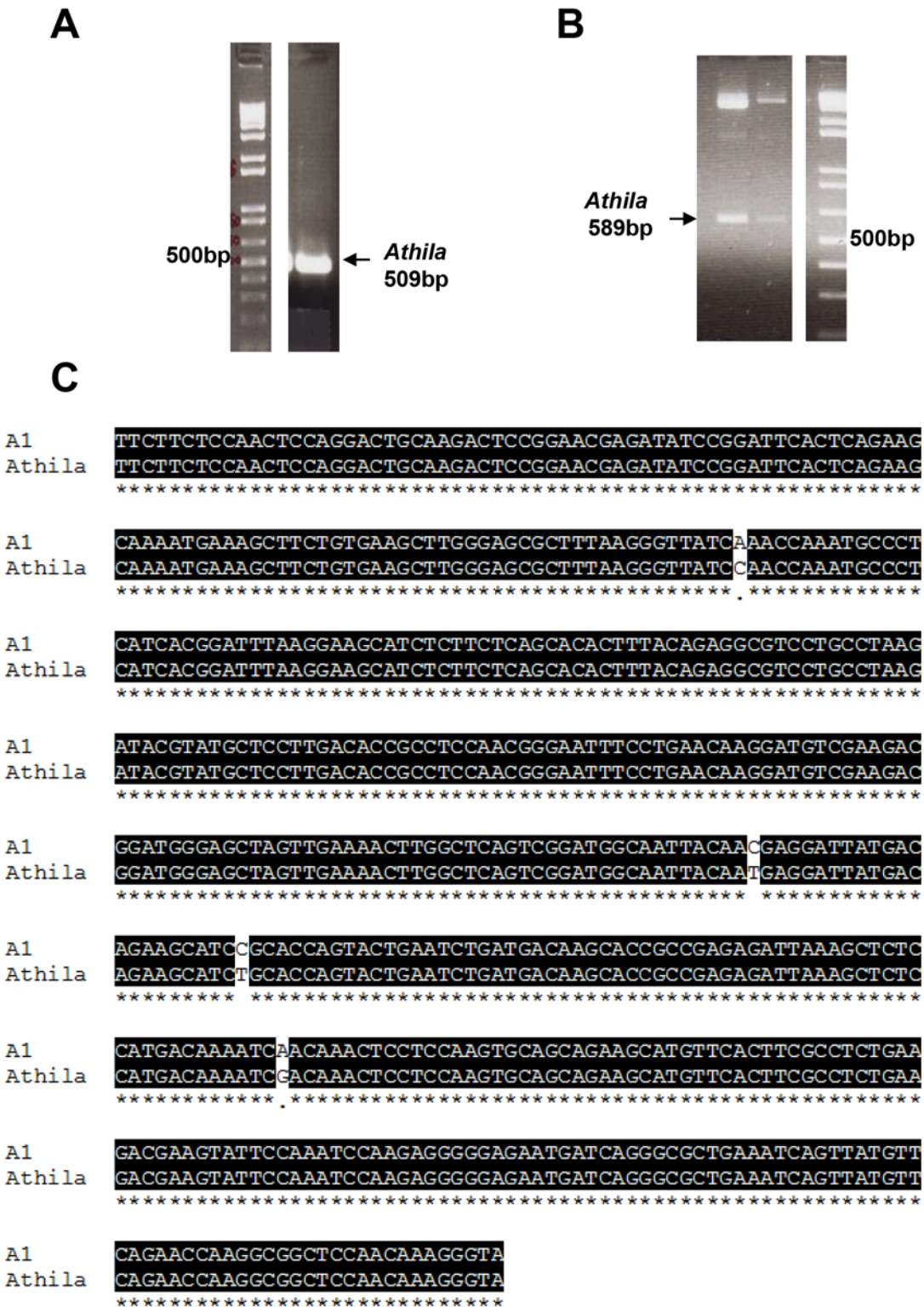

Figure 1.3. Generation of the *Athila* probe for Southern blot analysis. (**A**) The *Athila* probe was generated using primers designed from the accession X81801.1, (Trompa *et al.*, 2002). The 509 bp amplified PCR fragment was cloned into pGEM-T Vector. (**B**) Two clones were analyzed by restriction analysis (*Sac*I + *Apa*I), and the fragment of 589 bp was generated. The clones were confirmed by DNA sequencing. (**C**) Sequence of clone A1 shows homology to *Athila* sequence (identical nucleotides are marked with asterisk) and thus used as a probe for Southern blot analysis.

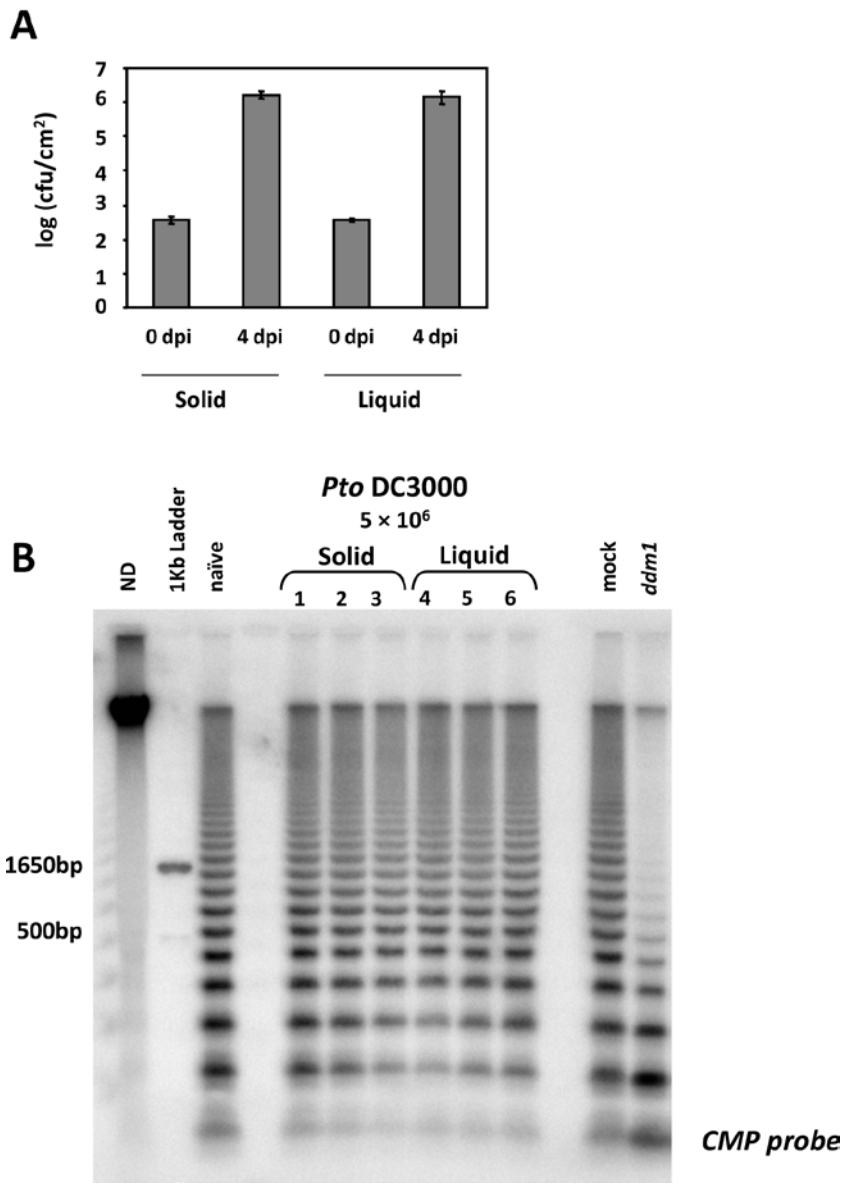

Figure 1.4. Southern blot analysis of plants infected with inocula from different sources. (**A**) *In planta* bacterial replication was analysed in *Arabidopsis* (Col-0) plants infiltrated with a lower concentration (5x10^4 cfu/ml) of the same bacterial solution used for Southern blot experiment (Fig. 1.4B). Plant tissue was processed at day 0 and day 4 post inoculation (0 dpi and 4 dpi). Three disc leaves per plant were collected and processed just after the inoculation (0 dpi), and at 4 dpi. Bacterial colonies were counted and represented in logarithmical scale. Bars represent the mean values from 3 plants per time point. Error bars represent the standard error. (**B**) Southern blot of genomic DNA obtained from *Arabidopsis* (Col-0) plants infected with 5x10^6 cfu/ml of *Pto* DC3000 previously grown in either liquid or solid LB medium. Samples were collected at 24 hours post infection (24 hpi). Three leaves per plant were harvested and processed for each sample. Genomic DNA was digested with the methylation-sensitive endonuclease *Sau*3AI and hybridized with the *CMP* probe. Genomic DNA from naïve and mock-inoculated plants (plants infiltrated with 10mM $MgCl_2$ and harvested 24hpi), as well as undigested genomic DNA from naive plants (ND) were used as a reference. *Arabidopsis ddm1* mutant was used as a positive control, as it displays genome-wide hypomethylation.

Pavet et al. (2006) reported that hypomethylation of plant centromeric DNA took place regardless of the inoculation dose (from 10^5 cfu/ml to $5x10^7$ cfu/ml) and time (24 and 48 hpi). To test whether these differences could have an impact on our experiments explaining the results obtained in **Figure 1.4B**, we repeated the infection of *Arabidopsis* plants inoculating *Pto* DC3000 at either $5x10^6$ cfu/ml or $5x10^7$ cfu/ml, and collected samples both at 24 and 48 hpi (**Figure 1.5**). Bacterial replication assays were carried out in parallel as before and confirmed bacterial growth as expected (**Figure 1.5A**). Southern blot analysis of these samples was carried out as before. The hybridization with the CMP probe did not show any increase on small size bands on *Pto*-infected plants at either 24 or 48 hpi, with either dose of inoculation, and no differences could be detected either between *Pto*-infected and mock or naïve plants, while it was clearly displayed in the *ddm1* mutant plants (**Figure 1.5B**). A similar result was obtained when the same genomic samples were digested with *Sau*3AI and the Southern blot hybridization performed using another centromeric probe, the *Athila* retrotransposon (Pavet et al., 2006), **Figure 1.5C**). At the highest inoculation dose, the plant tissue was severely damaged by 48 hpi (**Figure 1.5D**) but no symptoms could be observed at 24 hpi. As high molecular bands displayed a slight reduction in leaves inoculated with *Pto* DC3000 at $5x10^7$ cfu/ml at 24 hpi, we selected these conditions for the following assays. We also tested whether the effect on centromeric DNA hypomethylation reported by Pavet *et al.* (2006) could be occurring at earlier times in our laboratory conditions, infecting *Arabidopsis* leaves with $5x10^7$ cfu/ml *Pto* DC3000 and collecting samples at 0, 12 and 24 hpi (**Figure 1.6**). A Southern blot carrying *Sau*3AI-digested genomic DNA from these samples was hybridized with *Athila* probe. No significant changes on band intensity, consistent with DNA hypomethilation, could be detected in infected leaves at 12 hpi compared with 0 hpi, but a slight reduction of the signal from the higher molecular bands, accompanied by an increase of the signal from the 500 pb-lower band could be observed again in the 24 hpi samples (**Figure 1.6A**). As in prior experiments, bacterial replication was also tested (**Figure 1.6B**).

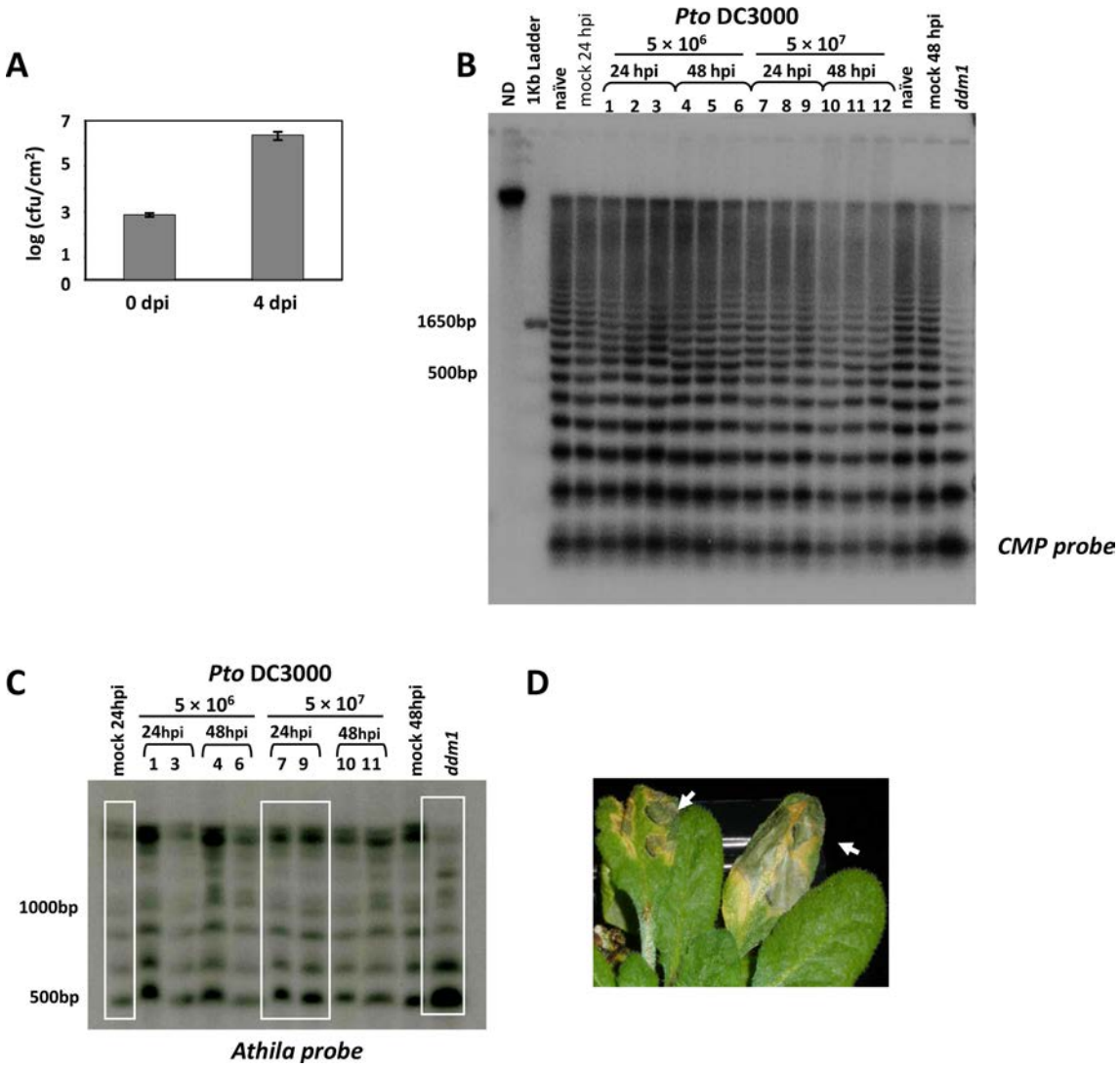

Figure 1.5. Southern blot analysis of *Pto*-infected plants with different inoculation dose. (**A**) *In planta* bacterial replication was analysed in *Arabidopsis* (Col-0) plants infiltrated with 5x10^4 cfu/ml of the same bacterial solution used for the Southern blot experiment (Fig. 1.5B and 1.5C). Plant tissue was processed at day 0 and day 4 post inoculation (0 dpi and 4 dpi). Three disc leaves per plant were collected and processed just after the inoculation (0 dpi), and at 4 dpi. Bacterial colonies were counted and represented in logarithmical scale. Bars represent the mean values from 3 plants per time point. Error bars represent the standard error. (**B**) Southern blot of genomic DNA obtained from *Arabidopsis* (Col-0) plants infected with 5x10^6 cfu/ml and 5x10^7 cfu/ml of *Pto* DC3000 previously grown in solid LB medium. Samples were collected at 24 and 48 hours post infection (24 hpi and 48 hpi). Three leaves per plant were harvested and processed for each sample. Genomic DNA was digested with the methylation-sensitive endonuclease *Sau*3AI and hybridized with the CMP probe. Genomic DNA from naïve and mock-inoculated plants (plants infiltrated with 10 mM $MgCl_2$), as well as undigested genomic DNA from naive plants (ND) were used as a reference. *Arabidopsis ddm1* mutant was used as a positive control, as it displays genome-wide hypomethylation. (**C**) Southern blot of samples 1, 3, 4, 6, 7, 9, 10 and 11, mock and *ddm1* used on Figure 1.5B. Genomic DNA was digested with the methylation-sensitive endonuclease *Sau*3AI and hybridized with *Athila* probe. (**D**) Symptoms of Arabidopsis Col-0 plants inoculated with 5 x 10^7 cfu/ml of *Pto* DC3000. Image shown was taken 48 hpi. Arrows indicate disease symptoms.

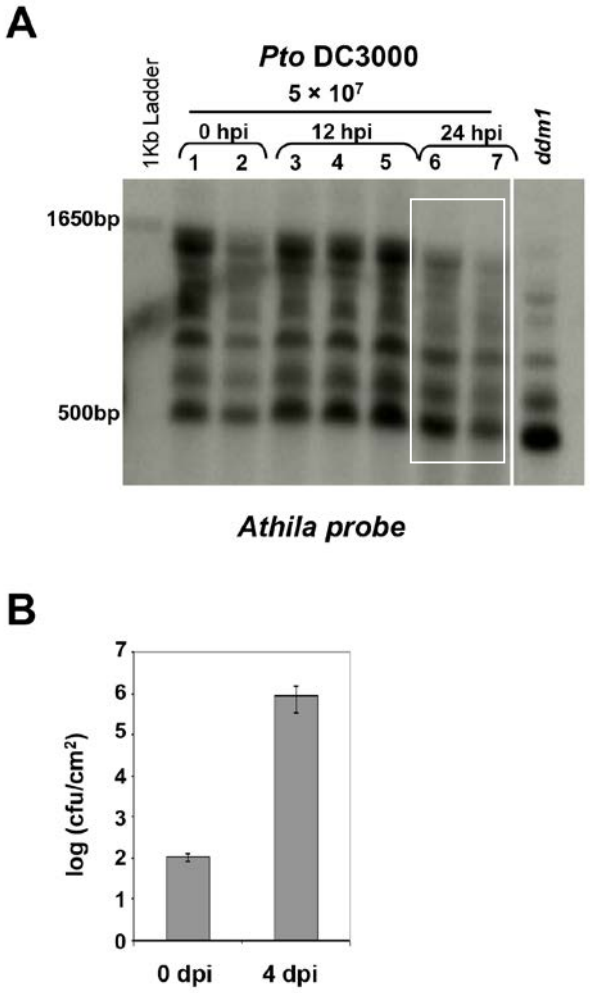

Figure 1.6. Southern blot analysis of plants infected during different time frames. (**A**) Southern blot of genomic DNA obtained from *Arabidopsis* (Col-0) plants infected with $5x10^7$ cfu/ml of *Pto* DC3000 previously grown in solid LB medium. Samples were collected at 0, 12 or 24 hours post infection (0, 12 and 24 hpi). Three leaves per plant were harvested and processed for each sample. Genomic DNA was digested with the methylation-sensitive endonuclease *Sau*3AI and hybridized with *Athila* probe. Genomic DNA from *Arabidopsis ddm1* mutant was used as a positive control, as it displays genome-wide hypomethylation. (**B**) *In planta* bacterial replication was analysed in *Arabidopsis* (Col-0) plants infiltrated with $5x10^4$ cfu/ml of the same bacterial solution used for Southern blot experiment (Fig. 1.6A). Plant tissue was processed at day 0 and day 4 post inoculation (0 dpi and 4 dpi). Three disc leaves per plant were collected and processed just after the inoculation (0 dpi), and at 4 dpi. Bacterial colonies were counted and represented in logarithmical scale. Bars represent the mean values from 3 plants per time point. Error bars represent the standard error.

Bhardwaj and collaborators showed that *Arabidopsis* has a circadian clock-mediated variation in resistance to *Pto* DC3000 (Bhardwaj et al., 2011). Plants were less susceptible to infection in the subjective morning than in the subjective night as a result of a clock-mediated modulation of pathogen associated molecular pattern (PAMP)-triggered immunity. Due to this temporal variation in susceptibility to *Pto* infection, we decided to infect *Arabidopsis* at different circadian stages: just before the evening, what we called "night infection", as after the inoculation the plants were immediately placed for 16 hours in the dark followed by 8 hours of light, or just before the morning, what we called "day infection" as after the inoculation the plants were immediately placed for 8 hours with light followed by 16 hours of darkness. For each condition samples were taken at 0 and 24 hpi from three leaves from two to five *Arabidopsis* plants infiltrated with $5x10^7$ cfu/ml *Pto* DC3000 or a $MgCl_2$ solution (mock). Two independent set of plants for "day infection" and "night infection" were infiltrated with the same inoculum whose replication rate in the plant was also measured (**Figure 1.7A**). Genomic DNA was digested with *Sau*3AI, separated on an agarose gel and the blot was hybridized with *Athila* probe. In "day infection" samples (**Figure 1.7B**), we could detect a clear increase on the intensity of the 500 bp-lower band, accompanied by a decrease on the signal of higher molecular bands on *Pto*-infected samples at 24 hpi, compared to the 0 hpi and mock samples. These differences were even clearer on "night infection" conditions (**Figure 1.7C**) indicating that hypomethylation of centromeric DNA was easier to detect when the plant is more susceptible to the bacteria and thus confirming the data presented by Pavet and collaborators (2006).

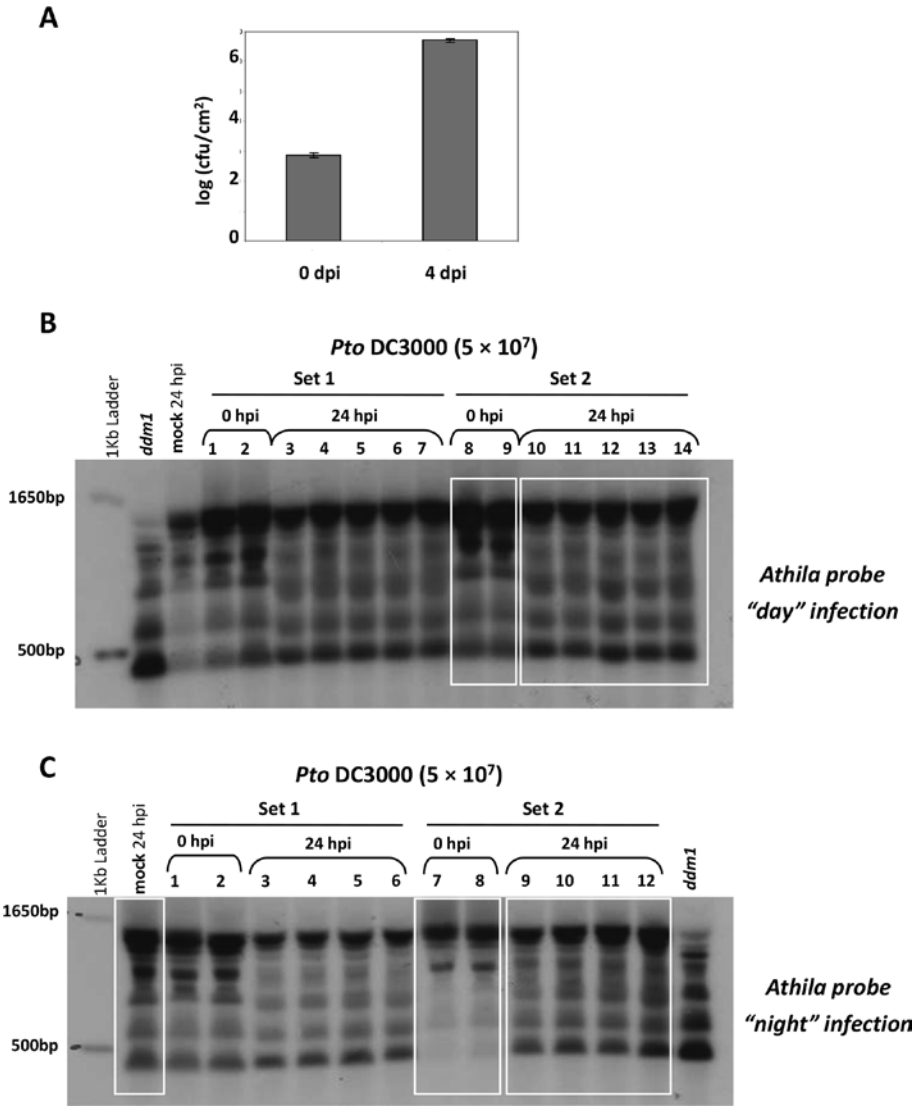

Figure 1.7. Southern blot analysis of Pto-infected plants in the subjective morning or in the subjective night. (**A**) *In planta* bacterial replication was analysed in *Arabidopsis* (Col-0) plants infiltrated with 5x10^4 cfu/ml of the same bacterial solution used for the Southern blot experiments (Fig. 1.7B and 1.7C). Plant tissue was processed at day 0 and day 4 post inoculation (0 dpi and 4 dpi). Three disc leaves per plant were collected and processed just after the inoculation (0 dpi), and at 4 dpi. Bacterial colonies were counted and represented in logarithmical scale. Bars represent the mean values from 3 plants per time point. Error bars represent the standard error. (**B**) Southern blot of genomic DNA obtained from *Arabidopsis* (Col-0) plants infected in the subjective morning (day infection) with 5x10^7 cfu/ml of *Pto* DC3000 previously grown in solid LB medium. Samples were collected at 0 and 24 hours post infection (0 hpi and 24 hpi). Two independent infections were performed with the same inoculum (Set 1 and Set 2). Three leaves per plant were harvested and processed for each sample. Genomic DNA was digested with the methylation-sensitive endonuclease *Sau*3AI and hybridized with *Athila* probe. Genomic DNA from mock-inoculated plants (plants infiltrated with 10mM $MgCl_2$ and harvested 24 hpi) was used as a reference. *Arabidopsis ddm1* mutant was used as a positive control, as it displays genome-wide hypomethylation. (**C**) The same as (B) but *Arabidopsis* (Col-0) plants were infected in the subjective night (night infection) with 5x10^7 cfu/ml of *Pto* DC3000 previously grown in solid LB medium.

1.3. Transcriptional activation of silent loci upon Pto DC3000 infection

The data presented by Dowen *et al.* (2012) confirmed the existence of genome-wide changes in DNA methylation levels in *Arabidopsis* in response to *Pto* infection, reinforcing the data presented by Pavet *et al.* (2006) and our own results. Dowen and collaborators went further by showing that these changes were intimately associated to differentially expressed genes in many loci. However, they did not addressed if the DNA hypomethylation of *Athila* also led to its transcriptional activation. To address this question, we measured the transcript levels of *Athila* on *Pto*-infected (with $5x10^7$ cfu/ml) *versus* control plants at 0 and 24 hpi under "night infection" conditions (**Figure 1.8**). All following *Pto* DC3000 infection experiments presented in this thesis were performed under these experimental settings, unless otherwise stated. *Athila* transcript accumulation was analysed by reverse transcription semi-quantitative PCR (RT-semi*q*PCR). *Athila* transcript accumulation was also analysed in *ddm1* plants as this mutant shows genome-wide hypomethylation and transcriptional activation of *Athila* (Vongs et al., 1993). By 24 hpi, *Pto*-infected plants showed a small increase on the transcript levels of *Athila* compared to samples taken at 0 hpi (**Figure 1.8A**). Quantification of this increase using the appropriate software support this conclusion since the differences measured were statistically significant (**Figure 1.8B**). Thus, these results indicate that *Athila* retrotransposon is transcriptionally activated during *Pto* DC3000 infection, and strongly suggest that it probably does so, by modifying the DNA methylation levels at this locus (**Figure 1.7 and 1.8**).

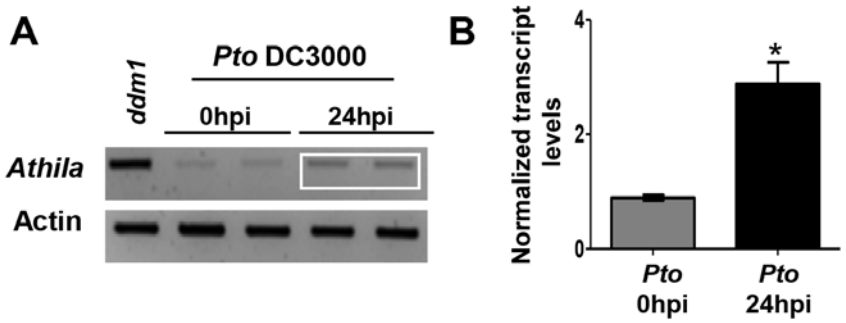

Figure 1.8. Accumulation of *Athila* transcripts in *Arabidopsis* infected plants. (**A**) Accumulation of *AtSN1* transcripts was analysed using reverse transcription semiquantitative PCR (RT-semi*q*PCR) in *Pto* DC3000-infected *Arabidopsis* plants, 0 and 24 hours post-inoculation (0 and 24 hpi). Three leaves per plant were harvested and processed for each sample. RNA from *ddm1* mutant was processed as a positive control for *Athila* expression. Amplification of actin transcript was used as a loading control. (**B**) Quantification of the RT-semiqPCR shown on (A) using ImageJ software. Transcript levels were normalised to actin and the results presented relative to the levels detected in *Pto* DC3000-infected plants 0 hpi. Bars represent the mean values from 2 plants. Error bars represent the standard error. Asterisks indicate samples that are statistically different from *Pto* DC3000-infected sample at 0 hpi as determined by Student's t-test at the 95% (*) confidence interval.

In order to investigate if under our laboratory conditions, *Pto* DC3000 infection also induces changes on the transcript levels of other transcriptionally silent loci (TGS-loci), we looked for TGS-loci which were previously reported to be activated in *Arabidopsis* mutants affected in DNA methylation, such as *met1-3* (METHYLTRANSFERASE 1 which is responsible for the maintenance of CG methylation) or *ddc* (a triple mutant on DOMAINS REARRANGED METHYLASE 1 and 2, and CHROMOMETHYLASE 3 which are involved in *de novo* DNA methylation and maintenance of CHG methylation, respectively). We selected four TGS-loci that were induced on *met1-3* or *ddc* mutant plants (Zhang et al., 2006): TE pseudogene (At1g38194), Ulp-like transposable element (At5g34900), CACTA-like DNA transposon (At2g04770) and *PHOSPHATE-INDUCED 1 (PHI-1,* At1g35140) and checked their transcript levels on *Pto*-infected *Arabidopsis* leaves. Leaves were infiltrated with $5x10^7$ cfu/ml *Pto* DC3000 under night infection conditions, and samples were collected at 0 and 24 hpi. Transcript levels for these TGS-loci were analysed by RT-semi*q*PCR (**Figure 1.9**) and samples

from *met1-3* and *ddm1* plants were included as positive controls. **Figure 1.9A** shows that by 24 hpi, *Pto*-infected plants display a significant increase on the levels of transcript for three out of the four TGS-loci analysed: the *TE pseudogene*, the *Ulp-like* transposable element, and the *CACTA* DNA transposon, although this increase is not as strong as that detected in *met1-3* or *ddm1* plants. These results indicate that infection with *Pto* triggers the transcriptional activation of a variety of epigenetically silenced-loci.

In the case of the fourth TGS-locus analysed, *PHI-1*, a locus induced on a *ddc* mutant (Zhang et al., 2006), we did not detect its transcriptional activation on *Pto*-infected plants at 24 hpi (**Figure 1.9B**). Surprisingly, transcript levels for *PHI-1* were activated on 0 hpi samples, and strongly reduced on *Pto*-infected plants at 24hpi. As we could not detect an induction on the chromatin remodeler mutant *ddm1* either, we reasoned that rather than a suppression of its transcription in *Pto*-infected plants at 24 hpi, our results support a fast activation of this locus upon inoculation, which is no longer detectable by 24 hpi. These results could indicate that mechanical damage associated to bacteria infiltration into the leave tissue, rather than interaction with *Pto* could be behind the activation of this locus. In order to confirm this, we analysed the transcript levels for *PHI-1* on naïve *versus* mock-infected plants (infiltrated with a $MgCl_2$ solution) at 0 hpi. As shown in **Figure 1.9B**, transcript levels for *PHI-1* were considerably higher in mock-inoculated than in naïve plants. Thus, we can conclude that *PHI-1* is transcriptionally activated by mechanical damage.

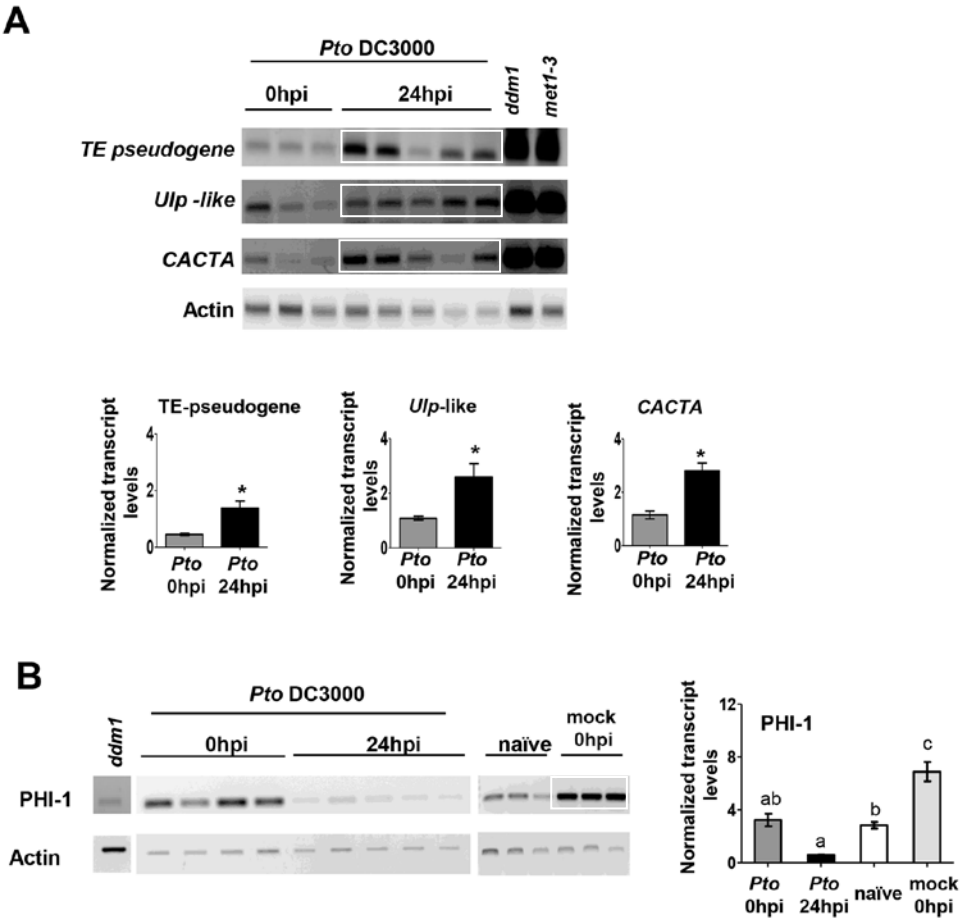

Figure 1.9. Accumulation of transcripts from TGS-loci in *Arabidopsis* infected plants. (**A**) Accumulation of transcripts from TE pseudogene (At1g38194), Ulp-like transposable element (At5g34900) and CACTA-like DNA transposon (At2g04770) was analysed using reverse transcription semiquantitative PCR (RT-semi*q*PCR) in *Pto* DC3000-infected *Arabidopsis* plants, 0 and 24 hours post-inoculation (0 hpi and 24 hpi). Three leaves per plant were harvested and processed on each line. RNA from *ddm1* and *met1-3* mutants was processed as a positive control for TGS-loci activation. Amplification of actin transcript was used as a loading control. (**A**, Bottom) Quantification of the RT-semi*q*PCR using ImageJ software. Gene expression levels were normalised to actin and the results presented relative to the levels detected in *Pto* DC3000-infected plants 0 hpi. Bars represent the mean values from 3-5 plants. Error bars represent the standard error. Asterisks indicate samples that are statistically different from the *Pto* DC3000-infected sample at 0 hpi as determined by Student's t-test at the 95% (*) confidence interval. (**B**) Accumulation of transcripts from PHOSPHATE-INDUCED 1 (PHI-1, At1g35140) was analysed using reverse transcription semiquantitative PCR (RT-semi*q*PCR) in *Pto* DC3000-infected *Arabidopsis* plants, 0 and 24 hours post-inoculation (0 hpi and 24 hpi). Naïve and mock-inoculated plants (10 mM $MgCl_2$ harvested 0 hpi) were included as controls for the basal transcript levels. Three leaves per plant were harvested and processed on each line. RNA from *ddm1* mutant was processed as a positive control for the TGS-loci expression. Amplification of actin gene was used as a loading control. (**B**, Right) Quantification of the RT-semi*q*PCR using ImageJ software. Transcript levels were normalised to actin and the results presented relative to the levels detected in *Pto* DC3000-infected plants 0 hpi. Bars represent the mean values from 4-6 plants. Error bars represent the standard error. Mean values marked with the same letter were not significantly different from each other as established by One-way ANOVA, Benferroni PosHoc test (95% confidence intervals).

Recently, the work from Yu *et al.* (2013) showed that some transposons such as *EVADE*, *Onsen* or *AtSN1* are demethylated and transcriptionally activated when *Arabidopsis* plants are exposed to the *Pto* flagellin-derived peptide flg22. Thus, we also analysed the transcript levels for *AtSN*1, a 170-bp SINE retrotransposon heavily methylated at non-CG and to a lesser extent at CG sites (Johnson et al., 2007) on *Arabidopsis* plants infected with *Pto* DC3000. Transcript levels were analysed on INFILTRATED leaves collected at 0 and 24 hpi. Transcript levels of *AtSN1* retrotransposon were also analysed by RT-semi*q*PCR, and samples from *ddm1* plants were used as positive control for *AtSN1* transcriptional activation. By 24 hpi, *Pto*-infected plants displayed a clear and significant increase on the transcript levels for *AtSN1* compared to the 0 hpi samples (**Figure 1.10**), indicating that *AtSN1* retrotransposon is also transcriptionallly activated during *Pto* DC3000 infection.

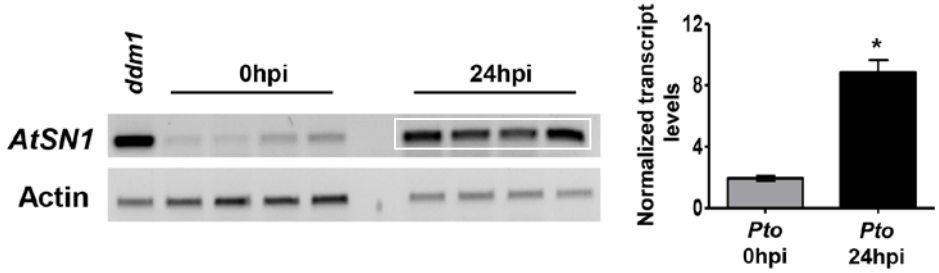

Figure 1.10. Accumulation of *AtSN1* transcripts in *Arabidopsis* infected plants. (**A**) Accumulation of *AtSN1* transcripts was analysed using reverse transcription semiquantitative PCR (RT-semi*q*PCR) in *Pto* DC3000-infected *Arabidopsis* plants, 0 and 24 hours post-inoculation (0 and 24 hpi). Three leaves per plant were harvested and processed for each sample. RNA from *ddm1* mutant was processed as a positive control for *AtSN1* expression. Amplification of actin gene was used as a loading control. (**B**) Quantification of the RT-semi*q*PCR shown on (A) using ImageJ software. Gene expression levels were normalised to actin and the results presented relative to the levels detected in *Pto* DC3000-infected plants 0 hpi. Bars represent the mean values from 4 plants. Error bars represent the standard error. Asterisks indicate samples that are statistically different from *Pto* DC3000-infected sample at 0 hpi as determined by Student's t-test at the 95% (*) confidence interval.

In order to better quantify the changes on the transcript levels of TGS-loci during *Pto*-infection in *Arabidopsis*, reverse transcription quantitative PCR (RT-*q*PCR) was performed on the two loci that showed a more consistent increase in transcript accumulation, *Athila* and *AtSN1*. Transcript levels for both loci were significantly induced by 24 hpi in *Pto*-infected plants, with the increase in *AtSN1* levels being stronger than that observed for *Athila* (**Figure 1.11A**).

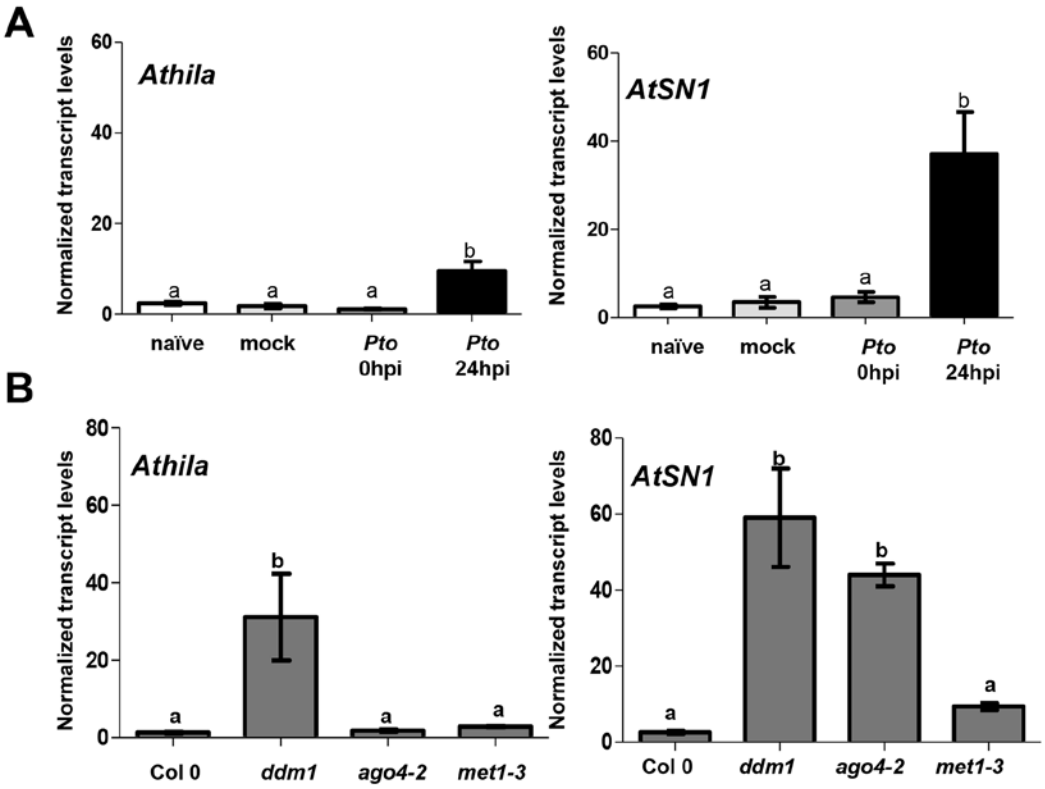

Figure 1.11. Transcript levels of *Athila* and *AtSN1* measured by RT-qPCR on *Arabidopsis* wild type and mutant plants with altered levels of DNA methylation. (**A**) Accumulation of *Athila* and *AtSN1* transcripts was analysed using reverse transcription quantitative PCR (RT-*q*PCR) in *Pto* DC3000-infected Col-0 plants at 0 and 24 hours post-inoculation (0 hpi and 24 hpi). Naïve and mock-inoculated plants (10 mM $MgCl_2$) were included as controls for basal transcript levels. Transcript levels were normalised to actin and the results presented as relative transcript accumulation compared to levels detected in plants inoculated with *Pto* DC3000 at 0 hpi. Bars represent the mean values from 1 independent experiment with 3-5 plants per sample. Error bars represent the standard error. Mean values marked with the same letter were not significantly different from each other as established by One-way ANOVA, Benferroni PosHoc test (99% confidence intervals). (**B**) Accumulation of *Athila* and *AtSN1* transcripts was analysed using RT-*q*PCR in Col-0, *ddm1, ago4-2, met1-3* plants. Transcript levels were normalised to actin and the results presented as relative transcript accumulation compared to levels detected in Col-0. Bars represent the mean values from 1 experiment with 3-5 plants per sample. Error bars represent the standard error. Mean values marked with the same letter were not significantly different from each other as established by One-way ANOVA, Benferroni PosHoc test (99% confidence intervals).

Transcriptional regulation of *Athila* depends on *DDM1*, whereas the involvement of *AGO4* (ARGONAUTE 4, silencing effector involved in RNA-dependent DNA methylation, RdDM) in its regulation has not been determined (Keith Slotkin, 2010). On the other hand, *AtSN1* activation has been shown to de dependent on *AGO4* (Agorio and Vera, 2007), and our results demonstrate that it also depends on *DDM1* (**Figure 1.10**). Thus, we analysed the transcriptional activation of these two loci in *Arabidopsis* Col-0, *ddm1, ago4-2* and *met1-3* mutants using RT-qPCR (**Figure 1.11B**), and found that whereas the transcriptional regulation of *Athila* does not depend on *AGO4* or *MET1*, that of *AtSN1* depends on *AGO4*, *DDM1*, and perhaps to a lesser extent on *MET1*.

1.4. Changes on AtSN1 methylation levels by Chop-PCR

Our results and others (Dowen et al., 2012; Yu et al., 2013) showed that several TGS-loci are transcriptionally activated during *Pto*-infection. Transcriptional activation of many of these loci is due to reduce DNA methylation levels, including that of *Athila* or *AtSN1*, the two loci displaying the strongest activation. To confirm that transcriptional activation of TGS loci was also due to DNA hypomethylation in our system, we used chop-PCR to analyse any changes on the DNA methylation status of *AtSN1* on *Pto*-infected plants. Chop-PCR is an assay in which genomic DNA is subjected to digestion with a methylation-sensitive or methylation-dependent restriction endonuclease and then tested as a template for PCR amplification using primers flanking the restriction sites (Earley et al., 2010; Oakes et al., 2009). *McrBC* is a restriction enzyme widely used for this type of analysis. It recognizes the two half-sites of the form 5′-G/A^{m}C-3′ that can be separated up to 2kb (5´…Pu^{m}C ($N_{40\text{-}2000}$) Pu^{m}C…3´), with an optimal separation of 55-103 bp. *McrBC* is methylation-dependent and thus cuts methylated but not unmethylated DNA. The McrBC enzyme only requires two methylated half-sites within the PCR-amplified region to cleave DNA, despite the methylation status of other sites. If a genomic region becomes hypomethylated, the enzyme will cut to a lesser extend and this will increase the amount of DNA that can be amplified by PCR. Ten Arabidopsis plants were infiltrated with

Pto DC3000 ($5x10^7$ cfu/ml, night infection) and samples were taken at 0 and 24hpi. Mock samples were included to determine wild-type levels of DNA methylation of *AtSN1* and samples from *ago4-2* plants were analysed as a positive control as this transposon becomes hypomethylated in this mutant (Agorio and Vera, 2007). Three leaves from each plant were independently macerated and frozen tissue was split in two to extract RNA and DNA. RNA was used to confirm transcriptional activation of *AtSN1* by RT-*q*PCR, and genomic DNA used to perform the chop-PCR assay. Genomic DNA was digested with *McrBC* and a *q*PCR performed using primers flanking the region of *AtSN1* that has been previously described to be most intensely methylated (Agorio and Vera, 2007; Xie et al., 2004; Yu et al., 2013). Although we could detect the transcriptional activation of *AtSN1* on *Pto*-infected plants by 24 hpi (**Figure 1.12A**), we found no evidence of hypomethylation for the transposon on the same infected plants (**Figure 1.12B**). To rule out the possibility that DNA hypomethylation was taking place at an earlier time on the infection process, we repeated these assays analysing samples at 3 and 9 hpi. No evidence for hypomethylation of *AtSN1* during *Pto* infection could be detected at these time points either (**Figure 1.12C**). This failure to detect DNA hypomethylation of *AtSN1* during *Pto* infection could be due to technical reasons, i.e. a low sensitivity of the chop-PCR assay, which could perhaps be solved by using other methylation-sensitive enzymes and other primers for *AtSN1* flanking their corresponding restriction sites, or due to the nature of the assay. This later possibility is supported by the small differences in methylation levels found for *AtSN1* by Yu and collaborators (Yu et al., 2013) following flg22 treatment. Flg22 treatment is expected to induce stronger changes than those taking place during infection since higher amounts of flagellin are thus presented to the plant. Furthermore, Yu and collaborators proposed that changes due to interaction with *Pto* occurs only in cells adjacent to bacteria, leading to leaf samples including cells with altered, as well as cells with normal DNA methylation levels, thus potentially diluting the changes and reducing the sensitivity of the assay. Any of these reasons could explain our negative results.

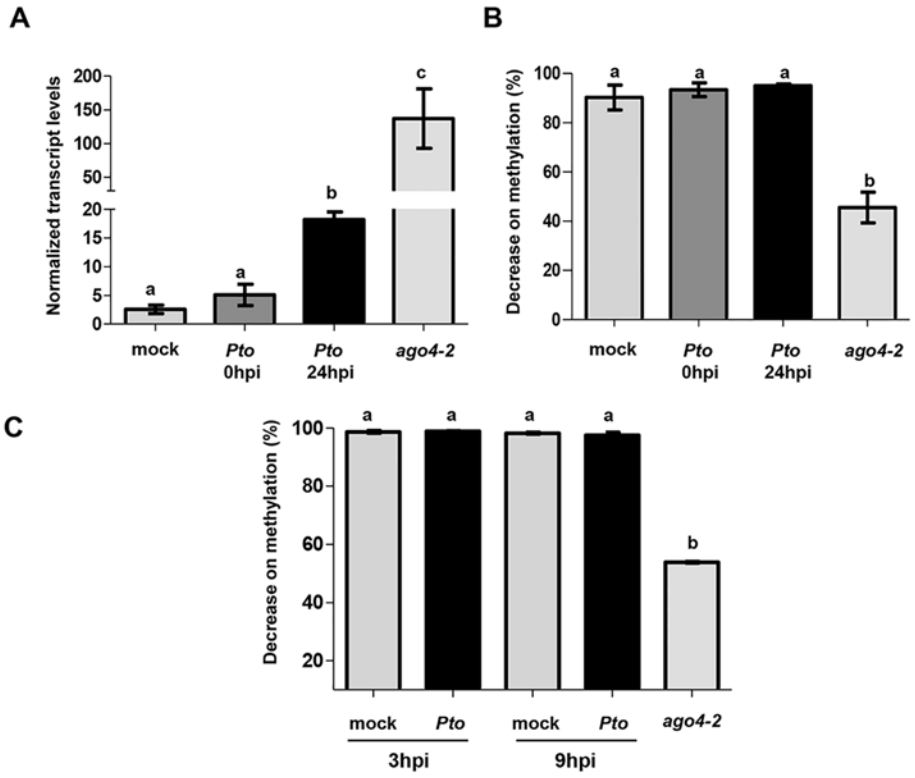

Figure 1.12. DNA methylation status of *AtSN1 in Pto* DC3000-infected *Arabidopsis* plants by Chop-PCR. (A and B) *Arabidopsis* plants were infected with *Pto* DC3000 and samples were harvested at 0 and 24 hours post-inoculation (0 hpi and 24 hpi). Mock-inoculated plants (10 mM $MgCl_2$) and *ago4-2* were included as negative and positive controls, respectively. Macerated tissue was split in two and samples were processed for RT-*q*PCR on (A) and for chop-PCR on (B). (**A**) Accumulation of *AtSN1* transcripts was analysed using RT-*q*PCR. Transcript levels were normalised to actin and the results presented as relative transcript accumulation compared to levels detected in plants inoculated with *Pto* DC3000 at 0 hpi. (**B**) Genomic DNA was digested with the methylation-dependent enzyme McrBC and an *AtSN1* fragment was amplified by PCR. A fragment from locus At3g18780 known to be non-methylated (Widman et al., 2009), was used to normalize the PCR amplified levels. The experiment was performed two times and one representative biological replicate is shown. Bars represent the mean values from 1 experiment with 3 (mock), 4 (0 hpi) and 10 (24 hpi) plants. Error bars represent the standard error. Mean values marked with the same letter were not significantly different from each other as established by One-way ANOVA, Benferroni PosHoc test (99% confidence intervals). (**C**) *Arabidopsis* plants were infected with *Pto* DC3000 and samples were harvested at 3 and 9 hours post-inoculation (3 hpi and 9 hpi). Mock-inoculated plants (10 mM $MgCl_2$) and *ago4-2* were included as negative and positive controls, respectively. Genomic DNA was digested with the methylation-dependent enzyme McrBC and an *AtSN1* fragment was amplified by PCR. A fragment from locus At3g18780 known to be non-methylated, was used to normalize the PCR amplified levels. Bars represent the mean values from 1 experiment with 3-4 plants. Error bars represent the standard error. Mean values marked with the same letter were not significantly different from each other as established by One-way ANOVA, Benferroni PosHoc test (99% confidence intervals).

1.5. Activation of a transcriptionally silent GUS transgene upon Pto DC3000 infection

Yu *et al.* (2013) generated an *Arabidopsis* transgenic line named *AtGP1 LTR:GUS,* which contains the β-glucuronidase GUS reporter gene fused to the LTR (long-terminal repeat) of *AtGP1*, a gypsy retrotransposon strongly targeted by siRNA-directed DNA methylation. The expression of GUS in this line is restored upon application of a DNA methyltransferase inhibitor, supporting transcriptionally silencing for this reporter transgene (Yu et al., 2013). Expression of *AtGP1 LTR:GUS* is activated after treating *Arabidopsis* leaves with flg22. In order to determine if during infection with *Pto* DC3000 this transcriptionally silent *GUS* transgene was also activated, we infected leaves of *AtGP1 LTR:GUS* plants ($5x10^7$ cfu/ml) and stained them to detect GUS signal at 0, 3 and 9 hpi. The presence of *Pto* DC3000 in the apoplast rapidly activates GUS expression as *Pto*-infected but not mock-infected leaves at 0 hpi displayed intense GUS staining, suggesting that activation of the transgene occurs immediately upon bacteria recognition by the plant. *Pto*-infected leaves displayed an even stronger GUS staining at 3 hpi with a small decrease at 9 hpi, indicating that the transgene becomes additionally activated during the initial hours of the interaction with *Pto* DC3000 (**Figure 1.13**). The changes occurring at the chromatin level in this transgenic line should be addressed in a future.

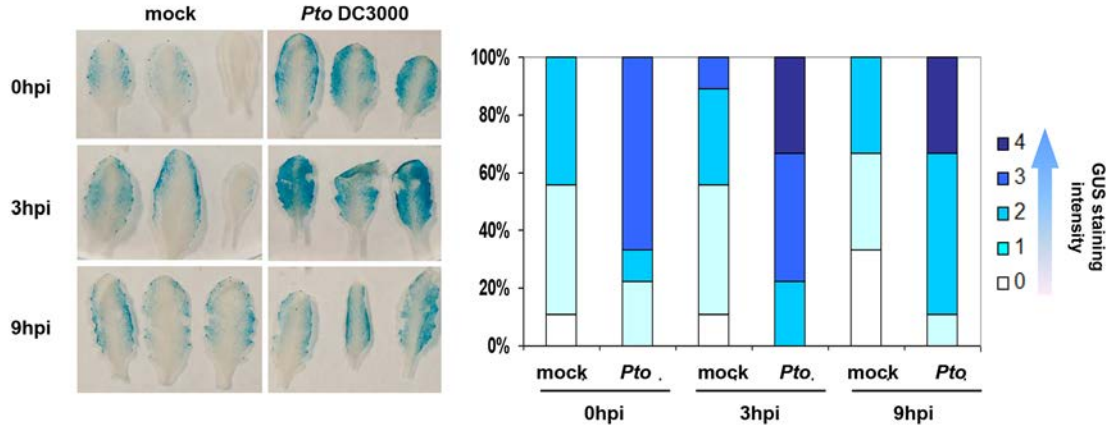

Figure 1.13. GUS staining of *Pto* DC3000-infected *Arabidopsis* transgenic line *AtGP1 LTR:GUS*. Six week-old *Arabidopsis* transgenic line *AtGP1 LTR:GUS*, which contains the β-glucuronidase GUS reporter gene fused to the LTR (long-terminal repeat) of *AtGP1*, was infiltrated with $5x10^7$ cfu/ml of *Pto* DC3000. In each experiment three leaves per 3 plants were infiltrated and leaves were GUS histologically stained at 0, 3 and 9 hours post-infiltration (0, 3, 9 hpi). Mock-inoculated plants (10 mM $MgCl_2$) were included as controls for the basal GUS expression level. The experiment was performed 3 times and the images correspond to a representative GUS histologically stained infiltration experiment. The graph summarizes the GUS staining intensity for that representative experiment.

Chapter 2

Role of bacterial virulence determinants in the transcriptional activation of the retrotransposon *AtSN1*

2.1. Role of the T3SS in determining AtSN1 transcript levels

Pavet and collaborators (2006) showed that hypomethylation of *Arabidopsis* DNA during *Pto* DC3000 infection requires a functional *hrpL* gene. HrpL activates the transcription of the genes necessary for coronatine production as well as the genes encoding the type III secretion system (T3SS). We chose to use the retrotransposon *AtSN1*, the TGS-locus displaying the strongest activation during infection with *Pto* DC3000 (**Figures 1.10** and **1.11**), as a reporter to analyse the role of different bacterial virulence determinants, including HrpL and the T3SS, in the modification of the plant epigenome. We analysed *AtSN1* transcript levels in plants infected with either *Pto* DC3000 or its mutant derivatives. The mutants analysed included: a *Pto* DC3000 carrying a knockout mutation in *hrcV*, encoding an inner membrane component of the T3SS (**Figure 2.1A**), a double mutant (*cfa*6::Tn*5 cma*::Tn*5*) COR$^-$, which fails to synthesize the toxin coronatine (**Figure 2.1B**), and a Δ*hrpL* mutant. Mutants in *hrcV* lack a functional T3SS and are thus not capable of delivering effector proteins inside of the host cell, do not cause infection in susceptible hosts, nor do they induce the HR in resistant hosts (Alfano and Collmer, 1997). No significant accumulation of *AtSN1* transcript was detected in *Arabidopsis* plants inoculated with either the Δ*hrpL* or the Δ*hrcV* mutants at 24 hpi. Plants inoculated with a COR$^-$ mutant accumulated significantly higher levels of *AtSN1* transcript than those inoculated with either Δ*hrpL* or Δ*hrc* mutants (**Figure 2.1B**), although this level was significantly lower than that accumulated in plants inoculated with the wild type strain.

To further confirm the differences found between the levels of *AtSN1* transcript accumulated following the inoculation with these strains, we analyzed the three mutant strains (Δ*hrpL,* Δ*hrcV* and COR$^-$) side by side (**Figure 2.1C**). Thus, our results indicate that the lack of transcriptional activation of *AtSN1* observed in plants inoculated with the *hrpL* mutant can be fully explained by its failure to secrete effectors. However, they also indicate that in the context of a fully functional T3SS, the synthesis of coronatine is necessary for full activation of *AtSN1.*

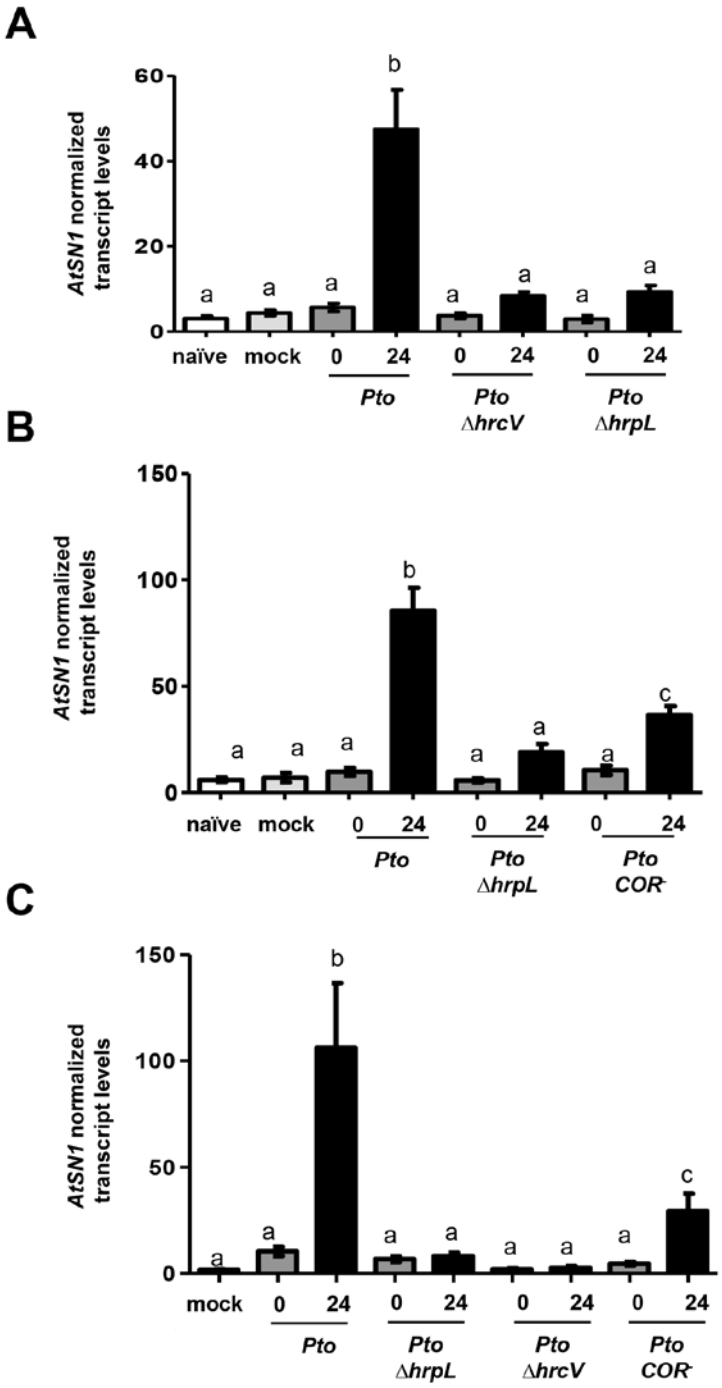

Figure 2.1. Accumulation of *AtSN1* transcript 24 hours post-inoculation with *Pto* DC3000 requires HrpL and a functional T3SS, and is partially dependent on coronatine synthesis. (**A-C**) Accumulation of *AtSN1* transcript was analysed using RT-*q*PCR in Col-0 plants 24 hours post-inoculation with *Pto* DC3000, *Pto* T3SS mutants (Δ*hrpL* and Δ*hrcV*) or COR$^-$ mutant. Naïve plants as well as plants mock-inoculated, were collected at 24 hpi and included as controls. Bars represent the mean values from 3 independent experiments with 3-6 plants per sample and experiment. Error bars represent the standard error. Samples represented in (**C**) were analyzed side by side within the same experiment. *AtSN1* transcript levels were normalised to actine and the results presented as relative transcript accumulation compared to the levels detected in *Pto* DC3000-infected plants 0 hpi. Mean values marked with the same letter were not significantly different from each other as established by One-way ANOVA, Benferroni PosHoc test (99% confidence intervals).

2.2. Identification of type III effector proteins potentially involved in the transcriptional activation of the retrotransposon AtSN1

Pto DC3000 actively deploys at least 28 *bona fide* effectors and several other proteins associated with extracellular functions of the T3SS (Schechter et al., 2006). The majority of these well-expressed DC3000 type III effectors are encoded within six clusters in the DC3000 genome (Wei et al., 2007) (**Table 2.1**). The genome also harbours 12 putative effector pseudogenes and 7 effector genes that appear only weakly expressed (Chang et al., 2005). To determine the role of the T3SS translocated effectors (T3Es) in the activation of *AtSN1* transcription during *Pto* DC3000 infection, we analysed *AtSN1* transcript accumulation in plants inoculated with a series of mutants in multiple effector genes, carrying deletions of different groups of *Pto* DC3000 effector genes. Growth within the plant of *Pto* Δ*28E*, a *Pto* DC3000 mutant derivative which lacks all 28 well expressed effector genes, is severely reduced in *Arabidopsis* and is not accompanied by lesion formation in the plant (Wei et al., 2007). We found that *AtSN1* transcript levels did not increase in plants inoculated with the *Pto* Δ*28E* mutant strain, being those observed at 24 hpi not significantly different from the levels displayed by plants inoculated with the Δ*hrcV* T3SS defective mutant (**Figure 2.2A**). This indicates that the transcriptional activation of *AtSN1* requires one or several of the 28 effectors translocated by the *Pto* DC3000 T3SS and supports the result obtained for Δ*hrcV* and Δ*hrcL* mutants which lack a functional T3SS (**Figure 2.1**).

We also analysed mutant strains lacking different clusters of effector genes in order to determine which effectors are involved in *AtSN1* transcriptional activation. As a first step, we analysed plants inoculated with two mutant strains: strain CUCPB5459, missing clusters I, II, IV, IX and X and therefore lacking 9 well expressed effectors and 3 putative pseudogenes, and strain CUCPB5451, missing clusters II, IV and IX, and lacking 15 well expressed effectors and 3 putative pseudogenes (**Figure 2.2B**). The level of *AtSN1* transcripts accumulated in plants inoculated with the CUCPB5459 strain was not significantly different from that accumulated in plants inoculated

with the wild type strain, suggesting that the effectors missing in this strain are not required for *AtSN1* transcriptional activation. Surprisingly, the accumulation of *AtSN1* transcripts was significantly higher in plants inoculated with strain CUCPB5451 than in those inoculated with the wild type. The simplest explanation for this result is that one or more effector(s) among the 15 effectors or 3 putative pseudogenes missing in this strain (CUCPB5451) could act as a suppressor(s) of *AtSN1* transcriptional activation. If *AtSN1* transcriptional activation was part of effector-triggered immunity (ETI) triggered against *Pto* DC3000, an effector capable of suppressing it could represent an adaptative advantage.

Table 2.1. Effector gene clusters in *Pseudomonas syringae* pv. *tomato* DC3000

Cluster	Effector genes
I	*hopU1, hopF2*
II	*hopH1, hopC1*
III	*hopAJ1, (hopAT')*
IV	*hopD1, hopQ1-1, hopR1*
V	*(hopAG::ISPssy), (hopAH1), (hopAI1)*
VI	*hopN1, hopAA1-1, hopM1, avrE1*
VII	*(hopAH2-1), (hopAH2-2)*
VIII	*hopS2, (hopT2), (hopO1-3'), hopT1-2, hopO1-2, (hopS1::ISPssy)*
IX	*hopAA1-2, hopV1, hopAO1, (hopD::IS52), (hopH::ISPsyr4), hopG1, (hopQ1-2)*
pDC3000A	*hopAM1-2, hopX1, hopO1-1, hopT1-1*

Clusters are numbered in the order of their location on the DC3000 chromosome. Putative pseudogenes are indicated with parenthesis. Cluster VI is also known as the conserved effector locus.

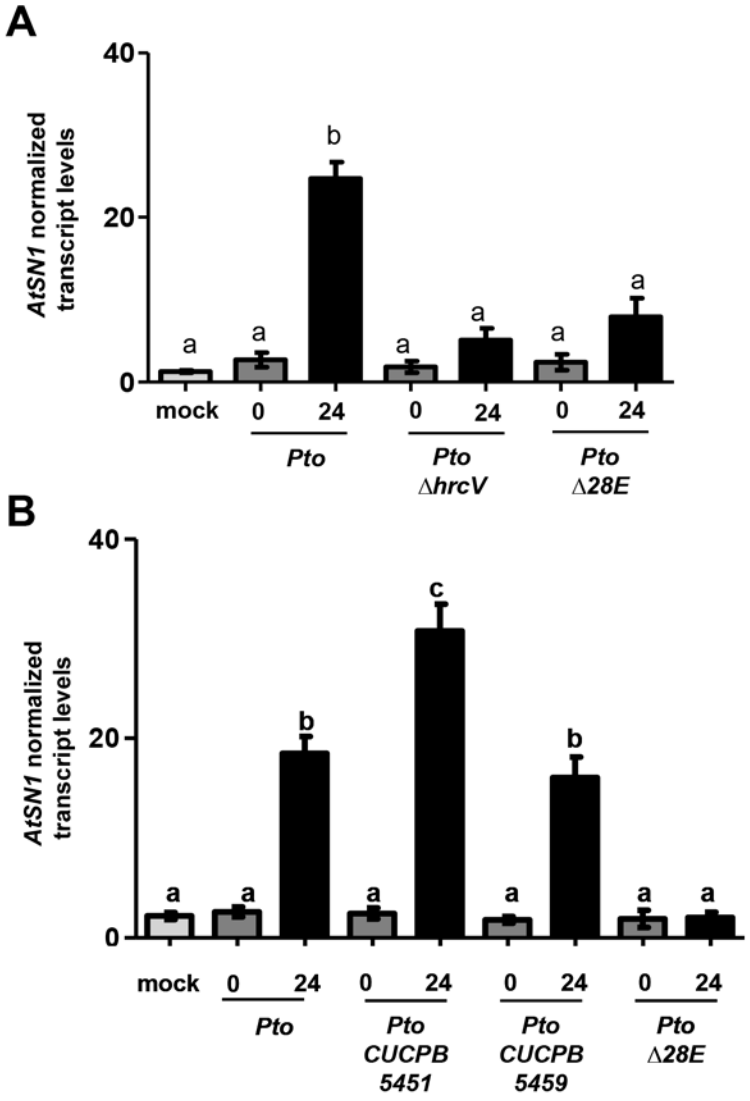

Figure 2.2. Accumulation of *AtSN1* transcript 24 hours post-inoculation with *Pto* DC3000 requires one or more effectors, and it is also suppressed by one or more effectors from the 28 well-expressed effector set. (A-B) Accumulation of *AtSN1* transcript was analysed using RT-*q*PCR in Col-0 plants 24 hours post-inoculation with *Pto* DC3000, or its Δ*hrcV* and Δ*28E* mutant derivatives (**A**) or with *Pto* DC3000, or its CUCPB5451 (missing clusters II, IV and IX), CUCPB5459 (missing clusters I, II, IV, IX and X) and Δ*28E* mutant derivatives (**B**). Mock-inoculated plants were collected at 24 hpi and included as controls. Bars represent the mean values from 2 independent experiments with 3-5 plants per sample and experiment. Error bars represent the standard error. Experiments were done 3 times with similar results. *AtSN1* expression levels were normalised to actin and the results presented as relative mRNA accumulation compared to levels detected in *Pto* DC3000-infected plants 0 hpi. Mean values marked with the same letter were not significantly different from each other as established by One-way ANOVA, Benferroni PosHoc test (95% confidence intervals).

2.3. Generation of type III secretion system single mutant effectors from Pseudomonas syringae pv. tomato.

In parallel to the analysis of *Pto* DC3000 virulence determinants in the transcriptional activation of *AtSN1*, we generated a collection of single mutants in *Pto* DC3000 effector genes using a method previously developed by our laboratory (Zumaquero et al., 2010). It applies a series of sequential PCR reactions and a selectable cloning step, to generate allelic exchange vectors that could be directly introduced into the target strain to produce the mutants. Every knockout vector is generated by a 6-step procedure shown in **Figure 2.3** and **Table 2.2**. Briefly, approximately 500 bp flanking the target ORF is amplified from *Pto* DC3000 genomic DNA, using primers in combination 1+A and 2+B, for each flanking region (Material and Methods, **Table M3**). Primers A and B include an *EcoR*I restriction site, absent in the amplified flanking sequences, and the T7 primer sequence (**Figure 2.3, Step 1**). These fragments are joinet into a 1000 bp fragment by the homology provided by T7 primer sequence by a PCR without additional primers or template (polymerization PCR), thus generating the deletion allele (**Figure 2.3, Step 2**). A third PCR is performed by adding primers 2+3 to the reaction, to increase the amount of the PCR-generated deletion allele, which are then A/T cloned into pGEM-T Vector system (**Figure 2.3, Step 3**), and fully sequenced. To prevent the accumulation of PCR-associated mutations during the process, we used a high fidelity polymerase, DMSO, commercial water, and very few PCR cycles (Materials and Methods, Section 3). The deleted alleles were confirmed by restriction analysis and the knockout vectors, carrying the *nptII* gene cloned into the deletion alleles were generated as follows. As suitable, *Eco*RI, or *Bam*HI fragments containing the *nptII* gene were obtained from pGEMT-*nptII*-*Eco*RI, or pGEMT-*nptII*-*Bam*HI generated by Dr. A. Zumaquero (Zumaquero et al., 2010), respectively, and ligated into the *Eco*RI, or *Bam*HI, fragments of the corresponding pGEM-T derivatives carrying the deletion alleles. The knockout alleles thus generated are marked with a *nptII* kanamycin resistance gene flanked by FRT sites (**Figure 2.3, Step 4**), and introduced into *Pto* DC3000 by electroporation (**Figure 2.3, Step 5**) to obtain the knockout strains by allelic exchange. The resistance

gene, *nptII* kanamycin, flanked by FRT sites can be easily removed by flipase-mediated site-specific recombination to allow the generation of double mutant strains (**Figure 2.3, Step 6**).

Table 2.2. Generated single knockout mutants for 38 effector genes.

Pto mutants	Gene size	Localization	Generated mutants
hopO1-2	897 bp	chromosome	this work
hopX1	1155 bp	plasmid	this work
hopT1-2	1170 bp	chromosome	this work
hopAA1-2	1464 bp	chromosome	this work
hopD1	2118 bp	chromosome	this work
hopV1	1173 bp	chromosome	this work
hopR1	5874 bp	chromosome	this work
hopB1	1401 bp	chromosome	this work
hopAM1-2	831 bp	plasmid	this work
hrpL	555 bp	chromosome	this work
hopA1	1143 bp	chromosome	this work
avrPto1	495 bp	chromosome	this work
hopC1	810 bp	chromosome	Zumaquero A and Beuzón CR
hopY1	864 bp	chromosome	Zumaquero A and Beuzón CR
hopM1	2139bp	chromosome	Zumaquero A and Beuzón CR
hopN1	1053bp	chromosome	Zumaquero A and Beuzón CR
hopI1	1467 bp	chromosome	Zumaquero A and Beuzón CR
hopE1	636 bp	chromosome	Zumaquero A and Beuzón CR
hopH1	657 bp	chromosome	Zumaquero A and Beuzón CR
avrE1	5388 bp	chromosome	Zumaquero A and Beuzón CR
hopAA1-1	1461 bp	chromosome	Zumaquero A and Beuzón CR
hop Q1-1	1344 bp	chromosome	Zumaquero A and Beuzón CR
hopAB2	1662 bp	chromosome	Zumaquero A and Beuzón CR
hopAM1-1	831 bp	chromosome	Zumaquero A and Beuzón CR
hopG1	1482 bp	chromosome	Zumaquero A and Beuzón CR
hopK1	1017 bp	chromosome	Zumaquero A and Beuzón CR
hopU1	795 bp	chromosome	Zumaquero A and Beuzón CR
hopAF1	855 bp	chromosome	Zumaquero A and Beuzón CR
hopAO1	1407 bp	chromosome	Zumaquero A and Beuzón CR
hopF2	615 bp	chromosome	Zumaquero A and Beuzón CR
hopO1-1	852 bp	plasmid	Zumaquero A and Beuzón CR
hopT1-1	1137 bp	plasmid	Zumaquero A and Beuzón CR
hopAH1	1269bp	chromosome	Zumaquero A and Beuzón CR
hopS2	534 bp	chromosome	Zumaquero A and Beuzón CR
hopAQ1	252 bp	chromosome	Zumaquero A and Beuzón CR
hrcV	2088 bp	chromosome	Zumaquero A and Beuzón CR
hopP1	975 bp	chromosome	Zumaquero A and Beuzón CR
hopAI1	786 bp	chromosome	Zumaquero A and Beuzón CR

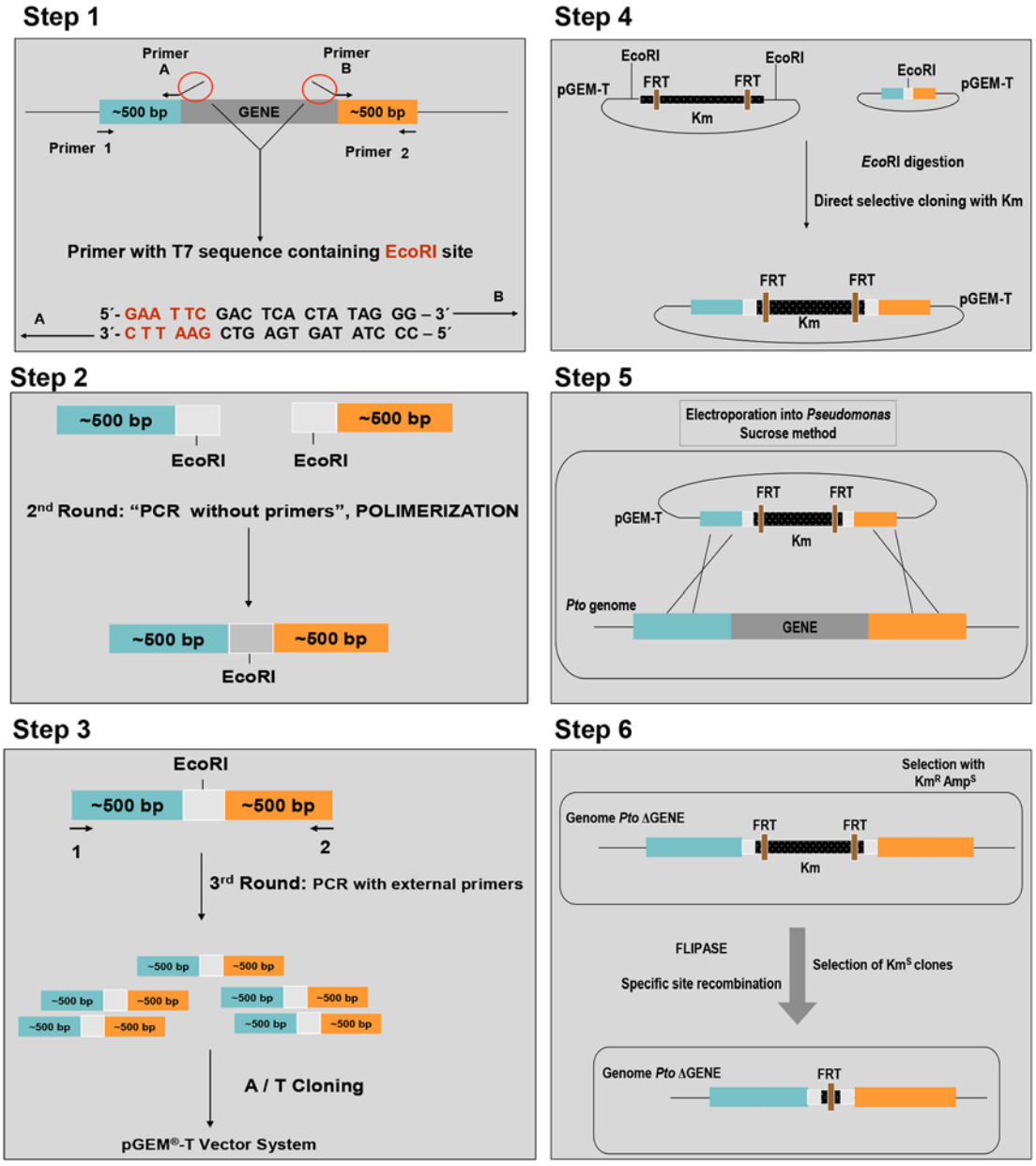

Figure 2.3. Method used for the generation of T3SS knockout mutants in *Pseudomonas syringae* pv. *tomato* DC3000. Step 1) Regions of approximately 500 bp flanking the target gene are amplified using primer combination A and 2 or B and 1. Primers A and B include an *EcoR*I site. **Step 2)** Polymerization PCR is carried out using both 500 bp flanking fragments without additional primers or template. Thus both fragments are joined together into 1000 bp fragment through the homology shared between primers A and B. **Step 3)** The resulting 1000 bp fragment (knockout allele) is amplified using external primers (1+2) and A/T cloned into pGEMT Vector. **Step 4)** The newly introduced restriction site (*EcoR*I) is used to clone an FRT-flanked fragment containing the *nptII* gene. **Step 5)** The knockout vector is introduced into the recipient strain by electroporation. **Step 6)** Transformants having undergone a double recombination event are selected and confirmed using antibiotic resistances. Knockout clones are expected to be resistant to kanamycine through the presence of the *nptII* gene in the knockout allele recombined into the chromosome, and ampicillin sensitive indicating the plasmid backbone is not integrated as well. Later on the *nptII* gene can be easily removed using flipase.

Thus, 38 single knockout mutants were generated in the laboratory lacking each of the complete T3SS effector inventory of *Pto* DC3000, 12 of which were generated as part of this Thesis. A full list of these effector genes, their sizes and genomic locations is presented in **Table M5**.

Two of these mutants, *hopAM1-2* and *avrPto1* gene, required a modification of the protocol since no transformants could be obtained, presumably due to a lower local recombination frequency. Indeed, allelic exchange was only achieved for these two loci after increasing the length of the flanking regions in the deletion allele up to 1000 bp, in keeping with the notion of a lower local recombination frequency that could be increased by providing a larger homologous region.

Although characterization of the role in activating or suppressing *AtSN1* transcription for all relevant effector mutants is yet to be completed, we did analyzed two single mutant strains during this thesis: Δ*hopAO1* and Δ*hopC1.* These genes encode two well-expressed effector proteins whose functional characterization has been already carried out by other laboratories (*hopC1* by Li *et al.,* (2005), and *hopAO1* by Underwood *et al.,* (2007), and Macho and Zipfel (2014)). Interestingly, when we measured the accumulation of *AtSN1* transcript in plants inoculated with either Δ*hopAO1* or Δ*hopC1* mutant strains at 24hpi*,* we found significantly lower levels of transcript in plants inoculated with Δ*hopC1* than in those inoculated with either Δ*hopAO1* or the wild-type (**Figure 2.4**). In fact, plants inoculated with Δ*hopC1* accumulate levels of *AtSN1* not significantly different from those observed immediately after inoculation (0 hpi) or at 24 hpi with a mock treatment. These results suggest that HopC1 is directly or indirectly responsible for the transcriptional activation of *AtSN1*. In the case of plants inoculated with Δ*hopAO1*, we consistently observed an increase in the levels of *AtSN1* transcript accumulated compared to wild type-inoculated plants, however these differences were not always statistically significant. Further analysis would be necessary to assess the possible role of HopAO1 as a suppressor of *AtSN1* transcriptional activation.

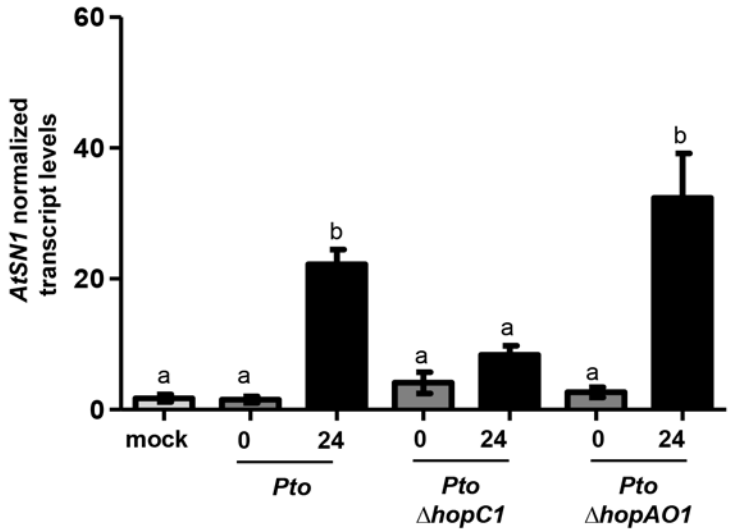

Figure 2.4. Accumulation of *AtSN1* transcript 24 hours post-inoculation with *Pto* DC3000 is significantly reduced in plants inoculated with Δ*hopC1*. Accumulation of *AtSN1* transcript was analysed using RT-*q*PCR in Col-0 plants 24 hours post-inoculation with *Pto* DC3000, or its Δ*hopC1* and Δ*hopAO1* mutant derivatives. Mock-inoculated plants were collected at 24 hpi and included as controls. Bars represent the mean values from 2 independent experiments with 3-6 plants per sample and experiment. Error bars represent the standard error. *AtSN1* expression levels were normalised to actin and the results presented as relative transcript accumulation compared to levels detected in *Pto* DC3000-infected plants 0 hpi. Mean values marked with the same letter were not significantly different from each other as established by One-way ANOVA, Benferroni PosHoc test (95% confidence intervals).

Both, *hopAO1* and *hopC1* are missing in *Pto* Δ*28E*, CUCPB5459 and CUCPB5451. Thus, to directly compare *AtSN1* transcript accumulation after infection with all these strains, we analyzed all of them side by side (**Figure 2.5**). ANOVA did not show statistically significant differences between the intermediate accumulation of *AtSN1* transcript in plants 24 hpi with Δ*hopC1* in this experiment, and those inoculated with either *Pto* DC3000, or its CUCPB5459 or Δ*28E* mutant derivatives. However, Student's t-test indicate that the levels of *AtSN1* transcript in plants 24 hpi with Δ*hopC1* is significantly lower than those displayed by plants inoculated with either *Pto* DC3000 (99% confidence interval), CUCPB5451 (99% confidence interval), CUCPB5459 (95% confidence interval), or Δ*hopAO1* (99% confidence interval), and significantly higher than the levels displayed by plants inoculated with Δ*28E* (99% confidence interval). Since all CUCPB5451, CUCPB5459 and *Pto* Δ*28E* mutants lack both *hopAO1* and *hopC1*, these results imply that there

must be other effector(s) directly or indirectly involved in determining the accumulation of *AtSN1* transcript, both increasing it and suppressing it.

Effector(s) candidate(s) that increase *AtSN1* transcripts accumulation could be encoded by cluster I (which includes effector genes *hopU1* and *hopF2*) or cluster X (which includes effector genes *hopAM1-2*, *hopX1*, *hopO1-1*, and *hopT1-1*). All these effectors genes (cluster I and X) are present in CUCPB5451 and are deleted in strains CUCPB5459 and Δ*28E*. Preliminary testing of mutants in either *hopU1* or *hopF2* show higher transcript levels by 24 hpi than those displayed by *Pto* DC3000, but these differences right in the limit of being statistically significant, perhaps due to functional redundancy (**Fig. 2.6**). Experiments analysing the accumulation of *AtSN1* transcript in plants inoculated with double (*hopU1 hopF2*) or triple mutants (*hopU1 hopF2 hopC1*) in these genes could shed light on their role in this process.

Nevertheless, the individual contribution of each effector is *AtSN1* expression is still complicated to clarify, because of the potentially complex and probable cross-talk between them. It is clear that several effectors directly or indirectly play a role in the determination of *AtSN1* transcript levels, although it is interesting and quite unexpected how, deletion of just one effector gene (e.g. *hopAO1*) can have a severe effect on the levels of transcript of this retrotransposon.

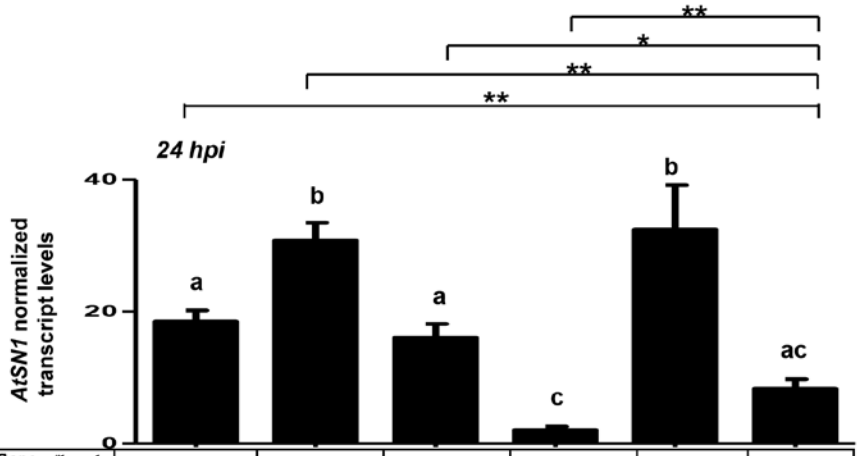

CLUSTERS	Gene "knock-out"	Pto DC3000	CUCPB5451	CUCPB5459	Δ28E	Δ hop AO1	Δ hop C1
	hopK1	hopK1	hopK1	hopK1	hopK1	hopK1	hopK1
	hopY1	hopY1	hopY1	hopY1	hopY1	hopY1	hopY1
I	hopU1	hopU1	hopU1	hopU1	hopU1	hopU1	hopU1
	hopF2	hopF2	hopF2	hopF2	hopF2	hopF2	hopF2
II	hopC1	hopC1	hopC1	hopC1	hopC1	hopC1	hopC1
	hopH1	hopH1	hopH1	hopH1	hopH1	hopH1	hopH1
IV	hopD1	hopD1	hopD1	hopD1	hopD1	hopD1	hopD1
	hop Q1-1	hop Q1-1	hop Q1-1	hop Q1-1	hop Q1-1	hop Q1-1	hop Q1-1
	hopR1	hopR1	hopR1	hopR1	hopR1	hopR1	hopR1
V	hopAH1	hopAH1	hopAH1	hopAH1	hopAH1	hopAH1	hopAH1
	hopAI1	hopAI1	hopAI1	hopAI1	hopAI1	hopAI1	hopAI1
	hop AM1-1	hop AM1-1	hop AM1-1	hop AM1-1	hop AM1-1	hop AM1-1	hop AM1-1
CEL (VI)	hopN1	hopN1	hopN1	hopN1	hopN1	hopN1	hopN1
	hop AA1-1	hop AA1-1	hop AA1-1	hop AA1-1	hop AA1-1	hop AA1-1	hop AA1-1
	hopM1	hopM1	hopM1	hopM1	hopM1	hopM1	hopM1
	avrE1	avrE1	avrE1	avrE1	avrE1	avrE1	avrE1
	hopB1	hopB1	hopB1	hopB1	hopB1	hopB1	hopB1
	hopAF1	hopAF1	hopAF1	hopAF1	hopAF1	hopAF1	hopAF1
	hopP1	hopP1	hopP1	hopP1	hopP1	hopP1	hopP1
	avrPto1	avrPto1	avrPto1	avrPto1	avrPto1	avrPto1	avrPto1
	hopE1	hopE1	hopE1	hopE1	hopE1	hopE1	hopE1
VIII	hopS2	hopS2	hopS2	hopS2	hopS2	hopS2	hopS2
	hopT1-2	hopT1-2	hopT1-2	hopT1-2	hopT1-2	hopT1-2	hopT1-2
	hopO1-2	hopO1-2	hopO1-2	hopO1-2	hopO1-2	hopO1-2	hopO1-2
	hopAQ1	hopAQ1	hopAQ1	hopAQ1	hopAQ1	hopAQ1	hopAQ1
IX	hopAA1-2	hopAA1-2	hopAA1-2	hopAA1-2	hopAA1-2	hopAA1-2	hopAA1-2
	hopV1	hopV1	hopV1	hopV1	hopV1	hopV1	hopV1
	hopAO1	hopAO1	hopAO1	hopAO1	hopAO1	hopAO1	hopAO1
	hopG1	hopG1	hopG1	hopG1	hopG1	hopG1	hopG1
	hopI1	hopI1	hopI1	hopI1	hopI1	hopI1	hopI1
	hopA1	hopA1	hopA1	hopA1	hopA1	hopA1	hopA1
X	hopAM1-2	hopAM1-2	hopAM1-2	hopAM1-2	hopAM1-2	hopAM1-2	hopAM1-2
	hopX1	hopX1	hopX1	hopX1	hopX1	hopX1	hopX1
	hopO1-1	hopO1-1	hopO1-1	hopO1-1	hopO1-1	hopO1-1	hopO1-1
	hopT1-1	hopT1-1	hopT1-1	hopT1-1	hopT1-1	hopT1-1	hopT1-1
	hopAB2	hopAB2	hopAB2	hopAB2	hopAB2	hopAB2	hopAB2
	avrPtoB	avrPtoB	avrPtoB	avrPtoB	avrPtoB	avrPtoB	avrPtoB
pseudogen	hopD´	hopD´	hopD´	hopD´	hopD´	hopD´	hopD´
"helper"	hopW1	hopW1	hopW1	hopW1	hopW1	hopW1	hopW1

Figure 2.5. Experimental and statistical analysis of the effector protein mutants used to confirm differences in accumulation of *AtSN1* transcript. Accumulation of *AtSN1* transcript was analysed using RT-*q*PCR in Col-0 plants 24 hpi with *Pto* DC3000, or its CUCPB5451 (missing clusters II, IV and IX), CUCPB5459 (missing clusters I, II, IV, IX and X), Δ*hopC1*, Δ*hopAO1*, and Δ*28E* mutant derivatives. Bars represent one experiment with 5 plants per strain. Error bars represent the standard error. *AtSN1* transcript levels were normalised to actin and the results presented as relative transcript accumulation compared to levels detected in *Pto* DC3000-infected plants 0 hpi . Mean values marked with the same letter were not significantly different from each other as established by One-way ANOVA, Benferroni PosHoc test. The values of each 24 hpi were compared to each other as well, as established by Student's T-test, (*95%, **99% confidence intervals).

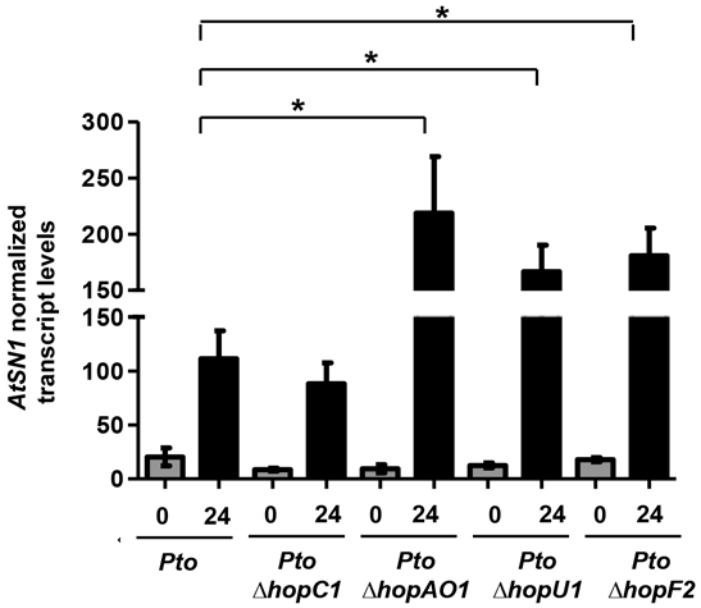

Figure 2.6. Accumulation of *AtSN1* transcript 24 hours post-inoculation with *Pto* DC3000 is significantly different in comparison to all single mutants used except of Δ*hopC1*. Accumulation of *AtSN1* transcript was analysed using RT-*q*PCR in Col-0 plants 24 hpi *Pto* DC3000, Δ*hopC1*, Δ*hopAO1*, Δ*hopU1* or Δ*hopF2* mutant derivatives. Bars represent the mean values from 2 independent experiments with 5-8 plants per sample and experiment. Error bars represent the standard error. *AtSN1* expression levels were normalised to actin and the results presented as relative mRNA accumulation compared to levels detected in *Pto* DC3000-infected plants 0 hpi. Mean values marked with the asterisk were significantly different from each other as established by Student T-test (95% confidence interval).

Chapter 3

AtSN1 transcript accumulation during different plant defence responses against *P. syringae*

3.1 AtSN1 transcript accumulation during basal defence response against P. syringae

The first line of defence against pathogens, the PAMP-triggered response or PTI, can be triggered by non-host pathogens, T3SS-deficient pathogen mutants (*e.g., ΔhrcV, ΔhrcC, ΔhrpL*) or externally applied PAMPs, such as flagellin. To determine if transcript levels for the retrotransposon *AtSN1* are also altered during PTI, we used the model bean pathogen *P. syringae* pv. *phaseolicola* 1448A (hereafter *Pph* 1448A), a non-host pathogen in *Arabidopsis* that causes no visible symptoms in Col-0 plants due to its triggering a strong, unsuppressed, PTI. No significant accumulation of *AtSN1* transcript was detected in plants 24 hpi with *Pph* 1448a (**Figure 3.1**), being this level not significantly different to those displayed by naïve, mock-inoculated or inoculated plants at 0 hpi, and clearly different from those displayed 24 hpi with *Pto* DC3000. These results are in keeping with our hypothesis of *AtSN1* transcript accumulation being the result of direct or indirect T3 effector activity.

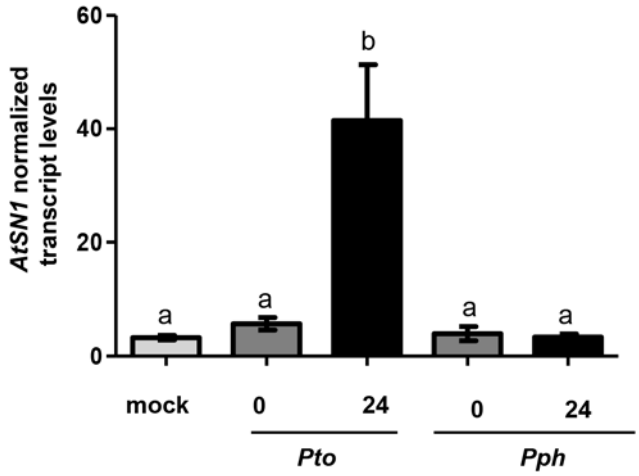

Figure 3.1. *AtSN1* transcript does not accumulate following inoculation with the non-host pathogen *Pph* 1448A. Accumulation of *AtSN1* transcript was analysed using RT-*q*PCR in Col-0 plants 24 hpi with *Pto* DC3000 or *Pph* 1448A. Mock-inoculated plants were collected at 24 hpi and served as a control for mechanical damage. Bars represent the mean values from 3 independent experiments with 3-5 plants per sample and experiment. Error bars represent the standard error. *AtSN1* transcript levels were normalised to actin and the results presented as relative transcript accumulation compared to levels detected in *Pto* DC3000-infected plants 0 hpi. Mean values marked with the same letter were not significantly different from each other as established by One-way ANOVA, Benferroni PosHoc test (99% confidence intervals).

FLS2 (Flagellin Sensing 2) senses the flagellin-derived peptide flg22, and triggers a signalling cascade which affects the expression of hundreds of genes (Boller and Felix, 2009; Navarro et al., 2004; Zipfel et al., 2004). Recently, it has been reported by Yu *et al.*, (2013) that flg22 depresses RNA-directed DNA Methylation (RdDM) in *Arabidopsis* leaves. RdDM is a plant regulatory mechanism that involves the biosynthesis of siRNAs that guide DNA methylation of transposons and repeats. These authors reported that external application of the flg22 peptide to *Arabidopsis* leaves induced the transcription of several transposons such as *EVD*, *Onsen* or *AtSN1*. To determine the role of flagellin in the transcriptional activation of transposons that takes place during infection with *Pto* DC3000, we analyzed the accumulation of *AtSN1* transcript in plants inoculated with a *Pto* DC3000 Δ*fliC* mutant derivative, which does not produce flagellin (Material and methods, **Table M1**). Since this strain does not carry any antibiotic resistance we confirmed the deletion of the *fliC* gene by PCR using primers listed in **Table M4** (**Figure 3.2A**), and confirmed its motility defect using a *swimming* assay (**Figure 3.2B**). As expected, the Δ*fliC* mutant is non-motile. When *AtSN1* transcript levels were measured 24 hpi in a Δ*fliC* mutant strain, we observed a significant accumulation of *AtSN1* transcript compared to 0 hpi, although this accumulation was significantly smaller than that detected in plants 24 hpi with *Pto* DC3000 (**Figure 3.2C**). Thus, we can conclude that in the context of an infection by *Pto* DC3000, flagellin also contributes to the transcriptional activation of *AtSN1* transcript, although it does not do so to the same extent than the T3SS. Moreover, transcriptional activation of *AtSN1* is not a general feature of all PTI responses since that triggered against *Pph* 1448a does not activate this transposon.

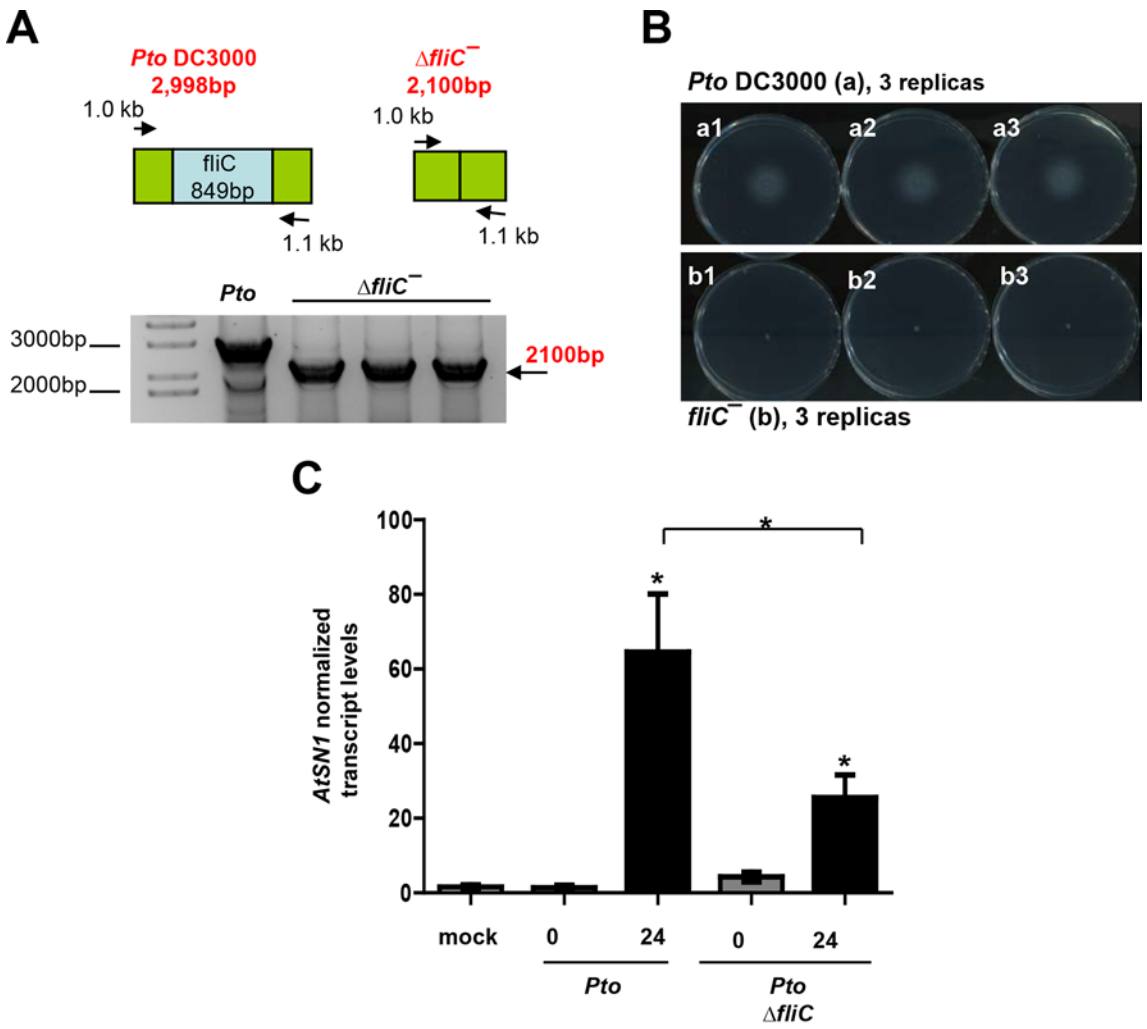

Figure 3.2. Accumulation of *AtSN1* transcript 24 hours post-inoculation with *Pto* DC3000 is partially dependent on flagellin. (**A**) PCR confirmation of the deletion of *fliC* in the Δ*fliC* strain. Genomic DNA of *Pto* DC3000 was used as a control. (**B**) Motility (swimming) assay. Bacterial strains were incubated for 2 days at 23°C on soft agar, King's B containing 10 mM $MgCl_2$ plate. The image shows 3 independent biological replicates for each strain (*Pto* DC3000; a1, a2, a3 and Δ*fliC;* b1, b2, b3) (**C**) Accumulation of *AtSN1* transcript was analysed using RT-*q*PCR in Col-0 plants 24 hpi with *Pto* DC3000 or *Pto* Δ*fliC*. Mock-inoculated plants collected at 24 hpi, were included as controls. Bars represent the mean values from 2 independent experiments with 3-5 plants per sample and experiment. Error bars represent the standard error. *AtSN1* transcript levels were normalised to actin and the results presented as relative transcript accumulation compared to levels detected in *Pto* DC3000-infected plants 0 hpi**.** Each time 0 hpi sample was compared to its 24 hpi. The values of each 24 hpi were compared to each other as well, and were shown to be statistically different as established by Student's T-test, (95% confidence intervals).

3.2 AtSN1 transcript accumulation is enhanced during effector-triggered immunity against P. syringae

The second layer of plant defence is associated to a severe rapid localized programmed cell death at the site of infection, called the HR (hypersensitive response) and triggered upon direct or indirect recognition of effectors, thus giving raise to its name of effector-triggered immunity (ETI) (Dangl and Jones, 2001). Our results show that accumulation of *AtSN1* transcript is dependent on a functional T3SS and activated by T3Es. However, transcriptional activation of *AtSN1* could be part of the virulence activity of T3Es, or part of the plant defence response triggered against them. The fact that our results also show that this activation can be suppressed by effectors, and it is partially dependent on flagellin, suggests the second hypothesis as the most likely, *i.e.,* that transcriptional activation of *AtSN1* could be part of the plant defence response, and be triggered during both PTI, and up to a larger extent ETI.

If accumulation of *AtSN1* during infection with *Pto* DC3000 is associated to ETI-defences, it would be expected to be significantly increased during an incompatible interaction, *i.e.* interaction with *Pto* expressing an effector that triggers the HR in *Arabidopsis*. To explore this possibility, we analyzed the accumulation of *AtSN1* transcript in Col-0 plants 24 hpi with *Pto* DC3000 constitutively expressing *Arabidopsis* avirulent genes (Avr) from a plasmid. Expression of these *avr* effector genes lead to activation of the HR, which is fully dependent on the corresponding R gene. We analyzed plants inoculated with *Pto* DC3000 expressing: (i) AvrRpt2, a well-characterized Avr effector whose activity is recognized by the product of the *RPS2* gene in *Arabidopsis*, encoding a typical CC-NB-LRR (coiled-coil, nucleotide-binding site and leucine-rich repeat) resistance protein whose activity depends on salicylic acid (SA) (Kunkel et al., 1993; Yu et al., 1993); (ii) AvrRpm1, whose activity is recognized by the product of *RPM1*, in a SA-independent manner (Dangl et al., 1992; Katagiri et al., 2002); (iii) AvrRps4, whose activity is recognized by RPS4, a member of the TIR (Toll and Interleukin-1 Receptor) subclass of NBS-LRR (Nucleotide-binding site leucine-rich repeat) which does not depend on SA (Hinsch and Staskawicz, 1996); and (iv) HopZ1a whose activity is

recognized by the product of *ZAR1*, an atypical R gene that acts independently of SA or other defence pathways previously described, and in whose functional characterization our laboratory has contributed (Macho et al., 2010). All these plasmids have been previously used in our laboratory and shown to determine the activation of the HR when expressed from *Pto* DC3000 and to cause a strong reduction of bacterial growth in *Arabidopsis* Col-0, both dependent on the functionality of the corresponding R genes. Analysis of *AtSN1* transcript accumulation during the activation of these four different defence pathways in Col-0 plants (**Figure 3.3A**) showed significantly increased levels of transcript in all four cases compared to those displayed by plants 24 hpi with *Pto* DC3000, independently of the type of signalling cascade defence response involved. These increases were not detected when plants carrying mutations in the corresponding R genes were used (**Figure 3.3B**). **Figure 3.3C** shows another representation of the results obtained in 3.3B for later comparison.

These results further support the notion of *AtSN1* transcriptional activation being part of the defence response of the plant to T3Es, *i.e.* part of the ETI or effector-triggered immunity, and not therefore the result of the virulence activity of one or more effectors. These results together with those obtained through the analysis of effector mutants in Chapter 2, suggest a model in which the plant defence response against some of the *Pto* DC3000 effectors would include the transcriptional activation of transposons, presumably prior modification of their chromatin, while the virulence activity of other T3Es would partially suppress it, directly or indirectly as part of a defence suppression mechanism.

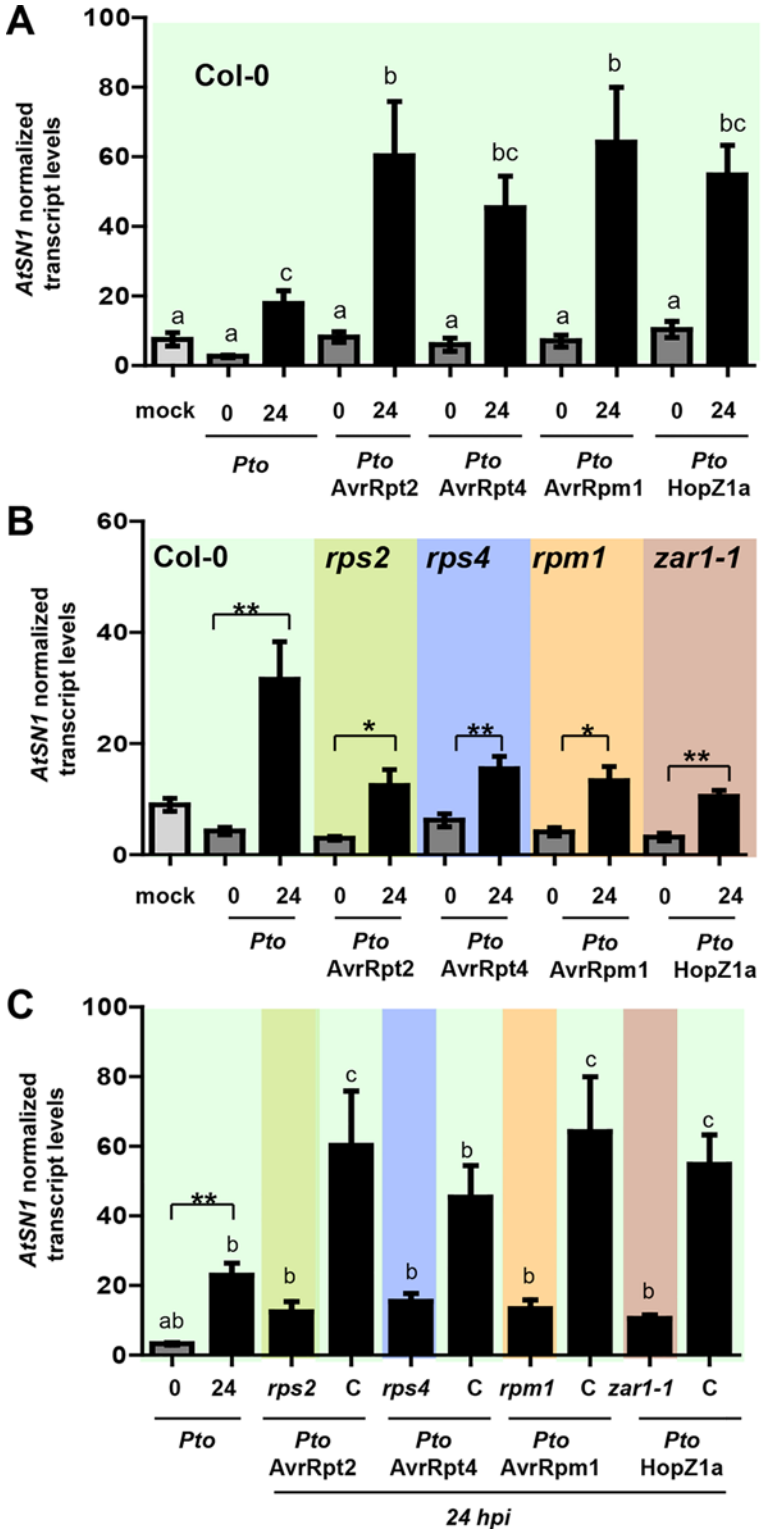

Pto overexpressing	R genes in *Arabidopsis*
AvrRpt2	RPS2
AvrRpt4	RPS4
AvrRpm1	RPM1
hopZ1a	ZAR1

Figure 3.3. Analysis of *AtSN1* transcript accumulation upon activation of different ETI responses. (**A**) Accumulation of *AtSN1* transcript 24 hpi with *Pto* DC3000 is increased when AvrRpt2, AvrRpt4, AvrRpm1 or HopZ1a are expressed from a plasmid. Accumulation of *AtSN1* transcript was analysed using RT-*q*PCR in Col-0 plants 24 hpi with *Pto* DC3000 or *Pto* overexpressing AvrRpt2, AvrRpt4, AvrRpm1 or HopZ1a. Mock-inoculated plants were collected at 24hpi and included as controls. Bars represent the mean values from 3 independent experiments with 5-15 plants per sample and experiment. Error bars represent the standard error. *AtSN1* transcript levels were normalised to

actin and the results presented as relative transcript accumulation compared to levels detected in *Pto* DC3000-infected plants 0 hpi. Mean values marked with the same letter were not significantly different from each other as established by One-way ANOVA, Benferroni PosHoc test, (95% confidence intervals). (**B**) Accumulation of *AtSN1* transcript 24 hpi of Col-0 plants with *Pto* DC3000 expressing AvrRpt2, AvrRpt4, AvrRpm1 or HopZ1a is reduced in mutants on the R genes responsible for the triggering immunity against AvrRpt2, AvrRpt4, AvrRpm1 and HopZ1a. Accumulation of *AtSN1* transcript was analysed using RT-*q*PCR in Col-0, *rps2*, *rps4*, *rpm1* and *zar1-1* plants 24 hpi with *Pto* DC3000 or *Pto* overexpressing AvrRpt2, AvrRpt4, AvrRpm1 or HopZ1a. Mock-inoculated plants at 24 hpi were included as controls. Bars represent the mean values from 2 independent experiments with 3-5 plants per sample and experiment. Error bars represent the standard error. *AtSN1* transcripts levels were normalised to actin and the results presented as relative transcript accumulation compared to levels detected in *Pto* DC3000-infected plants 0 hpi. Each time 0 hpi samples were compared to its 24 hpi and were shown to be statistically different as established by Student's T-test, (95% confidence intervals). (**C**) Accumulation of *AtSN1* transcript 24 hpi of Col-0 plants with *Pto* DC3000 overexpressing AvrRpt2, AvrRpt4, AvrRpm1 or HopZ1a in plants carrying mutations on the corresponding R genes is similar to that observed in Col-0 plants (marked with C) inoculated with *Pto* DC3000. Samples were analysed by One-way ANOVA, Bonferroni PosHoc test and mean values marked with the same letter were found to be not significantly different from each other (95% confidence intervals).

To support this model, we tested whether accumulation of *AtSN1* transcripts could be triggered by exogenous salicylic acid (SA) treatment. If this accumulation was associated to ETI responses, exogenous SA would be expected to trigger it. Previous data have shown that SA treatment induces changes in the DNA methylation profiles (hyper and hypomethylation) at transposons and other sequences, and that these changes are associated with transcriptional alterations (Dowen et al., 2012). However, no specific information about the levels of transcript for *AtSN1* during SA treatment was reported. Plants were sprayed with a hormone solution (Salicylic Acid, 5 days of 1 mM SA+ 0.01% of Silwet L-77) and analyzed 6 days after the treatment. Control plants (naïve and mock) were grown under the same conditions and analyzed in parallel. However, these control plants were maintained far apart from the treated group to avoid cross-activation. Mutants *ddm*1, *ago4-2* and *met1-3* were included as positive controls for *AtSN1* transcriptional activation. RT-semi*q*PCR analyses showed that *AtSN1* accumulated in plants treated with SA (**Figure 3.4A**). We also analyzed the accumulation of PR1 (pathogenesis-related protein 1, At2g14610) transcripts as a control of the activation of the SA response, since its expression has been previously shown

to be induced in response to exogenous SA application (Ryals et al., 1996), as well as the transcript levels of At1g13470 as this locus shows SA-dependent demethylation and transcriptional activation (Dowen et al., 2012). **Figure 3.4A** shows that *AtSN1* transcripts were induced after SA-treatment, supporting that its transcriptional activation was associated to plant defence responses. Plants treated with 1mM SA showed necrotic lesions on the leaves that started to appear 4 day post-treatment (**Figure 3.4B**), further confirming the activation of the SA-dependent defence response.

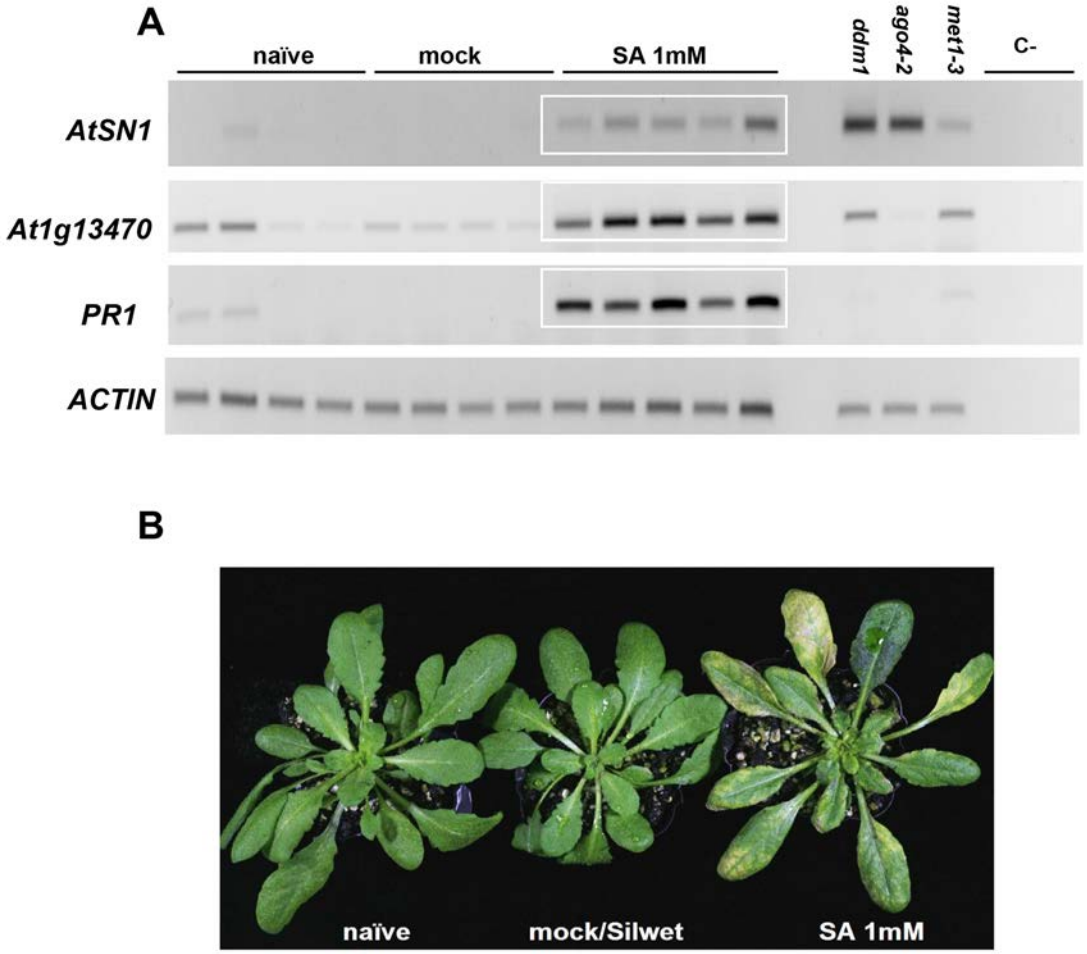

Figure 3.4. *AtSN1* transcript accumulates in plants treated with exogenous salicylic acid.
(**A**) RT-semi*q*PCR of *AtSN1, At1g13470* and *PR1* in Col-0 plants treated with salicylic acid. RT-semi*q*PCR was performed using cDNA obtained from leaves treated for 5 days with 1mM SA supplemented with 0.01% of Silwet, 24 hours after the treatment. Naïve samples were harvested on the sixth day together with the mock samples treated only with 0.01% Silwet. Accumulation of actin transcripts was determined and used as an internal control. *Arabidopsis ddM1, ago4-2* and *met1-3* mutants were used as a positive control for accumulation of *AtSN1* transcript. (**B**) Plants treated with 1mM SA display necrotic lesions after 4 days of treatment.

Chapter 4

Role of key genes in establishing and maintaining plant DNA methylation levels in the plant defence response against *Pto* DC3000

4.1 Analysis of the impact of Pto DC3000 infection on the expression of plant methylases and demethylases

Yu and collaborators (2013) previously reported that treatment of *Arabidopsis* leaves with the flagellin peptide flg22 represses RdDM (RNA-directed DNA methylation) activity by down-regulating some of the key components of this pathway, such as the Argonaute protein AGO4, the Nuclear RNA Polymerase D2 (NRPD2), the Nuclear RNA Polymerase E5 (NRPE5), or the chromatin-remodelling factor DRD1 (Defective in RNA-directed DNA methylation 1). Unexpectedly, this report did not include the analysis of the effects of flg22 treatment on the transcript levels of DRM2, a *de novo* DNA methyltansferase known to be involved in RdDM, reporting instead down-regulation of the maintenance DNA methyltransferase MET1. In addition, MET1 and the chromatin remodeler DDM1 are both down-regulated in response to *Pto* infection or salicylic acid treatment (Dowen et al., 2012). To gather additional insight on the effect of the infection with *Pto* on the plant DNA methylation machinery, we monitored transcript levels of the plant DNA methyltransferases, DRM2, MET1 and CMT3 as well as the demethylase ROS1 (a DNA glycosylase that removes methylcytosines from DNA, (Penterman et al., 2007)), during infection with *Pto* DC3000. *Arabidopsis* plants inoculated with *Pto* DC3000, showing activation of the retrotransposon *AtSN1* 24 hpi (**Figure 4.1**), displayed significant down-regulation of *MET1* and *ROS1* transcript levels. These results are in agreement with previous reports since *ROS1* is known to be robustly down-regulated in DNA methylation-defective mutants (Martínez-Macías et al., 2012; Mathieu et al., 2007). We did not find evidence of *Pto* DC3000 infection having any impact on *CMT3* transcript levels, but detected a robust up-regulation of *DRM2* (*de novo* DNA methyltransferase) not previously reported (**Figure 4.1**).

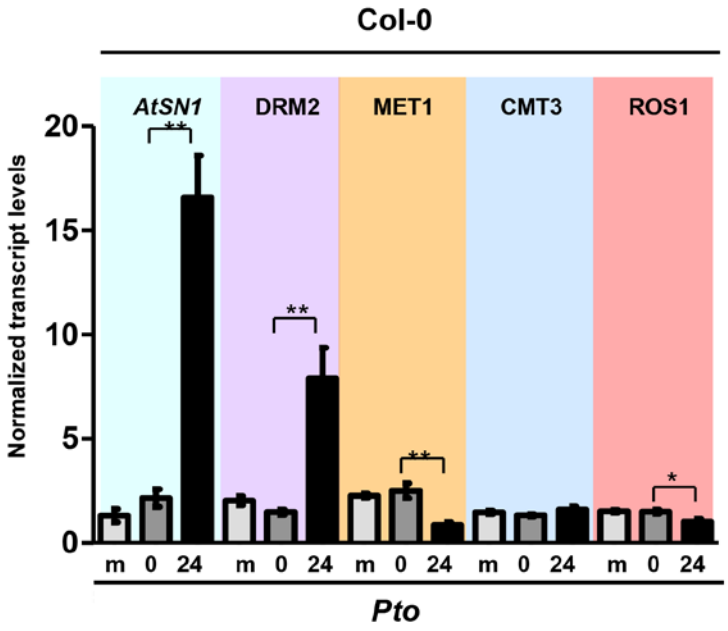

Figure 4.1. Expression of the plant DNA methyltransferases and demethylases upon *Pto* DC3000 infection. Normalized transcript levels of the retrotransposon *AtSN1*, de novo DNA methyltransferase (*DRM2*), the maintenance DNA methyltransferases (*MET1* and *CMT3*) and the DNA demethylase (*ROS1*) were determined by reverse transcription quantitative PCR (RT-*q*PCR) in *Pto* DC3000-infected *Arabidopsis* Col-0 plants 0 and 24 hpi. Mock-inoculated plants (m, 10 mM $MgCl_2$) were included as a control for the basal transcript levels. Transcript levels were normalised to actin and the results presented as relative transcript accumulation compared to levels detected in plants 0 hpi with *Pto* DC3000. Bars represent the mean values from 2 independent experiments with 2-5 plants per sample and experiment. Error bars represent the standard error. Asterisks indicate samples that are statistically different from 0 hpi sample as determined by Student's t-test with the 99% (**) or the 95% (*) confidence interval.

4.2 Bacterial entry and development of disease in plant DNA methylation mutants

Microbial entry into the host tissue is a critical first step of the infection process in both animals and plants. In plants, microscopic surface openings (such as stomata or hydathodes) or wounds, serve as ports of bacterial entry during infection (Melotto et al., 2006). Upon detection of incoming bacteria the plant triggers stomata closure as part of the innate immunity response to prevent entry of the pathogen. These initial steps of the bacteria-plant interaction are bypassed when plants are inoculated by infiltration, an inoculation procedure that artificially delivers bacteria directly underneath the epidermis. However, natural infection, including these early steps, can be

mimicked through dip or spray inoculation. These means of inoculation are less efficient and more variable but can provide additional information about the relevance of the early steps on the different outcomes of the plant-pathogen interaction. Previous reports have demonstrated that the loss of DNA methylation enhances resistance to bacteria inoculated by infiltration (Agorio and Vera, 2007; Dowen et al., 2012). Thus, we considered of interest to analyse how the methylation status of the plant affects the interaction with spray-inoculated bacteria.

We spray-inoculated plants with bacterial strains carrying mutations on genes relevant to the early steps of the infection process, *i.e.* a mutant defective in flagellin or coronatine production, as well as with wild type and wild type expressing the avirulence determinant AvrRpt2, as controls. We analysed their interaction with plants carrying each one of the following mutations: *met1-3, ago4-2, ddc,* and *ros1-4*. Symptom development was monitored after spray-inoculating 1 x 10^7 cfu/ml of the different strains, an inoculation dose sufficient to induce stomata closure at 1 hpi and coronatine-mediated stomata reopening at 3 hr in wild type infections (Melotto et al., 2006).

Wild-type Col-0 plants inoculated with *Pto* DC3000 developed yellow necrotic lesions typical of disease development by 8 dpi, whereas those inoculated with *Pto* DC3000 expressing AvrRpt2 looked healthier, in keeping with AvrRpt2 triggering immunity (**Figure 4.2**). Plants inoculated with a COR$^-$ mutant, expected to be severely attenuated when inoculated onto the leaf surface, but not when infiltrated directly into the apoplast (Brooks et al., 2004; Mittal and Davis, 1995), displayed symptoms more similar to mocked-inoculated plants than to plants inoculated with the wild-type strain. Interestingly, plants inoculated with a Δ*fliC* mutant, which does not trigger FLS2-mediated PTI, displayed stronger disease symptoms that those inoculated with the wild-type strain (**Figure 4.2**). Although the role of FLS2-mediated PTI in plant defence against *P. syringae* is undisputed (Jones and Dangl, 2006), this has been established using exogenously applied flg22 and the interaction between strains deficient in flagellin production and the plant has never been previously characterised.

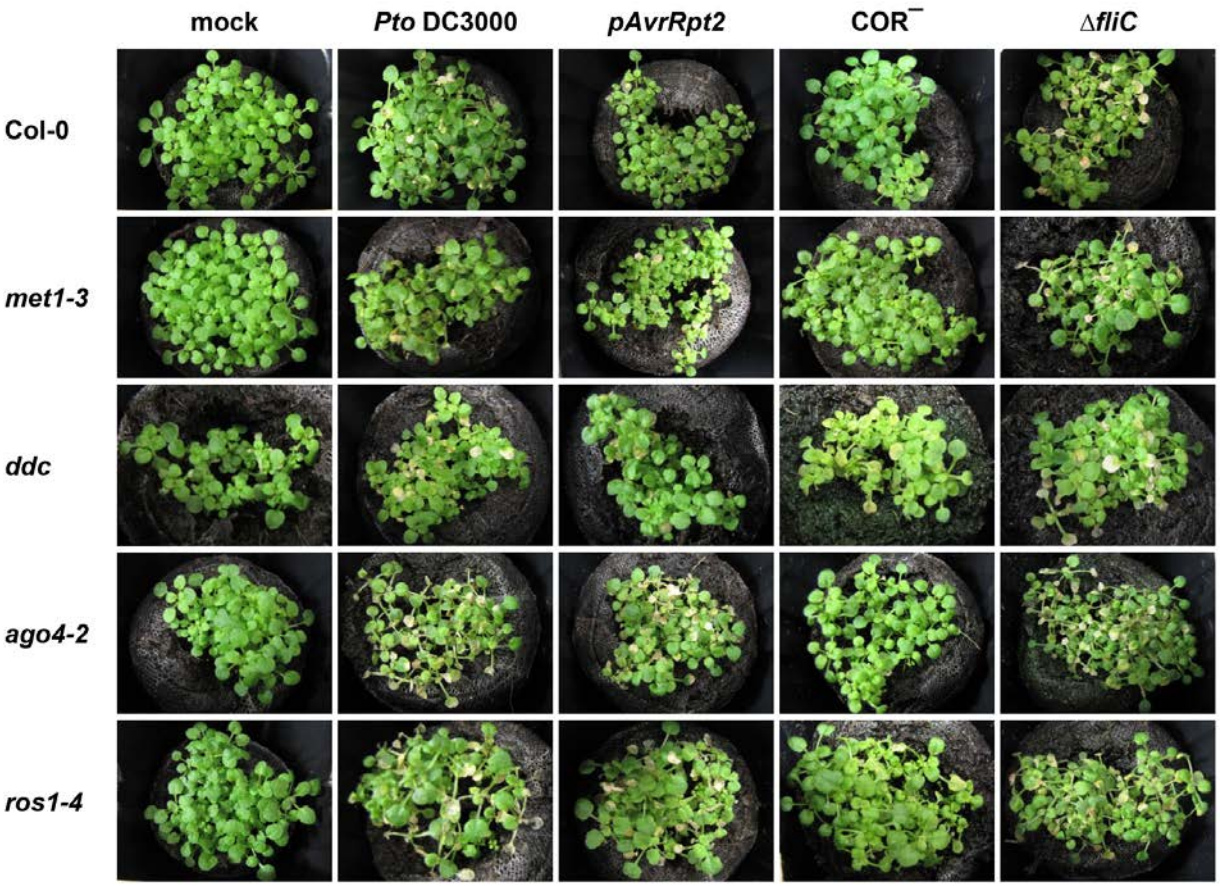

Figure 4.2. Plant genotypes affected in DNA methylation differentially affect disease development following spray-inoculation. Symptom development was monitored and documented in Col-0 wild type, *met1-3*, *ddc*, *ago4-2*, and *ros1-4* spray-inoculated with 0.02% of Silwet and $1x10^7$ cfu/ml of either *Pto* DC3000, *Pto* DC3000 expressing AvrRpt2, Δ*fliC*, or COR$^-$. Images shown were taken 8 dpi and are representative of 6 replicates per bacterial strain and plant genoptype. The experiment was repeated 3 times with similar results.

When *met1-3* plants were inoculated, we obtained similar results to those displayed by wild-type plants for all inoculated strains. When the triple mutant strain *ddc* was surveyed, plants inoculated with wild type, and remarkably with COR$^-$, but not Δ*fliC* or *Pto* DC3000 expressing AvrRpt2 displayed stronger symptoms than the corresponding wild-type plants (**Figure 4.2**), suggesting than defences different from FLS2-mediated PTI, or RPS2-mediated ETI, may be compromised in this plant genotype. The fact that clear symptoms can be observed in *ddc* mutants inoculated with COR$^-$ raises the interesting possibility of these plants being impaired for stomata closure upon pathogen detection.

The *ago4-2* mutant displayed stronger disease symptoms than wild type when inoculated with *Pto* DC3000, *Pto* DC3000 expressing AvrRpt2 or Δ*fliC* (**Figure 4.2**), in keeping with previous reports indicating than these plants are more susceptible to *Pto* DC3000 regardless of whether they are in a compatible or an incompatible interaction (Agorio and Vera, 2007). However, the fact that *ago4-2* plants inoculated with COR$^-$ do not display any symptoms support the notion that, regardless of their general defect on defences, they are still capable of closing stomata upon pathogen detection.

Finally, when *ros1-4* plants were analysed, enhanced symptoms could be observed for all strain tested, including COR$^-$ was used (**Figure 4.2**). These results are very interesting since they suggest the implication of ROS1 in both ETI and PTI defences, including stomata closure. However, the difference in plants inoculated with Δ*fliC* were not as clear. In order to obtain a clearer view on this issue, we spray-inoculated 3 week old plants (1 week older than those showed in **Figure 4.2**), five plants per pot (total of 25 plants), of each Col-0 and *ros1-4* genotypes with either *Pto* DC3000 or Δ*fliC* strains (**Figure 4.3**). By 14 dpi, *ros1-4* mutant plants inoculated with *Pto* DC3000 showed more susceptibility, displayed as stunted growth and stronger yellowing, than Col-0 plants inoculated with *Pto* DC3000. Moreover, in keeping with the results shown in **Figure 4.2**, wild-type plants inoculated with the Δ*fliC* mutant strain displayed stronger symptoms than those inoculated with wild type bacteria. This increase in the severity of the symptoms developed upon inoculation with the Δ*fliC* strain was also apparent when *ros1-4* plants were analyzed. Thus, the results indicate that the increased susceptibility observed in *ros1-4* mutant inoculated with the wild-type strain is not due to a failure to establish flagellin-mediated PTI. This is of particular relevance considering that Yu and collaborators (Yu et al., 2013) recently reported that treatment with flg22 triggers local hypomethylation and activation of transcriptionally silenced loci in a *ROS1*-dependent manner, and therefore support the involvement of ROS1 in more than one type of defence response.

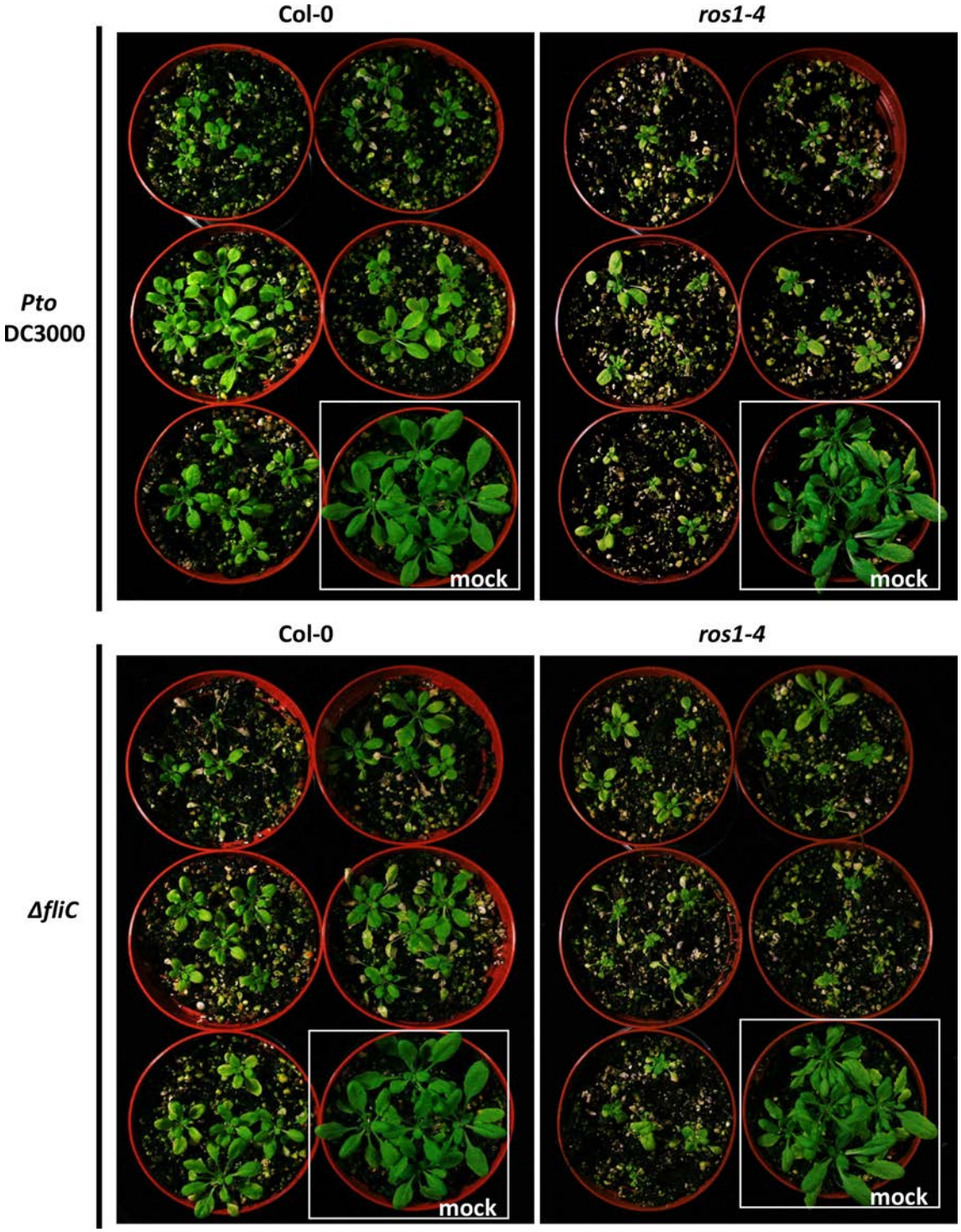

Figure 4.3. Mutant *ros1-4* shows increased susceptibility to wild type and *ΔfliC* bacteria. Symptoms development was monitored and documented in Col-0 wild type and *ros1-4* spray-inoculated with 0.02% of Silwet and 1x10^7 cfu/ml of either *Pto* DC3000 or Δ*fliC*. Images shown were taken 14 dpi and are representative of 3 independent experiments with 15 plant replicates per bacterial strain and plant genotype. The experiment was repeated 3 times with similar results.

To further explore the link between ROS1 and antibacterial defence, we tested the resistance of the *ros1-4* mutant to proliferation of infiltrated *Pto* DC3000. By 4 dpi, we could observe a mild, although significant increase in wild type bacterial growth in *ros1-4* plants compared to growth observed in wild type plants (**Figure 4.4A**). These results are in keeping with a role of ROS1-dependent DNA demethylation in antibacterial resistance. Since Yu and collaborators described this role as flagellin-dependent, but our results suggest its additional involvement in flagellin-independent defence responses, including stomata closure, we also tested growth of the Δ*fliC* and COR$^-$ in *ros1-4* plants. Both mutant strains grew significantly better in *ros1-4* than in Col-0 plants indicating that the effect of *ros1-4* on bacterial growth still takes place in the absence of flagellin, so it is not flagellin-dependent, and it also takes place in the absence of coronatine, so it is not coronatine-dependent either.

Finally, we also analysed whether the effects of *ros1-4* on bacterial growth would also affect growth of a Δ*hrcV* mutant, which lacks a type III secretion system (**Figure 4.4B**). Although in this experiment the effect of *ros1-4* in growth of *Pto* DC3000 was below statistical significance, the increase in growth of both the Δ*fliC* and COR$^-$ mutants was clearly observed. Surprisingly, growth of the Δ*hrcV* was not increased but significantly decreased in comparison to the growth observed in Col-0 wild type plants. This bacterial strain lacks a functional T3SS and does not translocate any effector inside the host cell, but produces coronatine and possesses all functional elicitors of PTI (e.g. flagellin), which in the absence of effectors are not suppressed (Katagiri and Tsuda, 2010).

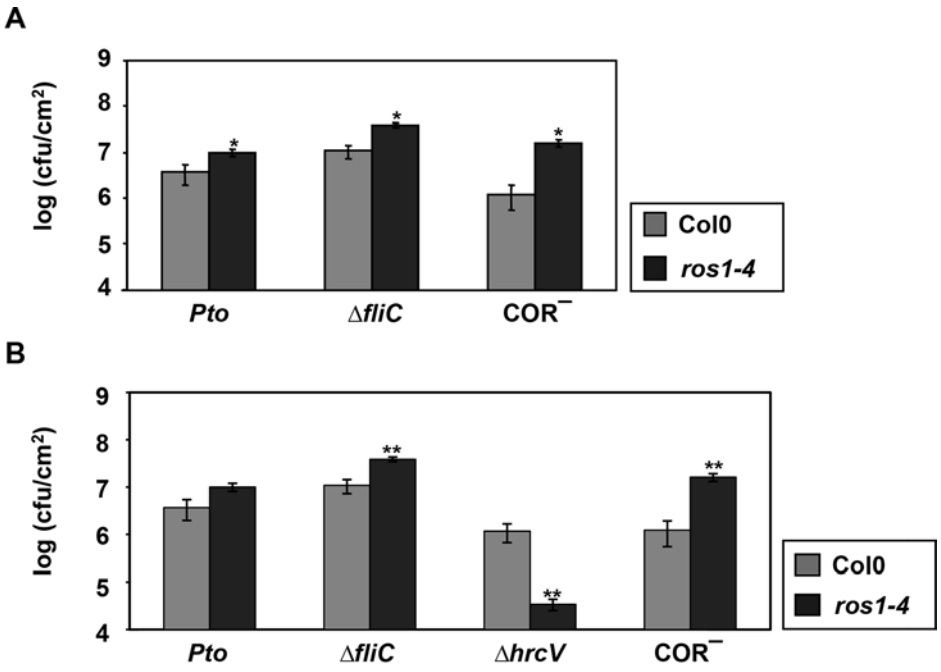

Figure 4.4. Bacterial replication is increased in the DNA methylation mutant *ros1-4*. Plants of Col-0 and *ros1-4* were inoculated with 5x10^4 cfu/ml of either *Pto* DC3000 (**A** and **B**), Δ*fliC* (**A** and **B**), *ΔhrcV* (**B**) or COR$^-$ (**A** and **B**). Three disc leaves per plant were collected and processed just after the inoculation (0 dpi), and by 4 dpi. Bacterial colonies were counted and represented in logarithmical scale. Error bars represent the standard error. Mean cfu values obtained from *ros1-4* plants were compared to the corresponding value obtained for the same strain and time point from Col-0 wild type plants. Asterisks indicate significant differences as established by Student t-test, with 95% (*), 99% (**) confidence interval difference. Experiment was repeated twice with similar results.

4.3 Bacterial replication in DNA methylation mutant plants

Some plant genotypes with altered DNA methylation levels (*met1-3*, *ddc*, *ddm1*, *drd1*, *nrpd1a,* etc.) have been previously reported to differentially affect growth of *P. syringae* (Agorio and Vera, 2007; Dowen et al., 2012; Yu et al., 2013)). Among the mutants analysed in this work, *ros1-4, ago4-2* and *met1-3* have been previously tested for growth of *P. syringae.* Whereas *Pto* DC3000 has been reported to grow more in an *ago4-2* and *ros1-4* mutant than in wild-type plants (Agorio and Vera, 2007, Yu et al., 2013), it was reported to growth less in a *met1-3* mutant (Dowen et al., 2012). While the results reported for *ago4-2* plants are in keeping with the results shown in **Figure 4.2** where *ago4-2* plants displayed stronger disease symptoms following inoculation with *Pto* DC3000 than wild type, those reported for *met1-3* mutant are not so clear, since no changes in the development of symptoms associated to *Pto* DC3000 infection could be observed in these

plants when compared to wild type plants (**Figure 4.2**). To gather additional insight on the effect of these two plant genotypes in our system and experimental conditions, we analysed growth of *P. syringae* strains using two different approaches, individual and mixed infections.

First, *Pto* DC3000 was inoculated by infiltration into wild type, *ago4-2* and *met1-3* plants and bacterial growth was analysed 2 and 4 dpi (**Figure 4.5**). In keeping with previous results and reports, the changes in methylation of the *ago4-2* mutant benefit the pathogen, since a significant increase in growth could be already detected by 2 dpi. By 4 dpi, replication levels in the mutant were almost 10-fold higher than those reached in wild type Col-0 plants (**Figure 4.5**). When bacterial growth was analyzed in *met1-3* plants we observed a significant decrease in bacterial growth in comparison to that found in wild-type plants (**Figure 4.5**). By 4 dpi, replication levels in the mutant were almost 10-fold higher than those reached in wild type Col-0 plants (**Figure 4.5**). When bacterial growth was analyzed in *met1-3* plants, we observed a significant decrease in bacterial growth in comparison to that found in wild-type plants (**Figure 4.5)**. This result is in keeping with previous reports and supports a role for MET1 in disease development, since in its absence bacterial growth is impaired.

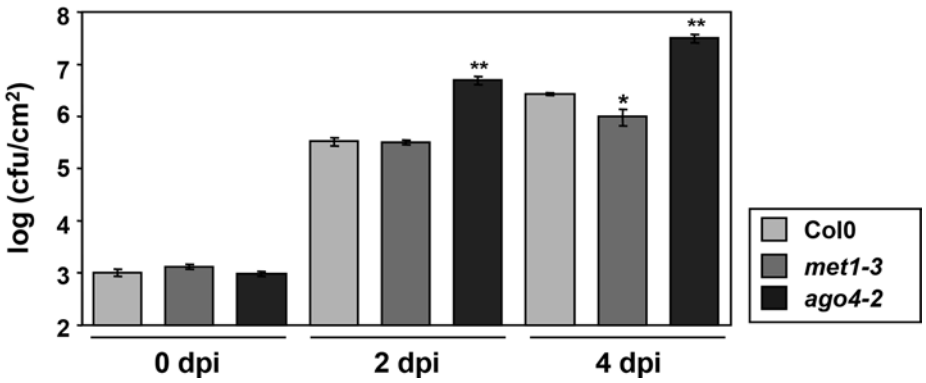

Figure 4.5. Bacterial replication is differentially altered in plant genotypes affected in DNA methylation. Plants of Col-0, *met1-3* and *ago4-2* were inoculated with 5x10⁴ cfu/ml of *Pto* DC3000. Three disc leaves per plant were collected and processed just after the inoculation (0 dpi), and by 4 dpi. Bacterial colonies were counted and represented in logarithmical scale. Error bars represent the standard error. Mean cfu values obtained from mutant plants were compared to the corresponding value obtained for the same strain and time point from Col-0 wild type plants. Asterisks indicate significant differences as established by Student t-test, with 95% (*), 99% (**) confidence interval difference. Experiment was repeated twice with similar results.

To further characterize the impact that changes in methylation have on bacterial growth, we applied Competitive Index (CI) assays. CI assays are based on directly comparing growth of two strains within the same plant by co-inoculating them in equal amounts and analysing their ratio after growth within the plant. If a CI is not significantly different to one, growth within the plant of the co-inoculated strains is not significantly different, while if the value of the CI is significantly less than one, *in planta* growth of one of the strains is significantly worse than growth of the other (Macho et al., 2007). CI assays can also be used to determine the impact on bacterial growth of a plant genotype, but in this case bacterial cfu for each of the strains used in each CI values have to be taken into account as well (Macho and Beuzón, 2010; Macho et al., 2010). For this purpose, we determined the CIs in these three plant genotypes, wild type, *ago4-2* and *met1-3* plants of three different strains (Δ*hrcV*, COR⁻ and pAvrRpt2) against the wild type *Pto* DC3000 (**Figure 4.6**, left panels). The cfu numbers corresponding to each CI is also represented (**Figure 4.6**, right panels).

Although no significant changes could be established for the CI of the Δ*hrcV* mutant between Col-0 and the *ago4-2* and *met1-3* mutant plants, and as

expected they all showed significant attenuation for the Δ*hrcV* mutant (CIs significantly different from 1), significant changes in bacterial counts were detected between the plant genotypes (**Figure 4.6A**). Growth of the Δ*hrcV* mutant was significantly increased in both *met1-3* and *ago4-2* plants. However, growth of the wild type strain was only significantly changed in *ago4-2* plants, where it was increased compared to growth in Col-0 and *met1-3* plants. These results as well as those shown in **Figure 4.2**, suggest that the involvement of MET1 in the development of disease is not as determinant as the role of AGO4 in the establishment of plant defences.

In addition, to determine the ability of these plant mutants to trigger a SA-dependent ETI, we analysed the CI of *Pto* DC3000 constitutively overexpressing AvrRpt2 from a plasmid, in mixed infection with the wild type strain, in wild type Col-0, *met1-3* and *ago4-2* plants. The CI of this strain in wild-type plants showed an attenuation close to 100-fold (**Figure 4.6B**), as expected from the expression of AvrRpt2 triggering *RPS2*-mediated resistance (Macho et al., 2010; Macho et al., 2009). No significant changes were observed between the CIs obtained in these three plant genotypes. No significant changes were observed in growth of any of the co-inoculated strains in *met1-3* plants either, in line with the results obtained in previous experiments where the contribution of MET1 to bacterial growth and disease development is not always clear. Interestingly, growth of *Pto* DC3000 expressing AvrRpt2, but not that of *Pto* DC3000, was significantly higher in *ago4-2* plants than in wild-type Col-0 (**Figure 4.6B**). These results indicate that *AGO4* is also required for effector-triggered ETI immunity, as expected from the results shown in **Figure 4.2** as well as with previous reports (Agorio and Vera, 2007). Moreover, since growth of the wild type strain in *ago4-2* plants is significantly increased compared to growth in Col-0 plants when following individual inoculation (**Figure 4.5**), these results also show that co-inoculation with *Pto* DC3000 expressing AvrRpt2 in *ago4-2* seems to limit growth of the wild type strain. Previous work has shown than in Col-0 plants co-inoculation of *Pto* DC3000 with $5x10^4$ cfu/ml *Pto* DC3000 expressing AvrRpt2 avoids interference between AvrRpt2-triggered immunity and growth of the wild type strain, whereas higher inoculation doses lead to a dominant

negative effect on the growth of the wild type bacterial strain (Macho et al., 2007). Thus, the observed limitation of growth of *Pto* DC3000 when co-inoculated with *Pto* DC3000 expressing AvrRpt2 in *ago4-2* is likely to be the result of a dominant negative effect caused by an enhanced defence response against AvrRpt2 in the absence of AGO4.

We also determined the CIs for the COR$^-$ mutant in these plant mutant backgrounds. No significant growth attenuation was detected for the COR$^-$ mutant strain in Col-0 plants, since the CI obtained was not significantly different from 1 (**Figure 4.6C**). This result is in agreement with previous reports, since the CIs were carried out by infiltration and the main role of coronatine as a virulence factor is suppression of stomatal closure following spray or dip-inoculation (Brooks et al., 2004; Mittal and Davis, 1995). No significant changes were observed when the CI of COR$^-$ was determined in either *met1-3* or *ago4-2* plants. No significant changes were observed either in the growth of any of the co-inoculated strains in *met1-3* plants. However, as observed in **Figure 4.6A**, growth of both co-inoculated strains was significantly increased in *ago4-2* plants, further supporting a role for AGO4 in all plant defences tested.

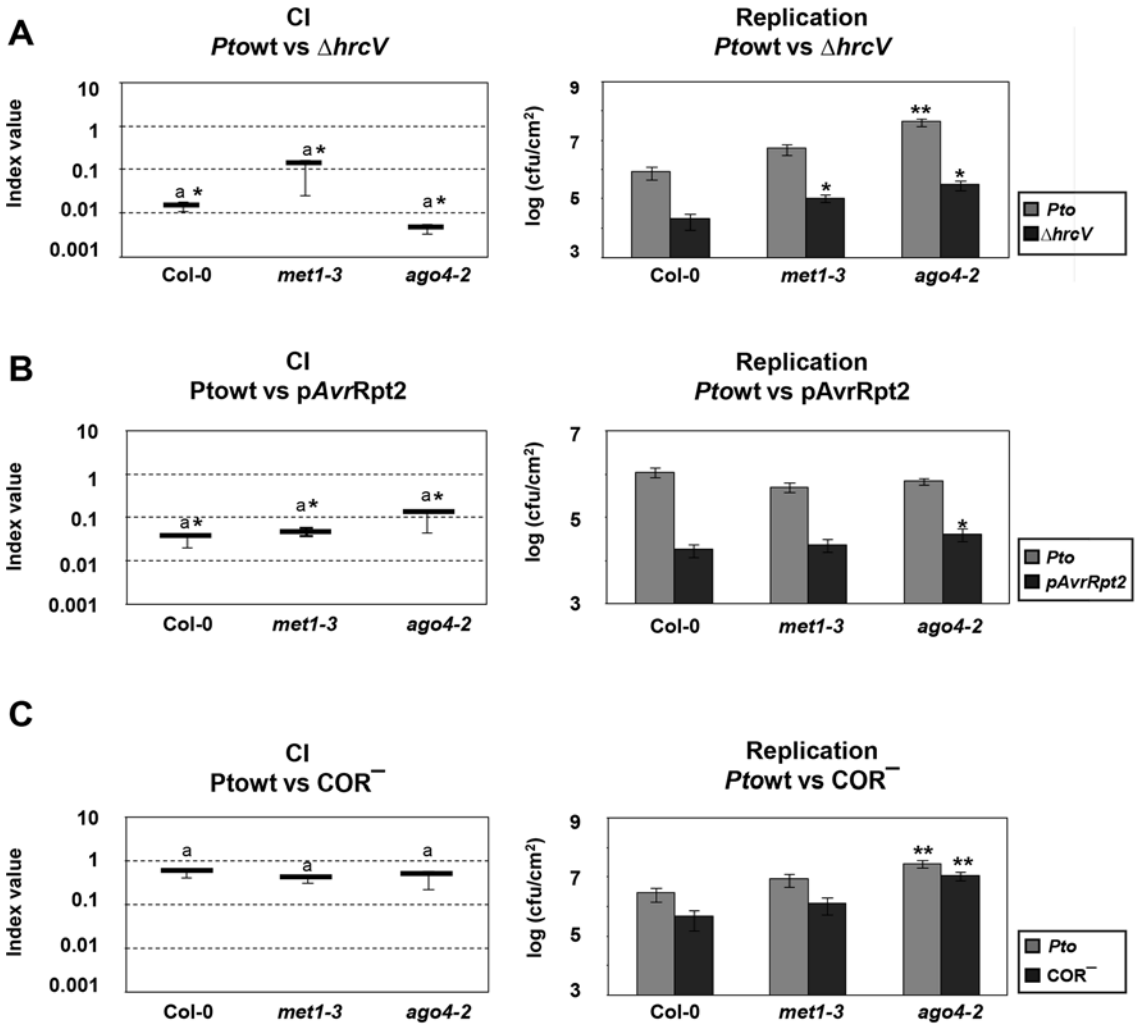

Figure 4.6. Competitive Index (CI) analysis and its corresponding bacterial replication within mixed infections in plant genotypes affected on DNA methylation. (**A**) Graphical representation of CIs and bacterial growth resulting from the mixed infection of *Pto* DC3000 and Δ*hrcV* in either Col-0 wild type, *met1-3*, or *ago4-2*. (**B**) Graphical representation of CIs and bacterial growth resulting from mixed infection of *Pto* DC3000 and *Pto* DC3000 expressing AvrRpt2 in either Col-0 wild type, *met1-3*, or *ago4-2*. (**C**) Graphical representation of CIs and bacterial growth resulting from mixed infection of *Pto* DC3000 and a COR$^-$ mutant in either Col-0 wild type, *met1-3*, or *ago4-2*. Inoculation was carried out by infiltrating with a 5x10^4 cfu/ml of the mixed bacterial suspension in the indicated genotypes, and growth was analysed 4 dpi. Index values correspond to the mean of 9 plants (3 samples per experiment in 3 independent experiments), and error bars represent the standard error. Mean CI values (left panels) marked with the same letter were not significantly different as established by One-way ANOVA, Benferroni PosHoc test (99% confidence intervals). Asterisk associated to CI values (left panels) indicates results significantly different from 1.0, as established by Student, t-test (95%). Bacteria were differentiated using antibiotic selection. Asterisks associated to cfu values for each of the strains within the mixed infection (right panels) indicate significant differences between growth in the mutant genotype and growth of the same strain within Col-0 wild type, as established by Student, t-test, 95% (*), 99% (**).

4.4 Analysis of the role of ROS1 in activation of AtSN1 during the infection

The recent study published by Yu and collaborators (2013) also linked *ROS1* to activation of *AtSN1* in response to flg22 treatment. When wild type Col-0 and *ros1-4* plants were treated with flg22, an enhanced expression of *AtSN1* was detected by 9 hpi in wild type Col-0, but not *ros1-4* plants, leading to the hypothesis that activation of *AtSN1* is carried out by ROS1 in response to flagellin. Since our results indicate that ETI responses also lead to activation of *AtSN1,* we analysed accumulation of *AtSN1* transcript at 24 hpi with *Pto* DC3000 and Δ*fliC* in wild type and *ros1-4* plants (**Figure 4.7**). Our findings show that the activation of *AtSN1* during infection with *Pto* DC3000 occurs independently of *ROS1*, since the differences in the accumulation of *AtSN1* in both wild type and *ros1-4* plants are not statistically significant. The activation of *AtSN1* is partially but not fully dependent on flagellin, since transcript accumulation in both Col-0 and *ros1-4* plants inoculated with the Δ*fliC* mutant was reduced in comparison to those inoculated with *Pto* DC3000, but the differences are not always statistically significant.

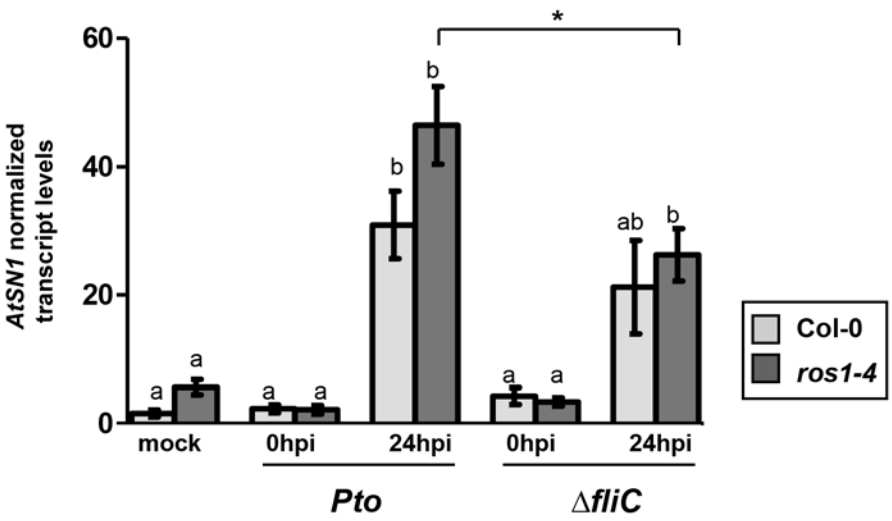

Figure 4.7. Accumulation of *AtSN1* transcript does not depend on flagellin in Col-0 or *ros1-4* infected-plants. Accumulation of *AtSN1* transcript was analysed using RT-*q*PCR in Col-0 and *ros1-4* plants infected with *Pto* DC3000 or a flagellin mutant (Δ*fliC*) at 0 and 24 hours post-inoculation (0 hpi and 24 hpi). Mock-inoculated plants (10 mM $MgCl_2$) were included as a control for the basal transcript levels. Gene expression levels were normalised to actin and the results presented as relative transcript accumulation compared to levels detected in *Pto* DC3000 infected Col-0 plants 0 hpi with *Pto* DC3000. Bars represent the mean values from 2 independent experiments with 3-6 plants per sample and experiment. Error bars represent the standard error. Mean values marked with the same letter were not significantly different from each other as established by One-way ANOVA, Benferroni PosHoc test (99% confidence intervals). Asterisks indicate samples that are statistically different from *Pto* DC3000 infected-sample at 24 hpi as determined by Student's t-test at the 99% (**) or the 95% (*) confidence interval.

Concluding remarks

Pseudomonas syringae pv. *tomato (Pto)* strain DC3000 in its interaction with *Arabidopsis* constitutes a well characterized model system. The ability of these bacteria to infect *Arabidopsis* depends on the Hrp T3SS, and the role of the T3SS and that of its translocated effectors in suppressing the plant defence have been the focus of many recent reports. However, the particular mechanisms by which different T3Es interfere with the plant defences are still largely unknown. When this work begun there was one report that indicated that the plant DNA methylation status changed during infection with *Pto* (Pavet et al., 2006). Interference with the host DNA methylation status and/or with other epigenetic mechanisms have been shown to be an important virulence mechanism in mammalian pathogens (Gómez-Díaz et al., 2012; Hamon and Cossart, 2008; Paschos and Allday, 2010). Although less was known in plants, plant viruses do suppress repressive methylation and transcriptional silencing of viral, transgenic and endogenous loci during the infection (Raja et al., 2010; Rodríguez-Negrete et al., 2013; Zhang et al., 2011). Thus, the report by Pavet and collaborators (2006) raised the interesting possibility of plant pathogenic bacteria also altering the host epigenome during infection. Such was the initial interest of these observations that gave raise to the objectives of this thesis. Pavet and collaborators reported that infection with *Pto* induced rapid DNA hypomethylation at pericentromeric chromatin (by 24 hpi), including repeats such as the 180-bp unit and *Athila* retrotansposon, and that this hypomethylation was not associated to DNA replication, suggesting the involvement of an active demethylation process.

The initial work of this thesis encountered many technical difficulties in reproducibly replicating the results presented by Pavet and collaborators, probably due to the fact that epigenetic changes do not take place in all plant cells on the inoculated tissue but only in those adjacent to the invading bacteria. However, these difficulties allowed us to make some interesting observations such as, the fact that plant DNA hypomethylation is clearer when the initial stages of the infection take place at a subjective night (under *night conditions*, *i.e.* the inoculation takes place immediately before the 16 h dark period). We also established that accompanying these changes, which

occur during the first 24 hours of *Pto* infection, TGS loci become transcriptionally active. Among other loci, we could detect the transcriptional activation of the retrotransposon *AtSN1* but direct demonstration of its hypomethylation has evaded us, probably also due to its being restricted to bacteria-adjacent cells and thus diluted in the inoculated tissue analysed. *AtSN1* was later shown to become transcriptionally active through DNA hypomethylation upon treatment with exogenous bacterial flagellin (flg22), supporting that its activation during *Pto* infection is probably due to plant DNA hypomethylation (Yu et al., 2013).

The use of the highly activated TGS locus *AtSN1* as a reporter has been greatly useful in the analysis of the role that *Pto* virulence determinants have in altering the transcriptional status of TGS loci, and probably in altering plant DNA methylation levels. Thus, we showed that as could be expected from the work of Pavet and collaborators (2006), transcriptional activation of *AtSN1* requires the transcriptional activator of T3SS genes, HrpL. We also established that this is due to the requirement of a functional T3SS since a mutant in a gene encoding one of the structural components, which does not translocate any effectors, also fails to activate transcription of *AtSN1*. Interestingly, in the context of a fully functional T3SS, coronatine is also necessary for full activation of *AtSN1* transcription supporting that functional redundancy is a common element between plant pathogenic virulence determinants.

Analysis of mutants lacking one or more effectors has also proven interesting. We have shown that one or more of the 28 *bona fide Pto* DC3000 effectors is required to activate *AtSN1*. Moreover, we have found that deletion of different groups of effectors may lead to either a failure to activate *AtSN1*, or an enhanced activation, indicating that effectors are involved in both triggering the transcriptional activation of *AtSN1* and in suppressing it. One candidate effector involved in triggering its activation is HopC1, although the difficulties for reproducibly and further support the involvement of more than one effector in the process. Similarly HopAO1 is a candidate effector to suppress activation of *AtSN1* but again functional redundancy is expected.

The fact that *Pto* T3Es act both activating and suppressing *AtSN1* suggests that one or the other is part of the plant defence response. In this regard, a second report studying the changes on DNA methylation during *Pto* infection profiled the entire *Arabidppsis* DNA methylome during the interaction with both virulent and avirulent *Pto,* revealing that many genomic regions enriched in transposon sequences became differentially methylated, affecting transcription of neighbouring protein-coding genes, including defence-related genes (Dowen et al., 2012). These changes also took place following treatment with exogenous SA. If we also take into account that Yu and collaborators (2013) showed activation of *AtSN1* through changes in methylation upon treatment with exogenous bacterial flagellin (flg22) all these results suggest activation of *AtSN1* is likely part of the plant defence response against *Pto*, and thus *Pto* encodes effector(s) directly or indirectly capable of suppressing this activation. Our results show that this is indeed the case. We found that in keeping with the results presented by Yu and collaborators (2013) activation of *AtSN1* is partially dependent on the bacterial production of flagellin, since accumulation of *AtSN1* transcript is reduced but not abolished in plants inoculated with a *ΔfliC* mutant, thus supporting the involvement of transcriptional activation of TGS loci in PTI. However, this is not a universal feature of flagellin-dependent PTI in *Arabidopsis* since inoculation with the non-host bacteria *P. syringae* pv. *phaseolicola* does not induce accumulation of *AtSN1.* Furthermore, this is not the only defence response in which activation of TGS loci takes place since levels of *AtSN1* transcript are significantly higher during the incompatible interaction of *Arabidopsis* with *Pto* expressing the heterologous effectors AvrRpt2, AvrRps4, AvrRpm1 or HopZ1a, and these increased levels require effector recognition dependent on their corresponding R genes, *RPS2*, *RPS4*, *RPM1* and *ZAR1*, respectively. Thus our results demonstrate that transcriptional activation of TGS loci also takes place as part of the ETI.

In keeping with the relation between the changes in DNA methylation, activation of TGS loci and plant defences, we found that transcription of the genes encoding the maintenance DNA methyltransferase MET1 and the demethylase ROS1 were downregulated during infection with *Pto*, whereas

transcription of the gene encoding the DNA methyltransferas DRM2 was upregulated.

The involvement of the changes in DNA methylation and activation of TGS loci in different types of plant defences is additionally supported when bacterial growth is analysed in plant mutants affected in these processes. We found that the triple mutant *ddc* (*drm1-2 drm2-2 cmt3-11*) that presents alteration in DNA methylation mainly at CHG and CHH sites is impaired in defences different from flagellin-triggered PTI or *RPS2*-triggered ETI, which include stomata closure upon pathogen detection since a COR$^-$ mutant induces stronger symptoms in this plant mutant. Reversely, flagellin-triggered PTI and *RPS2*-triggered ETI, but not stomata closure were impaired in *ago4-2* mutants leading to a significant increase on bacterial growth within this plant genotype. We also found the *met1-3* mutant more susceptible to *Pto* than the wild type, although this is not always clear depending on the virulence assay used. Finally, we also found that a *ros1-4* mutant is more susceptible to *Pto,* in agreement with Yu and collaborators (2013), however this is not only due to a failure to establish an effective PTI since this mutant is also more susceptible to a *ΔfliC* mutant, a COR$^-$, and to *Pto* expressing AvrRpt2.

To summarise, the results presented in this thesis support the notion initially proposed by recent studies of RNA-directed DNA methylation (RdDM) and transcriptional gene silencing (TGS) having an important role in plant defence against phytopathogenic bacteria (Pumplin and Voinnet, 2013). Dampening defence gene expression through RdDM could provide an effective mode of regulation because RdDM can be rapidly reversed by biotic and abiotic stress. The rapid activation of plant defences would require the presence of RdDM-prone genomic segments (transposons and repeats) in the vicinity of defence-related genes and the involvement of active demethylation pathways to ensure optimal and rapid defence gene induction on pathogen attack. In addition, the dampening of RdDM and the resulting defence gene activation occurs only transiently, to prevent the prolonged induction of these stress-responsive plant genes. This feature is foreseeably advantageous in the case of defence-related genes whose continuous expression reduces plant

fitness. In such a model, the acquisition of effectors capable of directly or indirectly suppressing this activation would represent a clear advantage for plant pathogenic bacteria.

Conclusions

1. *Pseudomonas syringae pv. tomato* DC3000 (*Pto* DC3000) infection induces the hypomethylation of the *Arabidopsis* retrotransposon, *Athila* and up-regulates transcriptionally silent loci, such as *Athila*, *CACTA,* TE-pseudogene, a *GUS* transgene, and *AtSN1*, being this last locus, the one that shows the highest activation.

2. The transcriptional activation of *AtSN1* during infection with *Pto* requires a functional type III secretion system. However, in the context of a fully functional T3SS, the synthesis of coronatine is also necessary for full transcriptional activation of *AtSN1.*

3. Flagellin partially contributes to trigger the accumulation of *AtSN1* transcripts during infection with *Pto*, since activation of this retrotransposon is less efficient during infection with a *ΔfliC* mutant than during infection with the wild-type strain. However, this is not a general feature of all *P. syringae* strains since *Pph* 1448a, which triggers a strong flagellin-dependent PTI, does not activate *AtSN1* transcription.

4. Type III-secreted effectors from *Pto* DC3000 are directly or indirectly involved in both activation and suppression of *AtSN1*.

5. The activation of *AtSN1*_during infection with *Pto* is associated to effector-triggered responses (ETI) against type III-secreted effectors and is stronger when *Pto* expresses HR-inducing effectors. These results suggest that the transcriptional activation of *AtSN1* can be triggered during both, PTI (PAMP-triggered immunity) and up to a larger extent ETI (effector-triggered immunity).

6. The DNA methylation at CHG or CHH sites, both of which are altered in the *Arabidopsis* triple mutant *ddc* (*drm1-2 drm2-2 cmt3-11*) is important for the establishment of plant defences against *P. syringae* different from FLS2-mediated PTI or RPS2-mediated ETI. In addition these functions might be

important for stomata closure upon pathogen detection, as COR$^-$ displayed stronger symptoms on *ddc* than on wild-type plants.

7. *Arabidopsis* mutants *ago4-2* and *ros1-4* show flagellin-independent increased susceptibility to *Pto* supporting a relevant role for RNA-directed DNA methylation of plant cytosine residues and their demethylation in the plant defence against *Pto*.

8. AGO4 and ROS1, but not MET1, are required for effector-triggered ETI immunity.

References

Agorio, A. and Vera, P. (2007) ARGONAUTE4 is required for resistance to *Pseudomonas syringae* in *Arabidopsis*. *Plant Cell* **19**, 3778-3790.

Alfano, J.R. and Collmer, A. (1997) The type III (Hrp) secretion pathway of plant pathogenic bacteria: Trafficking harpins, Avr proteins, and death. *Journal of Bacteriology* **179**, 5655-5662.

Anderson, J.P., Gleason, C.A., Foley, R.C., Thrall, P.H., Burdon, J.B. and Singh, K.B. (2010) Plants versus pathogens: An evolutionary arms race. *Functional Plant Biology* **37**, 499-512.

Anderson, J.P. and Singh, K.B. (2011) Interactions of *Arabidopsis* and *M. truncatula* with the same pathogens differ in dependence on ethylene and ethylene response factors. *Plant Signaling and Behavior* **6**, 551-552.

Asai, T., Tena, G., Plotnikova, J., Willmann, M.R., Chiu, W.L., Gomez-Gomez, L., Boller, T., Ausubel, F.M. and Sheen, J. (2002) Map kinase signalling cascade in *Arabidopsis* innate immunity. *Nature* **415**, 977-983.

Averre, C.W. and Kelman, A. (1964) Severity of bacterial wilt as influenced by ratio of virulent to avirulent cells of *Pseudomonas solanacearum* in inoculum. *Phytopathology* **54**, 779-783.

Bender, C.L., Alarcon-Chaidez, F. and Gross, D.C. (1999) *Pseudomonas syringae* phytotoxins: Mode of action, regulation, and biosynthesis by peptide and polyketide synthetases. *Microbiology and Molecular Biology Reviews* **63**, 266-292.

Bender, J. (2004) DNA methylation and epigenetics. *Annual Review of Plant Biology* **55**, 41-68.

Bertrand, C., Bergounioux, C., Domenichini, S., Delarue, M. and Zhou, D.-X. (2003) *Arabidopsis* histone acetyltransferase AtGCN5 regulates the floral meristem activity through the WUSCHEL/AGAMOUS pathway. *Journal of Biological Chemistry* **278**, 28246-28251.

Bhardwaj, V., Meier, S., Petersen, L.N., Ingle, R.A. and Roden, L.C. (2011) Defence responses of *Arabidopsis thaliana* to infection by *Pseudomonas syringae* are regulated by the circadian clock. *PLoS ONE* **6**.

Bird, A. (2002) DNA methylation patterns and epigenetic memory. *Genes and Development* **16**, 6-21.

Boller, T. and Felix, G. (2009) A renaissance of elicitors: Perception of microbe-associated molecular patterns and danger signals by pattern-recognition receptors. *Annual Review of Plant Biology* **60**, 379-407.

Boller, T. and He, S.Y. (2009) Innate immunity in plants: An arms race between pattern recognition receptors in plants and effectors in microbial pathogens. *Science* **324**, 742-743.

Bostock, R.M. (2005) Signal crosstalk and induced resistance: Straddling the line between cost and benefit. In: *Annual Review of Phytopathology* pp. 545-580.

Brooks, D.M., Bender, C.L. and Kunkel, B.N. (2005) The *Pseudomonas syringae* phytotoxin coronatine promotes virulence by overcoming salicylic acid-dependent defences in *Arabidopsis thaliana*. *Molecular Plant Pathology* **6**, 629-639.

Brooks, D.M., Hernández-Guzmán, G., Kloek, A.P., Alarcón-Chaidez, F., Sreedharan, A., Rangaswamy, V., Peñaloza-Vázquez, A., Bender, C.L. and Kunkel, B.N. (2004) Identification and characterization of a well-defined series of coronatine biosynthetic mutants of *Pseudomonas syringae* pv. *tomato* DC3000. *Molecular Plant-Microbe Interactions* **17**, 162-174.

Buchmann, R.C., Asad, S., Wolf, J.N., Mohannath, G. and Bisaro, D.M. (2009) Geminivirus AL2 and L2 proteins suppress transcriptional gene silencing and cause genome-wide reductions in cytosine methylation. *Journal of virology* **83**, 5005-5013.

Cameron, R.K., Dixon, R.A. and Lamb, C.J. (1994) Biologically induced systemic acquired resistance in *Arabidopsis thaliana*. *Plant Journal* **5**, 715-725.

Chang, J.H., Urbach, J.M., Law, T.F., Arnold, L.W., Hu, A., Gombar, S., Grant, S.R., Ausubel, F.M. and Dangl, J.L. (2005) A high-throughput, near-saturating screen for type III effector genes from *Pseudomonas syringae*. *Proceedings of the National Academy of Sciences of the United States of America* **102**, 2549-2554.

Choi, K.H., Kumar, A. and Schweizer, H.P. (2005) A 10-min method for preparation of highly electrocompetent *Pseudomonas aeruginosa* cells: application for DNA fragment

transfer between chromosomes and plasmid transformation. *J Microbiol Methods* **64**, 391-397.

Choi, M.S., Kim, W., Lee, C. and Oh, C.S. (2013) Harpins, multifunctional proteins secreted by gram-negative plant-pathogenic bacteria. *Molecular Plant-Microbe Interactions* **26**, 1115-1122.

Collmer, A., Lindeberg, M., Petnicki-Ocwieja, T., Schneider, D.J. and Alfano, J.R. (2002) Genomic mining type III secretion system effectors in *Pseudomonas syringae* yields new picks for all TTSS prospectors. *Trends in Microbiology* **10**, 462-469.

Collmer, A., Schneider, D.J. and Lindeburg, M. (2009) Lifestyles of the effector rich: Genome-enabled characterization of bacterial plant pathogens. *Plant Physiology* **150**, 1623-1630.

Cunnac, S., Chakravarthy, S., Kvitko, B.H., Russell, A.B., Martin, G.B. and Collmer, A. (2011) Genetic disassembly and combinatorial reassembly identify a minimal functional repertoire of type III effectors in *Pseudomonas syringae*. *Proceedings of the National Academy of Sciences of the United States of America* **108**, 2975-2980.

Cunnac, S., Lindeberg, M. and Collmer, A. (2009) *Pseudomonas syringae* type III secretion system effectors: repertoires in search of functions. *Current Opinion in Microbiology* **12**, 53-60.

Cuppels, D.A. (1986) Generation and characterization of Tn5 insertion mutations in *Pseudomonas syringae* pv. *tomato*. *Applied and environmental microbiology* **51**, 323-327.

Dangl, J.L. and Jones, J.D.G. (2001) Plant pathogens and integrated defence responses to infection. *Nature* **411**, 826-833.

Dangl, J.L., Ritter, C., Gibbon, M.J., Mur, L.A.J., Wood, J.R., Goss, S., Mansfield, J., Taylor, J.D. and Vivian, A. (1992) Functional homologs of the *Arabidopsis* RPM1 disease resistance gene in bean and pea. *Plant Cell* **4**, 1359-1369.

Datsenko, K.A. and Wanner, B.L. (2000) One-step inactivation of chromosomal genes in *Escherichia coli* K-12 using PCR products. *Proceedings of the National Academy of Sciences* **97**, 6640-6645.

De Torres, M., Mansfield, J.W., Grabov, N., Brown, I.R., Ammouneh, H., Tsiamis, G., Forsyth, A., Robatzek, S., Grant, M. and Boch, J. (2006) *Pseudomonas syringae* effector AvrPtoB suppresses basal defence in *Arabidopsis*. *Plant Journal* **47**, 368-382.

Delaney, T.P., Friedrich, L. and Ryals, J.A. (1995) *Arabidopsis* signal transduction mutant defective in chemically and biologically induced disease resistance. *Proceedings of the National Academy of Sciences of the United States of America* **92**, 6602-6606.

Dowen, R.H., Pelizzola, M., Schmitz, R.J., Lister, R., Dowen, J.M., Nery, J.R., Dixon, J.E. and Ecker, J.R. (2012) Widespread dynamic DNA methylation in response to biotic stress. *Proceedings of the National Academy of Sciences* **109**, E2183–E2191.

Earley, K.W., Pontvianne, F., Wierzbicki, A.T., Blevins, T., Tucker, S., Costa-Nunes, P., Pontes, O. and Pikaard, C.S. (2010) Mechanisms of HDA6-mediated rRNA gene silencing: Suppression of intergenic Pol II transcription and differential effects on maintenance versus siRNA-directed cytosine methylation. *Genes and Development* **24**, 1119-1132.

Felix, G., Duran, J.D., Volko, S. and Boller, T. (1999) Plants have a sensitive perception system for the most conserved domain of bacterial flagellin. *Plant Journal* **18**, 265-276.

Feys, B.J.F., Benedetti, C.E., Penfold, C.N. and Turner, J.G. (1994) *Arabidopsis* mutants selected for resistance to the phytotoxin coronatine are male sterile, insensitive to methyl jasmonate, and resistant to a bacterial pathogen. *Plant Cell* **6**, 751-759.

Finnegan, E.J., Peacock, W.J. and Dennis, E.S. (1996) Reduced DNA methylation in *Arabidopsis thaliana* results in abnormal plant development. *Proceedings of the National Academy of Sciences of the United States of America* **93**, 8449-8454.

Freter, R., Allweiss, B., O'Brien, P.C., Halstead, S.A. and Macsai, M.S. (1981) Role of chemotaxis in the association of motile bacteria with intestinal mucosa: *in vitro* studies. *Infect Immun* **34**, 241-249.

Furner, I.J. and Matzke, M. (2011) Methylation and demethylation of the *Arabidopsis* genome. *Current Opinion in Plant Biology* **14**, 137-141.

Galán, J.E. and Collmer, A. (1999) Type III secretion machines: Bacterial devices for protein delivery into host cells. *Science* **284**, 1322-1328.

Gilardi, G.L. (1972) Infrequently encountered *Pseudomonas* species causing infection in humans. *Annals of Internal Medicine* **77**, 211-215.

Glazebrook, J. (2005) Contrasting mechanisms of defense against biotrophic and necrotrophic pathogens. *Annual Review of Phytopathology* **43**, 205-227.

Göhre, V. and Robatzek, S. (2008) Breaking the barriers: Microbial effector molecules subvert plant immunity. In: *Annual Review of Phytopathology* pp. 189-215.

Gómez-Díaz, E., Jordà, M., Peinado, M.A. and Rivero, A. (2012) Epigenetics of host–pathogen interactions: the road ahead and the road behind. *PLoS pathogens* **8**, e1003007.

Gómez-Gómez, L. and Boller, T. (2002) Flagellin perception: A paradigm for innate immunity. *Trends in Plant Science* **7**, 251-256.

González, A.J., Landeras, E. and Mendoza, M.C. (2000) Pathovars of *Pseudomonas syringae* Causing Bacterial Brown Spot and Halo Blight in *Phaseolus vulgaris* L. Are Distinguishable by Ribotyping. *Applied and environmental microbiology* **66**, 850-854.

Grant, M.R., Godiard, L., Straube, E., Ashfield, T., Lewald, J., Sattler, A., Innes, R.W. and Dangl, J.L. (1995) Structure of the *Arabidopsis* RPM1 gene enabling dual specificity disease resistance. *Science* **269**, 843-846.

Haag, J.R., Pontes, O. and Pikaard, C.S. (2009) Metal A and metal B sites of nuclear RNA polymerases Pol IV and Pol V are required for siRNA-dependent DNA methylation and gene silencing. *PLoS One* **4**, e4110.

Hamon, M. and Cossart, P. (2008) Histone modifications and chromatin remodeling during bacterial infections. *Cell Host & Microbe* **4**, 100-109.

Hanahan, D. (1983) Studies on transformation of *Escherichia coli* with plasmids. *Journal of Molecular Biology* **166**, 557-580.

Hayat, S., Ali, B. and Ahmad, A. (2007) Salicylic Acid: Biosynthesis, Metabolism and Physiological Role in Plants. In: *Salicylic Acid: A Plant Hormone* (Hayat, S. and Ahmad, A. eds), pp. 1-14. Springer Netherlands.

He, P., Shan, L., Lin, N.C., Martin, G.B., Kemmerling, B., Nürnberger, T. and Sheen, J. (2006) Specific Bacterial Suppressors of MAMP Signaling Upstream of MAPKKK in *Arabidopsis* Innate Immunity. *Cell* **125**, 563-575.

Henderson, I.R. and Jacobsen, S.E. (2007) Epigenetic inheritance in plants. *Nature* **447**, 418-424.

Hinsch, M. and Staskawicz, B. (1996) Identification of a new *Arabidopsis* disease resistance locus, RPS4, and cloning of the corresponding avirulence gene, avrRps4, from *Pseudomonas syringae* pv. *pisi*. *Molecular Plant-Microbe Interactions* **9**, 55-61.

Hirano, S.S. and Upper, C.D. (2000) Bacteria in the leaf ecosystem with emphasis on *Pseudomonas syringae* - A pathogen, ice nucleus, and epiphyte. *Microbiology and Molecular Biology Reviews* **64**, 624-653.

Holmes, D.S. and Quigley, M. (1981) A rapid boiling method for the preparation of bacterial plasmids. *Analytical Biochemistry* **114**, 193-197.

Hrabak, E. and Willis, D.K. (1992) The lemA gene required for pathogenicity of *Pseudomonas syringae* pv. *syringae* on bean is a member of a family of two-component regulators. *Journal of bacteriology* **174**, 3011-3020.

Jaenisch, R. and Bird, A. (2003) Epigenetic regulation of gene expression: How the genome integrates intrinsic and environmental signals. *Nature Genetics* **33**, 245-254.

Johnson, L.M., Bostick, M., Zhang, X., Kraft, E., Henderson, I., Callis, J. and Jacobsen, S.E. (2007) The SRA Methyl-Cytosine-Binding Domain Links DNA and Histone Methylation. *Current Biology* **17**, 379-384.

Jones, J.D.G. and Dangl, J.L. (2006) The plant immune system. *Nature* **444**, 323-329.

Kakutani, T., Jeddeloh, J.A., Flowers, S.K., Munakata, K. and Richards, E.J. (1996) Developmental abnormalities and epimutations associated with DNA hypomethylation mutations. *Proceedings of the National Academy of Sciences of the United States of America* **93**, 12406-12411.

Katagiri, F., Thilmony, R. and He, S.Y. (2002) The *Arabidopsis thaliana-Pseudomonas syringae* Interaction. *The Arabidopsis Book*, e0039.

Katagiri, F. and Tsuda, K. (2010) Understanding the plant immune system. *Molecular Plant-Microbe Interactions* **23**, 1531-1536.

Keith Slotkin, R. (2010) The epigenetic control of the athila family of retrotransposons in *Arabidopsis*. *Epigenetics* **5**, 483-490.

Kim, H.S., Desveaux, D., Singer, A.U., Patel, P., Sondek, J. and Dangl, J.L. (2005) The *Pseudomonas syringae* effector AvrRpt2 cleaves its C-terminally acylated target, RIN4, from *Arabidopsis* membranes to block RPM1 activation. *Proceedings of the National Academy of Sciences of the United States of America* **102**, 6496-6501.

King, E.O., Ward, M.K. and Raney, D.E. (1954) Two simple media for the demonstration of pyocyanin and fluorescin. *The Journal of Laboratory and Clinical Medicine* **44**, 301-307.

Kitten, T., Kinscherf, T.G., McEvoy, J.L. and Willis, D.K. (1998) A newly identified regulator is required for virulence and toxin production in *Pseudomonas syringae*. *Molecular microbiology* **28**, 917-929.

Klement, Z. and Lovrekovich, L. (1961) Defence Reactions Induced by Phytopathogenic Bacteria in Bean Pods. *Journal of Phytopathology* **41**, 217-227.

Kloek, A.P., Verbsky, M.L., Sharma, S.B., Schoelz, J.E., Vogel, J., Klessig, D.F. and Kunkel, B.N. (2001) Resistance to *Pseudomonas syringae* conferred by an *Arabidopsis thaliana* coronatine-insensitive (coi1) mutation occurs through two distinct mechanisms. *Plant Journal* **26**, 509-522.

Kunkel, B.N., Bent, A.F., Dahlbeck, D., Innes, R.W. and Staskawicz, B.J. (1993) RPS2, an *Arabidopsis* disease resistance locus specifying recognition of *Pseudomonas syringae* strains expressing the avirulence gene avrRpt2. *Plant Cell* **5**, 865-875.

Kunkel, B.N. and Brooks, D.M. (2002) Cross talk between signaling pathways in pathogen defense. *Current Opinion in Plant Biology* **5**, 325-331.

Kvitko, B.H., Park, D.H., Velásquez, A.C., Wei, C.F., Russell, A.B., Martin, G.B., Schneider, D.J. and Collmer, A. (2009) Deletions in the repertoire of *Pseudomonas syringae* pv. *tomato* DC3000 type III secretion effector genes reveal functional overlap among effectors. *PLoS Pathogens* **5**.

Law, J.A. and Jacobsen, S.E. (2010) Establishing, maintaining and modifying DNA methylation patterns in plants and animals. *Nature Reviews Genetics* **11**, 204-220.

Lennox, E. (1955) Transduction of linked genetic characters of the host by bacteriophage P1. *Virology* **1**, 190-206.

Li, X., Lin, H., Zhang, W., Zou, Y., Zhang, J., Tang, X. and Zhou, J.M. (2005) Flagellin induces innate immunity in nonhost interactions that is suppressed by *Pseudomonas syringae* effectors. *Proceedings of the National Academy of Sciences of the United States of America* **102**, 12990-12995.

Lindeberg, M., Cartinhour, S., Myers, C.R., Schlechter, L.M., Schneider, D.J. and Collmer, A. (2006) Closing the circle on the discovery of genes encoding Hrp regulon members and type III secretion system effectors in the genomes of three model *Pseudomonas syringae* strains. *Molecular Plant-Microbe Interactions* **19**, 1151-1158.

Macho, A.P. and Beuzón, C.R. (2010) Insights into plant immunity signalling: the bacterial competitive index angle. *Plant signaling & behavior* **5**, 1590-1593.

Macho, A.P., Guevara, C.M., Tornero, P., Ruiz-Albert, J. and Beuzón, C.R. (2010) The *Pseudomonas syringae* effector protein HopZ1a suppresses effector-triggered immunity. *New phytologist* **187**, 1018-1033.

Macho, A.P., Ruiz-Albert, J., Tornero, P. and Beuzon, C.R. (2009) Identification of new type III effectors and analysis of the plant response by competitive index. *Mol Plant Pathol* **10**, 69-80.

Macho, A.P. and Zipfel, C. (2014) Plant PRRs and the activation of innate immune signaling. *Molecular Cell* **54**, 263-272.

Macho, A.P., Zumaquero, A., Ortiz-Martin, I. and Beuzon, C.R. (2007) Competitive index in mixed infections: a sensitive and accurate assay for the genetic analysis of *Pseudomonas syringae*-plant interactions. *Mol Plant Pathol* **8**, 437-450.

Martienssen, R.A. and Richards, E.J. (1995) DNA methylation in eukaryotes. *Current Opinion in Genetics and Development* **5**, 234-242.

Martínez-Macías, M.I., Qian, W., Miki, D., Pontes, O., Liu, Y., Tang, K., Liu, R., Morales-Ruiz, T., Ariza, R.R., Roldán-Arjona, T. and Zhu, J.K. (2012) A DNA 3' Phosphatase Functions in Active DNA Demethylation in *Arabidopsis*. *Molecular Cell* **45**, 357-370.

Mathieu, O., Reinders, J., Čaikovski, M., Smathajitt, C. and Paszkowski, J. (2007) Transgenerational Stability of the *Arabidopsis* Epigenome Is Coordinated by CG Methylation. *Cell* **130**, 851-862.

Matzke, M., Kanno, T., Daxinger, L., Huettel, B. and Matzke, A.J. (2009) RNA-mediated chromatin-based silencing in plants. *Current Opinion in Cell Biology* **21**, 367-376.

Matzke, M.A., Mette, M.F. and Matzke, A.J.M. (2000) Transgene silencing by the host genome defense: Implications for the evolution of epigenetic control mechanisms in plants and vertebrates. *Plant Molecular Biology* **43**, 401-415.

Matzke, M.A. and Mosher, R.A. (2014) RNA-directed DNA methylation: An epigenetic pathway of increasing complexity. *Nature Reviews Genetics* **15**, 394-408.

Melotto, M., Underwood, W., Koczan, J., Nomura, K. and He, S.Y. (2006) Plant Stomata Function in Innate Immunity against Bacterial Invasion. *Cell* **126**, 969-980.

Melotto, M., Underwood, W. and Sheng, Y.H. (2008) Role of stomata in plant innate immunity and foliar bacterial diseases. *Annual Review of Phytopathology* **46**, 101-122.

Mittal, S. and Davis, K.R. (1995) Role of the phytotoxin coronatine in the infection of *Arabidopsis thaliana* by *Pseudomonas syringae* pv. *tomato*. *Molecular Plant-Microbe Interactions* **8**, 165-171.

Mohr, T.J., Liu, H., Yan, S., Morris, C.E., Castillo, J.A. and Jelenska, J. (2008) Naturally occurring non-pathogenic isolates of the plant pathogen species *Pseudomonas syringae* lack a Type III secretion system and effector gene orthologues. *J Bacteriol* **190**, 2858-2870.

Mudgett, M.B. and Staskawicz, B.J. (1999) Characterization of the *Pseudomonas syringae* pv. *tomato* AvrRpt2 protein: demonstration of secretion and processing during bacterial pathogenesis. *Molecular Microbiology* **32**, 927-941.

Naito, K., Taguchi, F., Suzuki, T., Inagaki, Y., Toyoda, K., Shiraishi, T. and Ichinose, Y. (2008) Amino acid sequence of bacterial microbe-associated molecular pattern flg22 is required for virulence. *Molecular Plant-Microbe Interactions* **21**, 1165-1174.

Navarro, L., Zipfel, C., Rowland, O., Keller, I., Robatzek, S., Boller, T. and Jones, J.D.G. (2004) The transcriptional innate immune response to flg22. Interplay and overlap with Avr gene-dependent defense responses and bacterial pathogenesis. *Plant Physiology* **135**, 1113-1128.

Nawrath, C., Heck, S., Parinthawong, N. and Métraux, J.P. (2002) EDS5, an essential component of salicylic acid-dependent signaling for disease resistance in *Arabidopsis*, is a member of the MATE transporter family. *Plant Cell* **14**, 275-286.

Nguyen, L., Paulsen, I.T., Tchieu, J., Hueck, C.J. and Saier Jr, M.H. (2000) Phylogenetic analyses of the constituents of Type III protein secretion systems. *Journal of Molecular Microbiology and Biotechnology* **2**, 125-144.

Oakes, C.C., La Salle, S., Trasler, J.M. and Robaire, B. (2009) Restriction digestion and real-time PCR (qAMP). *Methods in molecular biology (Clifton, N.J.)* **507**, 271-280.

Orth, K., Xu, Z., Mudgett, M.B., Bao, Z.Q., Palmer, L.E., Bliska, J.B., Mangel, W.F., Staskawicz, B. and Dixon, J.E. (2000) Disruption of signaling by yersinia effector YopJ, a ubiquitin-like protein protease. *Science* **290**, 1594-1597.

Paschos, K. and Allday, M. (2010) Epigenetic reprogramming of host genes in viral and microbial pathogenesis. *Trends in Microbiology* **18**, 439–447.

Pavet, V., Quintero, C., Cecchini, N.M., Rosa, A.L. and Alvarez, M.E. (2006) *Arabidopsis* Displays Centromeric DNA Hypomethylation and Cytological Alterations of Heterochromatin Upon Attack by *Pseudomonas syringae*. *Molecular Plant-Microbe Interactions* **19**, 577-587.

Peñaloza-Vazquez, A., Preston, G.M., Collmer, A. and Bender, C.L. (2000) Regulatory interactions between the Hrp type III protein secretion system and coronatine biosynthesis in *Pseudomonas syringae* pv. *tomato* DC3000. *Microbiology* **146**, 2447-2456.

Penterman, J., Zilberman, D., Jin, H.H., Ballinger, T., Henikoff, S. and Fischer, R.L. (2007) DNA demethylation in the *Arabidopsis* genome. *Proceedings of the National Academy of Sciences of the United States of America* **104**, 6752-6757.

Pumplin, N. and Voinnet, O. (2013) RNA silencing suppression by plant pathogens: defence, counter-defence and counter-counter-defence. *Nature Reviews Microbiology* **11**, 745-760.

Raja, P., Wolf, J.N. and Bisaro, D.M. (2010) RNA silencing directed against geminiviruses: Post-transcriptional and epigenetic components. *Biochimica et Biophysica Acta - Gene Regulatory Mechanisms* **1799**, 337-351.

Ranjan, R., Patro, S., Pradhan, B., Kumar, A., Maiti, I.B. and Dey, N. (2012) Development and functional analysis of novel genetic promoters using DNA shuffling, hybridization and a combination thereof. *PLoS One* **7**, e31931.

Reymond, P. and Farmer, E.E. (1998) Jasmonate and salicylate as global signals for defense gene expression. *Current Opinion in Plant Biology* **1**, 404-411.

Rich, J.J., Kinscherf, T.G., Kitten, T. and Willis, D.K. (1994) Genetic evidence that the gacA gene encodes the cognate response regulator for the lemA sensor in *Pseudomonas syringae*. *Journal of bacteriology* **176**, 7468-7475.

Rodríguez-Negrete, E., Lozano-Durán, R., Piedra-Aguilera, A., Cruzado, L., Bejarano, E.R. and Castillo, A.G. (2013) Geminivirus Rep protein interferes with the plant DNA methylation machinery and suppresses transcriptional gene silencing. *New Phytologist* **199**, 464-475.

Ronald, P.C., Salmeron, J., Carland, F. and Staskawicz, B. (1992) The cloned avirulence gene avrPto induces disease resistance in tomato cultivars containing the Pto resistance gene. *Journal of bacteriology* **174**, 1604-1611.

Ronemus, M.J., Galbiati, M., Ticknor, C., Chen, J. and Dellaporta, S.L. (1996) Demethylation-induced developmental pleiotropy in *Arabidopsis*. *Science* **273**, 654-657.

Ryals, J.A., Neuenschwander, U.H., Willits, M.G., Molina, A., Steiner, H.Y. and Hunt, M.D. (1996) Systemic acquired resistance. *Plant Cell* **8**, 1809-1819.

Ryan, C.A. and Pearce, G. (1998) Systemin: A polypeptide signal for plant defensive genes. In: *Annual Review of Cell and Developmental Biology* pp. 1-17.

Sandegren, L., Lindqvist, A., Kahlmeter, G. and Andersson, D.I. (2008) Nitrofurantoin resistance mechanism and fitness cost in *Escherichia coli*. *Journal of Antimicrobial Chemotherapy* **62**, 495-503.

Schechter, L.M., Vencato, M., Jordan, K.L., Schneider, S.E., Schneider, D.J. and Collmer, A. (2006) Multiple approaches to a complete inventory of *Pseudomonas syringae* pv. *tomato* DC3000 type III secretion system effector proteins. *Molecular Plant-Microbe Interactions* **19**, 1180-1192.

Schwessinger, B. and Zipfel, C. (2008) News from the frontline: recent insights into PAMP-triggered immunity in plants. *Current Opinion in Plant Biology* **11**, 389-395.

Soppe, W.J.J., Jacobsen, S.E., Alonso-Blanco, C., Jackson, J.P., Kakutani, T., Koornneef, M. and Peeters, A.J.M. (2000) The late flowering phenotype of *fwa* mutants is caused by gain-of-function epigenetic alleles of a homeodomain gene. *Molecular Cell* **6**, 791-802.

Stroud, H., Do, T., Du, J., Zhong, X., Feng, S., Johnson, L., Patel, D.J. and Jacobsen, S.E. (2014) Non-CG methylation patterns shape the epigenetic landscape in *Arabidopsis*. *Nature Structural and Molecular Biology* **21**, 64-72.

Takeda, S., Tadele, Z., Hofmann, I., Probst, A.V., Angelis, K.J., Kaya, H., Araki, T., Mengiste, T., Scheid, O.M., Shibahara, K.I., Scheel, D. and Paszkowski, J. (2004) BRU1, a novel link between responses to DNA damage and epigenetic gene silencing in *Arabidopsis*. *Genes and Development* **18**, 782-793.

Taylor, J.D., Teverson, D.M., Allen, D.J. and Pastor-Corrales, M.A. (1996) Identification and origin of races of *Pseudomonas syringae* pv. phaseolicola from Africa and other bean growing areas. *Plant Pathology* **45**, 469-478.

Taylor, R.K., Miller, V.L., Furlong, D.B. and Mekalanos, J.J. (1987) Use of phoA gene fusions to identify a pilus colonization factor coordinately regulated with cholera toxin. *Proceedings of the National Academy of Sciences of the United States of America* **84**, 2833-2837.

Tsuda, K., Sato, M., Glazebrook, J., Cohen, J.D. and Katagiri, F. (2008) Interplay between MAMP-triggered and SA-mediated defense responses. *Plant Journal* **53**, 763-775.

Underwood, W., Melotto, M. and He, S.Y. (2007) Role of plant stomata in bacterial invasion. *Cellular Microbiology* **9**, 1621-1629.

Van Der Biezen, E.A. and Jones, J.D.G. (1998) Plant disease-resistance proteins and the gene-for-gene concept. *Trends in Biochemical Sciences* **23**, 454-456.

Vongs, A., Kakutani, T., Martienssen, R.A. and Richards, E.J. (1993) *Arabidopsis thaliana* DNA methylation mutants. *Science* **260**, 1926-1928.

Wei, C.F., Kvitko, B.H., Shimizu, R., Crabill, E., Alfano, J.R., Lin, N.C., Martin, G.B., Huang, H.C. and Collmer, A. (2007) A *Pseudomonas syringae* pv. *tomato* DC3000 mutant

lacking the type III effector HopQ1-1 is able to cause disease in the model plant *Nicotiana benthamiana*. *The Plant Journal* **51**, 32-46.

Widman, N., Jacobsen, S.E. and Pellegrini, M. (2009) Determining the conservation of DNA methylation in *Arabidopsis*. *Epigenetics* **4**, 119-124.

Wierzbicki, A.T., Ream, T.S., Haag, J.R. and Pikaard, C.S. (2009) RNA polymerase v transcription guides ARGONAUTE4 to chromatin. *Nature Genetics* **41**, 630-634.

Wildermuth, M.C., Dewdney, J., Wu, G. and Ausubel, F.M. (2001) Isochorismate synthase is required to synthesize salicylic acid for plant defence. *Nature* **414**, 562-565.

Xie, Z., Johansen, L.K., Gustafson, A.M., Kasschau, K.D., Lellis, A.D., Zilberman, D., Jacobsen, S.E. and Carrington, J.C. (2004) Genetic and functional diversification of small RNA pathways in plants. *PLoS Biology* **2**.

Yu, A., Lepère, G., Jay, F., Wang, J., Bapaume, L., Wang, Y., Abraham, A.L., Penterman, J., Fischer, R.L., Voinnet, O. and Navarro, L. (2013) Dynamics and biological relevance of DNA demethylation in *Arabidopsis* antibacterial defense. *Proceedings of the National Academy of Sciences of the United States of America* **110**, 2389-2394.

Yu, G.-L., Katagiri, F. and Ausubel, F.M. (1993) *Arabidopsis* mutations at the RPS2 locus result in loss of resistance to *Pseudomonas syringae* strains expressing the avirulence gene avrRpt2. *MOLECULAR PLANT MICROBE INTERACTIONS* **6**, 434-434.

Yu, J., Penaloza-Vázquez, A., Chakrabarty, A.M. and Bender, C.L. (1999) Involvement of the exopolysaccharide alginate in the virulence and epiphytic fitness of *Pseudomonas syringae* pv. *syringae*. *Molecular Microbiology* **33**, 712-720.

Zemach, A., Kim, M.Y., Hsieh, P.H., Coleman-Derr, D., Eshed-Williams, L., Thao, K., Harmer, S.L. and Zilberman, D. (2013) The *Arabidopsis* nucleosome remodeler DDM1 allows DNA methyltransferases to access H1-containing heterochromatin. *Cell* **153**, 193-205.

Zhang, H. and Zhu, J.K. (2012) Active DNA demethylation in plants and animals. *Cold Spring Harbor Symposia on Quantitative Biology* **77**, 161-173.

Zhang, X., Dai, Y., Xiong, Y., DeFraia, C., Li, J., Dong, X. and Mou, Z. (2007) Overexpression of *Arabidopsis* MAP kinase kinase 7 leads to activation of plant basal and systemic acquired resistance. *Plant Journal* **52**, 1066-1079.

Zhang, X., Yazaki, J., Sundaresan, A., Cokus, S., Chan, S.W.L., Chen, H., Henderson, I.R., Shinn, P., Pellegrini, M., Jacobsen, S.E. and Ecker, J. (2006) Genome-wide High-Resolution Mapping and Functional Analysis of DNA Methylation in *Arabidopsis*. *Cell* **126**, 1189-1201.

Zhang, Z., Chen, H., Huang, X., Xia, R., Zhao, Q., Lai, J., Teng, K., Li, Y., Liang, L. and Du, Q. (2011) BSCTV C2 attenuates the degradation of SAMDC1 to suppress DNA methylation-mediated gene silencing in *Arabidopsis*. *The Plant Cell Online* **23**, 273-288.

Zipfel, C., Robatzek, S., Navarro, L., Oakeley, E.J., Jones, J.D.G., Felix, G. and Boller, T. (2004) Bacterial disease resistance in *Arabidopsis* through flagellin perception. *Nature* **428**, 764-767.

Zumaquero, A., Macho, A.P., Rufián, J.S. and Beuzón, C.R. (2010) Analysis of the role of the type III effector inventory of *Pseudomonas syringae* pv. *phaseolicola* 1448a in interaction with the plant. *Journal of bacteriology* **192**, 4474-4488.

"*One of the greatest discoveries a person makes, one of their great surprises, is to find they can do what they were afraid they couldn't do.*"

— Henry Ford

Resumen de la tesis en español

1. Pseudomonas syringae

Pseudomonas syringae es una bacteria en forma de bacilo, Gram-negativa, hemibiotrófa y con flagelos polares, que provoca una amplia variedad de síntomas en plantas, incluyendo, manchas necróticas y/o cloróticas y agallas.

La especie se divide en variantes patógenas (patovares, pv) que difieren en su rango de huéspedes (Peñaloza-Vázquez et al., 2000). Hay más de 50 patovares diferentes descritos, algunas de los cuales se subdividen en razas basándose en el rango de cultivares de la especie huésped que infectan (González et al., 2000; Hirano y Upper, 2000). *Pseudomonas syringae* sobrevive en las superficies de las hojas de las plantas como una epífita, antes de entrar en el espacio intercelular a través de aberturas naturales como estomas o heridas, para iniciar el proceso de infección (Hirano y Upper, 2000). *P. syringae pv. tomate* (en adelante *Pto*) DC3000, la principal estirpe modelo para el estudio de la interacción de *P. syringae* con el huésped, es el agente causante de la mancha bacteriana en tomate, y también puede causar enfermedad en la planta modelo *Arabidopsis thaliana*.

El genoma de *Pto* DC3000 (6,5 megabytes) contiene un cromosoma circular y dos plásmidos, que codifican en conjunto 5.763 ORFs (Collmer et al., 2002). La base genética de la patogénesis y la virulencia en *P. syringae* es compleja e incluye reguladores globales (Hrabak y Willis, 1992; Kitten et al., 1998; Rich et al., 1994), el conjunto de genes *hrp*, que codifica un sistema de secreción de tipo III (T3SS), así como factores de virulencia, tales como la fitotoxina coronatina, y exopolisacáridos (Bender et al., 1999; Yu et al., 1999). Una vez dentro de su huésped, *P. syringae* sobrevive y prolifera dentro de los espacios intercelulares, el apoplasto, donde a través de la acción del T3SS introduce un conjunto de proteínas altamente especializados, llamados efectores, a través de la pared en el citosol de la célula huésped. Una vez dentro del citosol, las proteínas efectoras trabajan para suprimir el sistema inmune de la planta, lo que permite el crecimiento del patógeno en el apoplasto (Göhre y Robatzek, 2008). Bacterias mutantes incapaces de introducir efectores en la célula huésped, es decir, mutantes en el T3SS, muestran un crecimiento

severamente restringido en el huésped debido a la acción del sistema inmune de la planta y no causan enfermedad (Mohr et al., 2008).

2. El sistema de secreción tipo III (Type III Secretion System, T3SS)

El T3SS es un aparato de secreción complejo compuesto de aproximadamente 30 proteínas diferentes. Este sofisticado aparato acopla la secreción a través de las membranas interna y externa de la bacteria, con la translocación a través de las membranas citoplasmáticas eucariotas, así como a través de la pared celular en el caso del T3SS de bacterias patógenas de plantas (Nguyen L. et al., 2000). Los T3SS son esenciales para la patogénesis (Cunnac et al., 2009). Los genes que codifican los componentes del T3SS, especialmente aquellos que codifican el aparato de secreción, se agrupan en *clusters*. En algunos organismos, estos grupos de genes se encuentran en plásmidos que son únicos para el agente patógeno y no se encuentran en parientes no patógenos (*Yersinia spp.*, *Shigella flexneri*, y *Ralstonia solanacearum*) (Galan y Collmer, 1999). En otros patógenos (*Salmonella typhimurium*, *Escherichia coli* enteropatógena (EPEC), *Pseudomonas aeruginosa*, *P. syringae*, *Erwinia amylovora* y *Xanthomoas campestris*) (Orth et al., 2000), los *cluster* para los genes del sistema de secreción tipo III, se localizan en el cromosoma y, a menudo parecen haber sido adquirido por transferencia horizontal, ya que las bacterias no patógenas relacionados, carecen de estas islas de patogénesis, pero comparten las correspondientes secuencias adyacentes.

Desde el punto de vista funcional, existen tres clases de proteínas diferentes en los T3SS; (*i*) las proteínas estructurales: que forman la base, la varilla interna y la aguja, (*ii*) las proteínas efectoras: que son introducidas en el interior de la célula huésped y promueven la infección a través de la supresión de las defensas de la planta, (*iii*) las chaperonas: que se unen a efectores en el citoplasma bacteriano, los protegen de la agregación y la degradación y los dirigen hacia el aparato de secreción (Anderson et al., 2010). Algunas estirpes de *P. syringae* también codifican proteínas que son secretadas de manera dependiente del sistema de secreción tipo III y que

pueden ayudar a translocar los efectores a través de la membrana de la célula de la planta, pero no entran en el citoplasma de la célula huésped, o que pueden permanecer en el exterior de la célula huésped, donde pueden provocar respuestas de defensa (Choi et al., 2013). El análisis funcional del genoma *Pto* DC3000 mostró varios grupos de genes que codificaban para efectores del sistema de secreción tipo III (T3Es), habiendo 31 confirmados y 19 predichos (Collmer et al., 2002). Los T3Es de *Pto* DC3000, conocidos como proteínas "Hop" (*HR and pathogenicity outer protein*) o proteínas "Avr" (*avirulence*), basándose en el fenotipo con el que fueron originalmente descritos (Collmer et al., 2002), han sido analizados de forma exhaustiva, y se ha demostrado que 28 de ellos, se expresan y se translocan correctamente durante la infección (Lindeberg et al., 2006). Los T3Es son en conjunto, esenciales para la patogénesis pero individualmente son prescindibles para derrotar las defensas, para crecer o para producir síntomas en las plantas. Dieciocho de los genes efectores *Pto* DC3000 se agrupan en seis islas / islotes genómicos (Collmer et al., 2009) y existen datos concluyentes que muestran que muchos de ellos se adquirieron por transferencia horizontal (Collmer et al., 2002).

3. La respuesta de defensa de la planta frente a P. syringae

Las plantas reaccionan al ataque de los patógenos mediante sucesivas respuestas de defensa en fase, que difieren principalmente en el tipo de moléculas del patógeno que se detectan en cada fase, y en la velocidad y en la intensidad de las respuestas resultantes. La primera fase o nivel de defensa, se activa tras la detección de patógenos a través de la acción de los receptores de reconocimiento de patrones (*pattern recognition receptors*, PRR).

3.1. Receptores de reconocimiento de patrones (Pattern recognition receptors) y patrones moleculares asociados a patógenos (pathogen-associated molecular patterns)

Las plantas son capaces de limitar la colonización y el crecimiento de un gran número de patógenos microbianos. Esto se debe principalmente a la activación de los receptores situados en la superficie celular de la planta denominados receptores de reconocimiento de patrones (*pattern recognition receptors*, PRRs). Estos receptores son proteínas que reconocen moléculas

específicas muy conservadas del microorganismo, y conocidas según los autores como patrones moleculares asociados a patógenos (*pathogen-associated molecular patterns*, PAMP) o patrones moleculares asociados a microbios (*microbe-associated molecular pattern* or MAMPs). *Arabidopsis* codifica numerosos PRRs (47 identificados hasta la fecha). Uno de los PRRs mejores caracterizados es FLS2, que percibe flagelina, el principal componente del flagelo bacteriano (Boller y Félix, 2009). FLS2 está altamente conservado entre las especies de plantas (Zipfel et al., 2004) y es capaz de alertar a la planta de la presencia de bacterias potencialmente invasoras, incluso antes de que las bacterias penetren en la hoja (Melotto et al., 2006). Muchas bacterias patógenas poseen flagelos, que están formado principalmente por un polímero de flagelina. A pesar de que la totalidad de la flagelina se considera que actúa como un PAMP, sólo un segmento de 22 aminoácidos del extremo N-terminal es necesario para el reconocimiento por parte de la célula vegetal (Felix et al., 1999). Este péptido de 22 aminoácidos está disponible comercialmente y es conocido como flg22. La mayoría de las mutaciones en flagelina que hacen que FLS2 no pueda reconocerla, causan su perdida de función y las bacterias que las codifican pierden por tanto su movilidad (Naito et al., 2008).

A partir del reconocimiento de estos patrones bacterianos conservados o PAMPs, la planta desencadena una respuesta inmune, que implica la activación de la cascada de señalización de las MAPK (*mitogen-activated protein kinase*) que conducen a la inducción de genes de defensa (*pathogen-response genes*), a la producción de especies reactivas de oxígeno (ROS) y a la deposición de calosa en los sitios de infección para reforzar las paredes celulares de la planta. Todas estas respuestas contribuyen a restringir el crecimiento bacteriano (Schwessinger y Zipfel, 2008). Este proceso se conoce como inmunidad producida por PAMP (*PAMP-triggered immunity*, PTI). La activación de PTI es un proceso lento y la intensidad de la respuesta se incrementa con el tiempo. Esta activación lenta es propia de una respuesta inmune que no distingue entre microorganismos patógenos y no patógenos y que permite a la planta prevenir la colonización por la mayoría de los microorganismos patógenos. Sin embargo, la lenta cinética inicial de

activación de PTI puede ser utilizada por patógenos adaptados, que han evolucionado para adquirir funciones adicionales que se dirigen específicamente y suprimen la PTI, y en ese caso esta primera respuesta de defensa puede ser insuficiente para proteger eficazmente la planta.

3.2. Supresión de PTI (inmunidad producida por PAMP, PAMP-triggered immunity, PTI) mediada por efectores

Los efectores han ido evolucionado contribuyendo así a incrementar la capacidad de la virulencia del patógeno y a superar las defensas del hospedador. La función principal del T3SS en bacterias fitopatógenas es suprimir la PTI en el huésped. Esta capacidad supresora de PTI ha sido demostrada para muchos de los efectores secretados por el sistema de secreción tipo III (T3Es), aunque todavía se desconocen los mecanismos moleculares implicados en dicha represión para la mayor parte de los efectores.

Trabajos recientes de los últimos años han mostrado las diferentes formas en que los patógenos son capaces de superar las defensas basales del huésped. Hay tres estrategias principales por las que los patógenos superan la PTI: (a) suprimir de la activación de PTI a través de la acción de los efectores, (b) circunnavegar las actividades PTI través de la producción de efectores tipo toxina o (c) degradar productos bioactivos de PTI a través de sofisticados mecanismos de desintoxicación (Anderson et al., 2011). Hay varios ejemplos de efectores de patógenos capaces de suprimir aspectos específicos de la defensa de la planta. Uno de estos ejemplos en *Arabidopsis*, es la supresión de la activación de la PTI tras la percepción de flg22 mediante los efectores denominados, AvrPto, AvrPtoB y HopAI1. Estos efectores de *Pto* suprimen PTI mediante el bloqueo de la activación de MAPK (de Torres et al., 2006; He et al., 2006; Zhang et al., 2007). Además de la supresión de las defensas del huésped, algunos efectores también pueden ayudar a los patógenos a evadir su detección mediante los PRRs del huésped, suprimiendo la señalización molecular que ocurre corriente abajo de PRR (Boller y He., 2009).

Por lo tanto, los patógenos adaptados son aquellos que utilizan efectores para superar eficazmente PTI y como resultado el patógeno pueden proliferar. En

este caso la planta se queda sometida a un proceso conocido como "susceptibilidad mediada por efector" (*effector-triggered susceptibility*, ETS) que conlleva al desarrollo de la enfermedad como un resultado de la interacción del patógeno con la célula huésped. Esto también se conoce como una interacción compatible. Sin embargo, durante la co-evolución planta-patógeno, las plantas han evolucionado genes de resistencia (R) que les permiten detectar los efectores de los patógenos (o el efecto de los efectores en la planta) y que activan respuestas de defensa de mayor intensidad y rápidez . Este reconocimiento conduce al establecimiento de la resistencia contra el patógeno y se conoce como inmunidad mediada por efector (*effector-triggered inmunity*, ETI) (Jones y Dangl, 2006).

3.3. Inmunidad mediada por efector (effector-triggered inmunity, ETI) y la supresión de la inmunidad mediada por efector

Los microorganismos invasores también pueden ser detectados a través del reconocimiento de sus efectores por parte de la planta. Los efectores específicamente reconocidos por proteínas de resistencia (R) de la planta, se denominan proteínas de avirulencia (Avr). Este tipo de reconocimiento es a menudo indirecto, a través de la detección de las modificaciones generadas por la actividad del efector en proteínas de la célula vegetal. El modelo por el cual se produce esta detección indirecta se conoce como la "hipótesis de guarda" (*guard hypothesis*, Van der Biezen y Jones, 1998). Esta hipótesis establece que las proteínas R interactúan o "guardan", una proteína que es el objetivo de una proteína Avr y que se conoce como "*guardee*". Cuando se detecta la interferencia con la proteína *guardee*, la proteína R activa una fuerte respuesta de resistencia contra el patógeno conocida como ETI. Las proteínas R son receptores intracelulares de proteínas del tipo NB-LRR (*Nucleotide-Binding, Leucine-Rich Repeat-containing proteins*).

Durante la activación de ETI, las células huésped vecinas al patógeno, se someten a un proceso de muerte celular programa conocido como "respuesta hipersensible" (*hypersensitive response*, HR) que resulta en la senescencia de la zona infectada y por lo tanto se restringe así el crecimiento y la propagación del patógeno (Jones y Dangl, 2006) . La HR se caracteriza por

una necrosis localizada del tejido y la producción de compuestos fenólicos y agentes antimicrobianos en el sitio de contacto con el patógeno. Esta interacción también se conoce como una interacción incompatible, y entonces el patógeno se considera avirulento, y el huésped, resistente.

En contraste con los PAMPs, los efectores son moléculas específicas de cada patógeno y su reconocimiento conduce a una respuesta de defensa más rápida, más intensa y más eficiente contra patógenos adaptados y presumiblemente más difícil de suprimir (Katagiri y Tsuda, 2010). El dispararse ETI generalmente previene la propagación de las bacterias invasoras a partes más distantes de la planta y se asocia a la activación de la inmunidad sistémica conocida como "resistencia sistémica adquirida" (*systemic acquired resistance*, SAR) (Cameron et al., 1994). Por lo tanto, SAR protege las partes distantes de la planta frente a nuevos ataques. Sin embargo, algunos patógenos también han adquirido, a través de la evolución, la capacidad de prevenir la activación de ETI, presumiblemente suprimiendo ETI incluso antes de que se dispare. Este paso lleva a la proliferación del patógeno y el desarrollo de la enfermedad y también se conoce como ETS (*effector-triggered susceptibility*, ETS). Se sabe menos acerca de los mecanismos mediante los cuales efectores suprimen ETI, haciéndolo algunos de manera muy específica, mientras que otros lo hacen de una manera más general (Macho et al., 2010; Macho y Beuzón, 2010).

Sin embargo, las plantas también pueden detectar a los efectores supresores de ETI a través de proteínas R adicionales. Por lo tanto, se establece una carrera de armamentos evolutiva en la interacción planta-patógeno que va de ETS (enfermedad de la planta y éxito para el patógeno) a ETI (resistencia y éxito para la planta hospedadora) según el plantel de efectores del patógeno y proteínas R de la planta disponibles en cada lado de la interacción.

3.4. El papel del ácido salicílico y la coronatina durante la interacción planta con Pseudomonas syringae pv. tomate (Pto)

La defensa de las plantas frente a patógenos está influenciada por la señalización endógena sistémica mediada por las hormonas vegetales (Hayat et al., 2007). *Arabidopsis thaliana* Col-0 tiene dos respuestas principales mediadas por hormonas, implicadas en las vías de señalización inducidas por defensa: las respuestas mediadas por el ácido salicílico (SA), y las mediadas por el ácido jasmónico o metiljasmonato (JA o MeJA). Estas vías suprimen el crecimiento de una amplia gama de patógenos microbianos, incluyendo muchos tipos diferentes de patógenos bacterianos (Bostock, 2005; Glazebrook, 2005; Kunkel y Brooks 2002).

Normalmente, la señalización mediada por SA conlleva a la resistencia frente a patógenos biotrófos y hemibiotrófos tales como *P. syringae*, mientras que la señalización mediada por MeJA se activa comúnmente en respuesta a heridas, insectos masticadores y patógenos necrotrófos (Ryan y Pearce, 1998). La acumulación de SA se produce cuando los receptores de la planta perciben los PAMPs (Tsuda et al., 2008) y conduce a la activación de la expresión génica de la defensa basal (Asai et al., 2002). Sorprendentemente, *Pto* produce una fitotoxina llamada coronatina (COR) que imita funcional y estructuralmente al MeJA y produce los mismos efectos que la activación de la respuesta mediada por MeJA (Brooks et al., 2005). La señalización de JA y SA puede ser antagónica (Kunkel et al., 2002), por lo tanto la activación de la señalización inducida por MeJA tiene como consecuencia la supresión de la vía de señalización SA, que es necesaria para una defensa basal eficaz contra *P. syringae* (Delaney et al., 1995; Nawrath, et al., 2002; Wildermuth et al., 2001). La producción de COR está implicada en la supresión del cierre de los estomas asociada a PTI (Melotto et al., 2008), está controlada por HrpL, que también regula la expresión del T3SS y se requiere para superar las defensas dependientes de SA (Brooks et al., 2005). Prueba de ello es que el mutante de *A. thaliana coi1* (coronatine insensitive mutant 1) que exhibe expresión constitutiva de las defensas dependientes de SA, presenta un fenotipo resistente a la infección por *P. syringae* (Feys et al., 1994). Esto proporciona evidencia genética de que la vía de señalización mediada por

MeJA regula negativamente la expresión de las defensas mediada por SA. Así *P. syringae* puede utilizar coronatina para activar la vía de señalización de MeJA, interfiriendo así con la inducción de la señalización dependiente de SA (Kloek et al., 2001). Esto podría inhibir o retrasar los mecanismo de defensa de la planta, dando así al patógeno una oportunidad de colonizar el tejido huésped (Reymond y Farmer, 1998).

4. Mecanismos epigenéticos: la metilación del DNA en plantas

La epigenética en su definición clásica, describe las modificaciones mitóticamente heredables del DNA o la cromatina que no alteran la secuencia primaria de nucleótidos (Bird, 2002; Jaenisch y Bird, 2003). Las modificaciones epigenéticas del DNA y de las histonas, los componentes básicos de la cromatina, consisten en modificaciones químicas que se asocian con cambios en la expresión de genes, son heredables y no alteran la secuencia primaria del DNA. Las modificaciones epigenéticas de la cromatina constituyen lo que se define como "el epigenoma" y representan un nuevo nivel de información que influye en la expresión de los genes subyacentes (Law y Jacobsen, 2010). Las modificaciones epigenéticas del DNA y de las histonas son cruciales para el desarrollo y la diferenciación de los diferentes tipos celulares. En las plantas, la metilación del DNA está implicada en el mantenimiento de la estructura de la cromatina y de los estados epigenéticos (Martienssen y Richards, 1995), en el control de desarrollo embrionario de la planta (Finnegan et al., 1996; Kakutani et al., 1996; Ronemus et al., 1996), en la impronta o *imprinting* genético, en la prevención de la recombinación homóloga (Bender, 2004), la transición a la fase reproductiva (Soppe et al., 2000) y el silenciamiento de fragmentos de DNA exógenos que se han incorporado en el genoma (Matzke et al., 2000).

En las plantas, la metilación del DNA ocurre comúnmente en las bases de citosina en los siguientes contextos de secuencia: la metilación simétrica en los contextos CG y CHG (donde, H = A, T o C) y la metilación asimétrica en el contexto CHH. Los niveles de metilación del DNA del genoma de *Arabidopsis* son aproximadamente el 24%, 6,7% y 1,7% para los contextos CG, CHG y CHH, respectivamente, y la metilación del DNA se produce

predominantemente en transposones y otros elementos de DNA repetitivo (Law and Jacobsen, 2010). Las metiltransferasas de DNA han sido bien caracterizadas en *Arabidopsis*. La metilación *de novo* es catalizada por las metiltransferasas de DNA denominadas DOMAINS REARRANGED METHYLTRANSFERASE 1 y 2 (DRM1 y DRM2) y la metilación es mantenida por tres vías diferentes: la metilación CG es mantenida por la METHYLTRANSFERASE 1 (MET1); la metilación CHG es mantenida por la CHROMOMETHYLASE 3 (CMT3), una metiltransferasa de DNA específica de plantas, y la metilación asimétrica CHH es mantenida mediante la persistente metilación *de novo* realizada por DRM1/DRM2 (Law y Jacobsen, 2010).

El establecimiento de la metilación del DNA en plantas está controlado por un mecanismo conocido de metilación del DNA dirigida por RNA (RNA-directed DNA methylation, RdDM) (Henderson y Jacobsen, 2007; Matzke et al., 2009). Durante el desarrollo de la planta, pequeños RNAs se unen a secuencias del genoma a las que son homólogas y esto conlleva a la metilación de las citosinas de dicha región en los tres contextos de secuencia, CG, CHG y CHH. Además de la maquinaria canónica del RNA interferente (RNA interference, RNAi) (miembros de las familias Dicer y Argonauta) y de la metiltransferasa *de novo* DRM2, RdDM necesita dos polimerasas de RNA específicas de plantas, Pol IV y Pol V, dos complejos putativos remodeladores de cromatina y varias otras proteínas recientemente identificadas (Matzke y Mosher, 2014). En resumen, el mecanismo de RdDM implica los siguientes pasos. La RNA polimerasa Pol IV produce largos transcritos que son transformados en RNA de doble cadena (dsRNA) y procesados por la enzima DICER-LIKE 3 (DCL3) en pequeños RNAs interferentes (small interfering RNAs, siRNAs) que se exportan al citoplasma. Una de las cadenas de los siRNAs es cargada en la proteína AGO4 y se importan al núcleo, donde el complejo siRNA-AGO4 guía mediante la complementariedad de secuencia, la formación de nuevos transcritos mediados por la RNA polimerasa PolV. En última instancia, este proceso recluta a la metiltransferasa de DNA (DRM2) para mediar la metilación *de novo* de las citosinas. Una vez establecidos los patrones globales de metilación del DNA en la célula, estos deben

mantenerse de forma estable tras las sucesivas mitosis (el genoma queda hemimetilado después de cada división celular) para asegurar que los transposones y demás elementos repetidos, permanecen silenciados y para preservar la identidad celular.

El mecanismo de RdDM parece actuar preferentemente en transposones ubicados en regiones eucromáticas, como es el caso del retrotransposón *AtSN1* que es un *locus* silenciado transcripcionalmente (TGS) y es un *locus* modelo de RdDM (Haag et al., 2009;. Wierzbicki et al., 2009). Por otro lado, el mecanismo de RdDM parece estar excluido en cierta medida de la heterocromatina pericentromérica, que está enriquecida en transposones más grandes. En cambio, las modificaciones en la heterocromatina pericentromérica (principalmente la metilación del DNA y la metilación de la lisina 9 de la histona H3, H3K9me) se producen principalmente de manera independiente a los siRNA y dependiente de MET1, CMT3 y DDM1 (DECREASED DNA METHYLATION 1, remodelador de cromatina) (Stroud et al., 2014; Zemach et al., 2013).

La metilación del DNA es una marca reversible y la desmetilación del DNA en plantas tiene lugar de forma pasiva y activa. La desmetilación pasiva se consigue mediante la inhibición de la actividad de las metiltransferasas de mantenimiento tras la replicación del DNA (Law y Jacobsen, 2010), mientras que los mecanismos de desmetilación activa son aquellos que eliminan activamente grupos metilo del DNA. En plantas, estudios genéticos y bioquímicos han revelado que las proteínas de *Arabidopsis* con dominio DNA glicosilasa como ROS1 (REPRESSOR OF SILENCING 1), DME (DEMETER) y las proteínas DEMETER-*like* (DML2 y DML3) funcionan como desmetilasas de DNA, siendo ROS1 la mejor caracterizada (Furner y Matzke, 2011). ROS1 participa en la desmetilación activa del DNA a través de la vía de reparación por escisión de base y preferentemente contrarresta la metilación inducida por RdDM (Zhang y Zhu, 2012).

5. El papel de la metilación y la desmetilación del DNA en respuesta al ataque del patógeno

Trabajos recientes realizados con patógenos de mamíferos han demostrado que las modificaciones en las histonas y la remodelación de la cromatina regulan la expresión génica y por tanto son las dianas principales utilizadas por los patógenos para manipular a la célula hospedadora durante la infección (Hamon and Cossart, 2008). En los últimos años, la modulación epigenética de los genes relacionados con la defensa del huésped, se ha convertido en un evento relativamente común de las infecciones virales y bacterianas (Gómez-Díaz et al., 2012; Paschos and Allday, 2010).

En las plantas, se conoce menos sobre cómo los patógenos alteran el epigenoma del huésped y las consecuencias que esto tiene en la interacción patógeno-huésped. Se ha propuesto que la metilación del DNA es uno de los principales mecanismos de defensa contra virus de DNA de plantas, tales como los geminivirus. Esto explicaría el hecho de que en estos virus se ha seleccionado la acción supresora que tienen algunas de la proteínas virales, para interferir con la metilación y el silenciamiento transcripcional del DNA viral (Raja et al., 2010). Al interferir con el correcto funcionamiento de los mecanismos de metilación de la planta, estas proteínas de los geminivirus revierten el silenciamiento génico transcripcional (TGS) de *loci* endógenos reprimidos transcripcionalmente y de transgenes (Raja et al., 2010; Rodríguez-Negrete et al., 2013; Zhang et al., 2011), confirmando que los virus modifican el epigenoma planta durante la infección.

Estudios que utilizan bacterias fitopatógenas han demostrado que los patógenos bacterianos de plantas también modifican el epigenoma del huésped y que las plantas han desarrollado defensas específicas contra la supresión del TGS orquestada por agentes patógenos.

Pavet y colaboradores fueron los primeros en mostrar que la infección con *Pto* DC3000 induce una rápida hipometilación del DNA en regiones pericentroméricas, incluyendo secuencias repetidas, como la repetición de 180 pb y el retrotransposón *Athila*, además de la descondensación de los cromocentros en *Arabidopsis* (Pavet et al., 2006). Los autores mostraron que estas respuestas se producen 24 horas después de la inoculación y que la

hipometilación del DNA inducida por *Pto* no está asociada a la replicación del DNA, lo que sugiere que se trata de un proceso de desmetilación activa (Pavet et al., 2006).

Un segundo trabajo que analizó mediante una aproximación genómica el estado de metilación del genoma completo de *Arabidopsis* (metiloma), reveló que numerosas regiones genómicas ricas en transposones, cambian su estado y patrón de metilación durante la interacción con estirpes de *Pto* virulentas o avirulentas o tras el tratamiento con SA exógeno. Además, muchos de estos cambios en la metilación del DNA, afectan a la expresión de genes vecinos, incluyendo genes relacionados con defensa (Dowen et al., 2012). Estos autores también demostraron que el crecimiento bacteriano de estirpes de *P. syringae* patógenas virulentas o avirulentas, estaba restringida en los mutantes afectados en la maquinaria de metilación de la planta y cuyo metiloma estaba alterado, tales como *met1-3* (alelo nulo de la metiltransferasa de mantenimiento, MET1) o *ddc* (mutante triple *drm1-2 drm2-2 cmt3-11*, afectado en las metiltransferasas DRM1, DRM2 y CMT3), lo que indica que la pérdida de metilación del DNA mejora la resistencia a las bacterias de manera inespecífica.

Un tercer trabajo reveló que el tratamiento de plantas de *Arabidopsis* con el péptido de flagelina flg22, conlleva a la disminución de la expresión de manera rápida y transitoria de los componentes clave del mecanismo de RdDM, incluyendo AGO4 y de la subunidad D 1A de la RNA polimerasa IV (Pol IV) (Yu et al., 2013). Esta supresión de la expresión de estos genes, se produce a las 3 horas tras el tratamiento con flg22 y es suficiente para reactivar la transcripción de varios *loci* endógenos cuyo silenciamiento depende de RdDM, como son los transposones *Onsen*, *EVADE* y *AtSN1*, así como del transgen *GUS* silenciado transcripcionalmente. Estos procesos son reversibles, ya que tanto la metilación del DNA como el silenciamiento transcripcional son restaurados a los niveles basales 9 horas después del tratamiento con flg22. Esta respuesta inducida por flg22 es facilitada por la desmetilasa ROS1, que es la principal desmetilasa en tejidos vegetativos. Los autores demostraron que *Pto* se replicaba mejor en el mutante *ros1-4* que en una planta silvestre y este hecho no se observaba en los mutantes

DEMETER-like (dml2 y dml3), apoyando un papel para la desmetilación del DNA mediada por ROS1 en la resistencia antibacteriana (Yu et al., 2013).
Mutantes del mecanismo de RdDM muestran HR espontánea y el aumento de la señalización mediada por SA. Estos procesos son indicativos de la activación constitutiva de los genes R, lo que sugiere que RdDM podría regular negativamente la expresión de algunos genes R. Yu y colaboradores demostraron que al menos dos genes R, RESISTANCE METHYLATED GENE 1 (RMG1) en plantas silvestres y WRKY22 en plantas tratadas con flg22, son sometidos a RdDM y se sobreexpresan en mutantes de RdDM (Yu et al., 2013) .
Estos estudios publicados de los ultimos años con bacterias fitopatógenas sugieren que la metilación de DNA dirigida por RNA (RdDM) y el silenciamiento génico transcripcional (TGS) juegan un papel importante en la interacción planta-huésped (Pumplin and Voinnet, 2013). La disminución de la expresión de genes de defensa a través de RdDM podría proporcionar un modo eficaz de regulación de la respuesta de defensa que puede inducirse por estrés biótico y abiótico. La rápida activación de defensas de las plantas requeriría la existencia de determinadas secuencias genómicas controladas por RdDM (transposones y repeticiones) en la proximidad de los genes relacionados con defensa y la implicación de las rutas de desmetilación del DNA activas, para garantizar una inducción óptima y rápida de genes de defensa ante el ataque del patógeno. Además, la disminución de la expresión de genes de RdDM y la activación de genes de defensa resultante se produciría sólo transitoriamente para evitar la inducción prolongada de estos genes. Esta característica sería previsiblemente ventajosa en el caso de los genes relacionados con la defensa, cuya expresión continua reduce el *fitness* de las plantas.
El objetivo de esta Tesis Doctoral ha sido profundizar en el conocimiento de la interacción planta-huésped a nivel epigenético. Para ello se han analizado los cambios que se producen en el estado de metilación del genoma de Arabidopsis y en la activación de *loci* silenciados transcripcionalmente, tras la infección por *Pto*. Se ha caracterizado la importancia de los determinantes virulencia de *P. syringae* y de los distintos mecanismos de defensa en la

activación de los *loci* silenciados transcripcionalmente. Además se profundizado en la importancia que tienen los procesos de metilación y desmetilación del DNA en la respuesta de defensa de *Arabidopsis* frente a *P. syringae*.

Notes